Universidade do Minho
Escola de Engenharia

Marco Aurélio Pinto da Silva

Optimization of Magnetoelectric Composites
Based on Electroactive Polymers for Energy
Harvesting and Sensor Application

setembro de 2015

Universidade do Minho
Escola de Engenharia

Marco Aurélio Pinto da Silva

Optimization of Magnetoelectric Composites
Based on Electroactive Polymers for Energy
Harvesting and Sensor Application

Tese de Doutoramento
Doutoramento em Engenharia de Materiais

Trabalho efectuado sob a orientação do
Professor Doutor Senentxu Lanceros-Méndez
Professor Doutor José Gerardo Vieira da Rocha
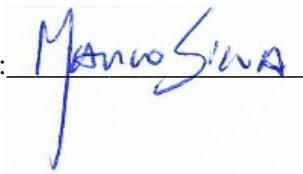Professor Doutor Pedro Libânio de Abreu Martins

setembro de 2015

I hereby declare having conducted my thesis with integrity. I confirm that I have not used plagiarism or any form of falsification of results in the process of the thesis elaboration. I further declare that I have fully acknowledged the Code of Ethical Conduct of the University of Minho.

University of Minho, Guimarães, 15 de setembro, 2015

Full name: Marco Aurélio Pinto da Silva

Signature:_____

I fully dedicate this work
to my mother, my father and my brother

Acknowledgments

I would like to thank to Portuguese Foundation for Science and Technology – FCT for the financial support (SFRH/BD/70303/2010) and to University of Minho for providing me all the conditions to develop my work.

Professor Senentxu, there is no words to express my deep gratitude and admiration for everything you taught me, for all the support, and for the friendship in every moment along this long journey.

To my co-supervisor Professor Gerardo, thank you for all the support and good advices you always gave me.

Many thanks to my co-supervisor doctor Pedro Martins, for all the friendship and support along this work.

Thank you Professor José Manuel Barandiarán and Professor Jon Gutierrez for the great time I have experienced with your research group at University of the Basque Country.

To my friends of the Electroactive Smart Materials Group, for all the amazing moments that we spent together, I will always remember you as my scientific family!

To the magnetoelectric group, you know how difficult is to work in this area, without you none of this would be possible. For your friendship, for all the moments that we help each other's. Many thanks my friends Silvinha, Renato, Andoni and Pedro Martins.

To all my friends that always helped me to be a better person every day.

And to my family for the love that always gave me. My dear mom and dad for the courage and to always look to the bright side of life. I owe you everything!

Abstract

Low power portable electronic devices and wireless sensors networks, for application in implantable biomedical sensors and monitoring for agricultural, environmental, building, military and industrial processes are typically powered by batteries, which have a finite supply of energy. The combination of an energy harvesting system with a rechargeable battery is the best way to self-power devices for their entirely lifetime. These harvesters collect energy (in the order of µW to mW) from ambient sources (thermal, mechanical or electromagnetic, among others).

Among them, energy harvesting from electromagnetic signals is one of the most challenging and interesting harvesting systems and has been poorly addressed. Magnetoelectric (ME) composite materials are an innovative tool that can convert such electromagnetic singnals into an electrical voltage and can be also be used as novel sensors and actuators.

The main objective of this work is to optimize ME laminated composites for sensor, actuators and energy harvesting devices. It is also an objective to find new applications for this ME effect.

From the different composite structures, laminated ME composites, comprising bonded piezoelectric and magnetostrictive layers, are the ones with the highest ME response, thus being the most studied materials for their implementation into technological applications. With high ME coupling, easy fabrication, large scale production ability, low-temperature processing into a variety of forms and, in some cases, biocompatibility, polymer based ME materials emerged as an original approach. In this work Vitrovac and Metglas were used as magnetostrictive materials due to their high magnetostriction at low fields, and .poly(vinylidene fluoride) was used as the polymeric piezoelectric material, due to his high piezoelectric constant compared to other polymers.

Thus, the effect of the bonding layer type and piezoelectric layer thickness is reported. Vitrovac/poly(vinylidene fluoride) magnetoelectric laminate were produced and experimental results show that the ME response increases with increasing piezoelectric thickness, the highest ME response of 53 V·cm^{-1}·Oe^{-1} being obtained for an 110 µm thick piezoelectric bonded with M- Bond epoxy. The behavior of the ME laminates with increasing temperatures up to 90 °C shows a decrease larger than 80% in the ME response. A finite element method (FEM) was used to evaluate the experimental

results. The obtained results show the critical role of the bonding layer and piezoelectric layer thickness in the ME performance of laminate composites

From the ME measurements it was concluded that tri-layered composites structures (Vitrovac/poly(vinylidene fluoride)/Vitrovac), show a high ME response (75 V cm^{-1} Oe^{-1}) and that the ME voltage coefficient decreases with increasing longitudinal size aspect ratio and increases with the lowest transversal aspect ratio between piezoelectric and magnetostrictive layers.

Relevant parameters such as sensibility, accuracy, linearity, hysteresis and resolution have been vaguely or never discussed in polymer-based ME composites. This work reports on those parameters on a Metglas/poly(vinylidene fluoride)/Metglas magnetoelectric laminate, the polymer-based composite with the highest ME response.

The sensibility and resolution determined for the DC (30 mV.Oe^{-1} and 8 μOe) and AC magnetic field sensor (992 mV.Oe^{-1} and 0.3 μOe) are favorably comparable with the most recent and sensitive polymer-based ME sensors.

The design and performance of five interface circuits, a full-wave bridge rectifier, two Cockcroft-Walton voltage multipliers (with 1 and 2 stages) and two Dickson voltage multipliers (with 2 and 3 stages), for the energy harvesting from a Metglas/PVDF/Metglas ME composite were discussed. Maximum power and power density values of 12 μW and 0.9 mW.cm^{-3} were obtained with the two stages Dickson voltage multiplier.

Finally, it is successfully demonstrated that nanoparticle's magnetostriction can be accurately determined based on the magnetoelectric effect measured on polymer composite materials. This represents a novel, simple and versatile method for the determination of particle's magnetostriction at the nano scale and in their dispersed state.

Thus, the developed polymer based magnetoelectric laminate composites showed suitable characteristics for applications in sensors and energy harvesting devices.

Resumo

Dispositivos eletrônicos portáteis de baixa potência e sensores de redes sem fio para implementação em sensores biomédicos, monitorização ambiental, gestão de agricultura, construção, aplicações militares e de processos industriais, normalmente são alimentados por baterias, que têm uma fonte finita de energia.

A combinação de um sistema de "energy harvesting" com uma bateria recarregável é a melhor forma de auto-alimentar um dispositivo durante o seu tempo de vida útil. Estes dispositivos ("harvesters") armazenam a energia proveniente de fontes presentes no ambiente (como térmica, mecânica e eletromagnética, entre outras). A energia produzida é na ordem de µW a mW. Entre estes sistemas, *energy harvesting* a partir de sinais eletromagnéticos é um dos desafios mais interessantes e tem sido pouco investigado. Materiais compósitos magnetelétricos (ME) são uma ferramenta inovadora que pode converter sinais eletromagnéticos em uma voltagem elétrica e também podem ser usados como novos sensores e atuadores.

O principal objetivo deste trabalho é otimizar compósitos laminados ME para sensores, atuadores e dispositivos de captação de energia. É também um objetivo de encontrar novas aplicações baseadas nestes materiais. De todas as diferentes estruturas compósitas, os compósitos laminados ME compostos pela colagem de camadas piezoelétricas e magnetostrictivas, são aqueles que apresentam a maior resposta ME, sendo desta forma os materiais mais estudados para a sua implementação em aplicações tecnológicas.

Com elevado acoplamento ME, fabrico fácil, capacidade de produção em grande escala, processamento a baixa temperatura numa grande variedade de formas e, em alguns casos, biocompatibilidade, materiais ME de base polimérica emergem como uma abordagem original.

Neste trabalho, Vitrovac e Metglas foram usados como materiais magnetostrictivos devido à sua elevada magnetostrição a baixos campos magnéticos. O poli (fluoreto de vinilideno) - PVDF foi usado como polímero piezoelétrico devido à sua elevada constante piezoelétrica entre os materiais poliméricos. De forma a resposta ME dos compósitos, o efeito do tipo da camada de adesão e a espessura da camada piezoelétrica foi avaliado.

Foi produzido um laminado magnetoelétrico (Vitrovac/PVDF) e os resultados experimentais mostram que a resposta ME aumenta com o aumento da espessura da camada piezoelétrica, a maior resposta ME foi de 53 V·cm^{-1}·Oe^{-1} para o laminado com uma espessura piezoelétrica de 110 µm colado com a resina epoxy M-Bond. Com o aumento da temperatura até 90ºC, os laminados ME mostram uma perda de resposta ME até 80%. O método dos elementos finitos (MEF) foi usado para avaliar os resultados experimentais. Os resultados obtidos mostram o papel crítico da camada de ligação e a espessura da camada piezoelétrica no desempenho de compósitos laminados ME. Através das medidas ME foi concluído que os compósitos de três camadas (Vitrovac/PVDF/Vitrovac), mostram a maior resposta ME (75 V cm^{-1} Oe^{-1}), e o coeficiente ME diminui com o aumento do *aspect ratio* longitudinal e aumenta com a diminuição do *aspect ratio* transversal entre a camada piezoelétrica e magnetostritiva.

Parâmetros relevantes, como sensibilidade, precisão, linearidade, histerese e resolução, tem sido pouco estudada em compósitos poliémicos ME,. Este trabalho investiga esses parâmetros num laminado ME (Metglas/PVDF/Metglas), o compósito polímero com a resposta.ME mais alta. A sensibilidade e resolução determinada para sensores de campo magnético DC (30 mV.Oe^{-1} and 8 µOe) e AC (992 mV.Oe^{-1} and 0.3 µOe) são favoravelmente comparadas com os mais recentes e sensíveis sensores baseados em compósitos ME de base polimérica. O *design* e a performance de cinco circuitos: retificador *full-wave bridge,* dois multiplicadores *Cockcroft-Walton* (com 1 e 2 andares) e dois multiplicadores *Dickson* (com 2 e 3 andares), para *energy harvesting* através de um laminado ME (Metglas/PVDF/Metglas) foi estudado e discutido. A máxima potencia e densidade de potência obtida foram 12µW e 0.9 mW.cm^{-3} usando um multiplicador Dickson de dois andares.

Por fim, é demonstrado com sucesso que a magnetostrição de nanopartículas pode ser determinada com precisão com base no efeito magnetoelétrico medido em materiais compósitos poliméricos. Isto representa um novo, versátil e simples método para a determinação de magnetostrição de partículas no seu estado disperso à escala nanométrica.

Assim, os compósitos laminados ME de base polimérica desenvolvidos, apresentam características adequadas para aplicações em sensores e dispositivos de *energy harvesting*.

Contents

List of tables

List of symbols

A	Area
A_P	Piezoelectric area
A_M	Magnetostrictive area
B_{AC}	AC magnetic field
C_{33}	Piezoelectric voltage
D	Electrical displacement
d_{3n}	Piezoelectric coefficient
E	Voltage
f_v	Force per unit volume
$g33$	Stiffness coefficient
I	Current intensity
I_{DC}	DC Current intensity
k	Bonding quality constant
P_{MAX}	Maximum power
$P_{density}$	Power density
R_{OPTIM}	Optimum resistance
T	Temperature
T_c	Curie temperature
t	Time
t	Thickness
$V_{DC}T$	Theoretical voltage
$V_{DC}R$	Measured voltage
V_{DC}	Voltage
V_n	Voltage
Y	Young´s Modulus
ν	Poisson´s Ratio
σ	Stress tensor
ρ	Density
$ρ_v$	Free electric charge density
$\nabla\cdot$	Divergence

α		ME coupling
λ		Magnetostriction
λ_{sat}		Magnetostriction saturation

List of abbreviations

CW	Cockcroft-Walton
DMC	Dimethyl carbonate
DMF	N,N-dimethylformamide
DSC	Differential scanning calorimetry
FE	Ferroelectric
FEM	Finite element method
FTIR	Fourier transformed infrared spectrostopy
FSO	Full scale output
LAR	Longitudinal aspect ratio
P(VDF-TrFE)	Poly(vinylidene fluoride-*co*-trifluoroethylene)
PMP	Piezoelectric/Magnetostrictive/Piezoelectric
PVDF	Poly(vinylidene fluoride)
PZT	Lead zirconate titanate
R_{Load}	Load resistance
SAMR	Small angle magnetization rotation
TAR	Transversal aspect ratio
ME	Magnetoelectric
MPM	Magnetostrictive/Piezoelectric/Magnetostrictive

1 Introduction

This chapter introduces the main topics related to the present work. It is to notice that the specific state of the art is provided in each of the chapters. A contextualization of the work is provided as well as the general and specific objectives of the study. Finally, the main structure of the document is presented.

1.1   Magnetoelectric effect

The main characteristic of magnetoelectric (ME) materials is the variation of the electrical polarization (P) in the presence of an applied magnetic field (H);

$$\Delta P = \alpha \Delta H \tag{1}$$

or the variation of the induced magnetization (M) in the presence of an applied electrical field (E):

$$\Delta M = \alpha \Delta E \tag{2}$$

Where α is the ME coupling coefficient. [1-4] Low Curie temperatures and weak ME coupling at room temperature hinder the technological applications of the first discovered ME materials, the single-phase ME materials [3, 5, 6]

To solve the limitations of single-phase materials the research interest began to focus in the ME effect on multiple-phase materials. Such effect is a result of the product of the magnetostrictive effect [1](magnetic/mechanical) within the magnetostrictive phase and the piezoelectric effect [2](mechanical/electrical) within the piezoelectric phase (equation 3).

$$ME_H effect = \frac{electric}{mechanical} \times \frac{mechanical}{magnetic} = \frac{\partial E}{\partial \lambda} \times \frac{\partial \lambda}{\partial B} \tag{3}$$

where $\partial \lambda/\partial B$ and $\partial E/\partial \lambda$ are the piezomagnetic coefficient and piezoelectric coefficients respectively. Thus, the ME effect in multiple-phase materials is extrinsic, strongly depending on the microstructure and coupling interaction across the magnetostrictive-piezoelectric interfaces.[7-9]

These ME composites produce a signal output at room temperature orders of magnitude larger than the single phase materials. Making them more suitable for technological applications such as magnetic sensors, among others.

---

[1]Magnetostriction is defined as the phenomenon where the dimensions or shape of a material change in response to an external applied magnetic field

[2]Piezoelectricity is defined as the ability of certain materials to generate an AC (alternating current) voltage when subjected to mechanical solicitations.

1.2 Magnetoelectric materials

Multiferroic (MF) materials show at least two of these three propertires: ferroelectricity, ferromagneticity, or ferroelasticity.[1, 3-5] Some of them are also magnetoelectric (ME) (Figure 1.1) Although the intrinsic ME effect can be found in some single-phase compounds, their low critical temperatures and/or weak ME coupling are not favorable to their practical applications.[3, 5, 6] Alternatively and with optimized design possibilities, multiferroic ME composites combining magnetostrictive and piezoelectric phases are gaining increasing attention since such composites combine large electric and magnetic responses at room temperature.
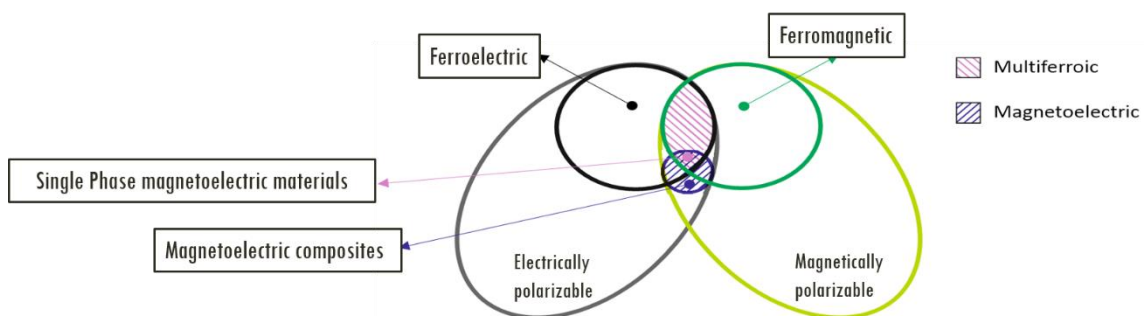
Figure 1.1 – Scheme of ferroic, multiferroic and magnetoelectric materials.

Thus, in such ME composites, neither of the constituent phases has ME properties, but the stress and elastic mediated coupling interaction between the phases gives rise to a strong ME effect.[6, 10, 11] There are two main groups of ME composites found in the literature: Non-polymer-based ME composites and polymer-based ME composites. [6, 10, 11]

Further, three main types of non-polymer-based ME composites are found in the literature: [1, 3, 6, 9, 12-15]

Non Polymer-based

Particulated composites of ferrites and piezoelectric ceramics (e.g., lead zirconate titanate (PZT)

Laminated composites of ferrites and piezoelectric ceramics;

Laminated composites of magnetostrictive metals/alloys (e.g., Terfenol-D or Metglas) and piezoelectric ceramics.
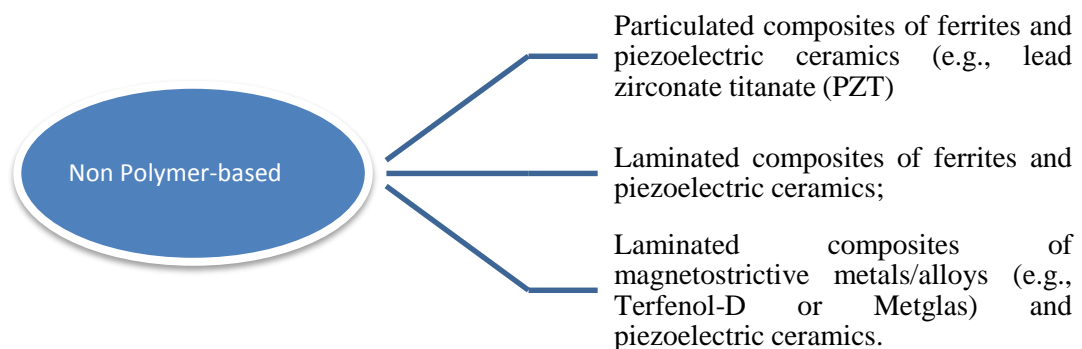
Figure 1.2 – Non Polymer based magnetoelectric materials.

Despite the ME coefficients obtained in ceramic-based ME composites being three orders of magnitude higher than in single-phase materials, such composites may become fragile and are limited by reactions at the interface regions, leading to high dielectric losses. They have low electrical resistivity, are dense, brittle and can lead to fatigue and failure during operation [1, 6].

The use of piezoelectric polymers, such as poly(vinylidene fluoride), PVDF, and its copolymers can solve some of the problems found in ceramic composites since they are flexible, show large electrical resistivity and small losses. Further, they can be easily fabricated by large- and small-scale low- temperature processing methods into a variety of forms.[6, 16, 17]

According to the literature, polymer-based ME composites also can be divided in three main types [18]
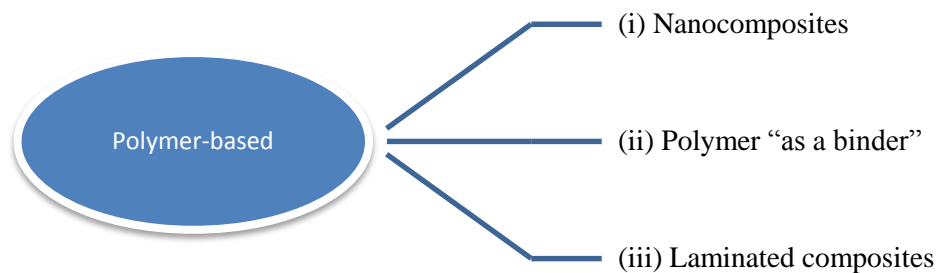
Figure 1.3 - Polymer based magnetoelectric materials

Within those composites, laminated polymer-based ME materials are those with the largest ME response, [19] being the highest value (21.46 V cm^{-1} Oe^{-1}) reported by Fang *et al*. for a three layer laminate comprising PVDF, Metglas and an epoxy resin. Such a value was achieved at non-resonance frequencies by taking advantage of the flux concentration effect, and is, so far, the highest response among this kind of materials at non- resonance frequencies.[19] On the other hand, the highest ME value reported by Jin *et al*. at the electromechanical resonance was 383 V cm^{-1} Oe^{-1} using cross-linked P(VDF-TrFE)/Metglas 2605SA1 composite bonded with an epoxy resin. [20]

1.3 Applications

The ME coefficient values found in ME laminates as well as the broad range of magnetic fields at which they respond, allow a large variety of applications in the areas of magnetic resonance imaging, multiple-state memories, filters, sensors, actuators, biomedical materials, energy harvesting systems among others. [17, 18] In some of these applications, polymeric based ME materials, due to the polymers unique characteristics can be taken to advantage.[18]

1.3.1 Sensors and actuators

The ME coefficients values found in polymer-based ME laminates as well as the broad range of the magnetic fields at which they respond, allow a large range of applications, in particular in the fields of magnetic sensors and actuators.[6, 21, 22]

Due to the limitations found in some of the conventional magnetic field sensors, including low operational temperatures, cost and high operational power[6, 23], self-powered polymer-based ME sensors are of increasing interest and applicability due to their novel working principle [6, 24, 25].

1.3.2 Energy harvesting

The ever decreasing power requirement of electronic sensors and devices has attracted attention to the energy harvesting technologies [26, 27].

Electronic devices steadily require lower power consumption and, due to this fact, the possibility of   feeding those devices by energy harvesting technologies increases. This creates a larger interest in investigating materials that may have the necessary characteristics for such harvesting.

Polymer-based ME composites have recently been evaluated for their use in energy-harvesting applications [6] . Such devices harvest energy from sources already present in the environment (thermal, mechanical and electromagnetic, among others). Currently one of the most rapidly developing technologies is the harvesting of energy from vibrations, with electromagnetic, electrostatic, magnetoelastic, or piezoelectric origin [28].

As described before, there has been significant advances in improving the magnitude of ME coefficient of laminate composites, which will improve the ME energy harvesting efficiency. ME materials based on piezoelectric polymers can be the next

generation of wearable energy-harvesting systems, due to their flexibility, versatility and low cost.

1.3.3   Magnetostriction measurements on particles

Materials with large magnetostriction, λ, are extensively used in sensors, actuators, micro-electromechanical systems and energy-harvesters, among others[29]. In this way, the magnitude of the magnetostrictive strain of a magnetic material is of great concern for the development and application on innovative technological devices.[30] Especially in applications that involve nanoparticles, the magnetostriction should be determined in their nanoscale in order to obtain more exact results.

The magnetostriction of a nanomaterial can be measured by direct or indirect methods. Direct methods enable the magnetostrictive strain to be measured as a function of the applied field, whereas indirect methods are suitable only for measuring the saturation magnetostriction λ_{sat}, often in an agglomerated state [31]

Through the ME effect, it is possible to accurately determinate nanoparticle's magnetostriction at the nano-sized state, by using polymeric-composite materials.

1.4 Objectives

The general objective of this work is the optimization of ME polymer based composites based on electroactive polymers for energy harvesting and sensor applications.

Thus, the specific objectives are:

- Develop composites and fabrication techniques for improving their ME response. The studied materials will be based on the piezoelectric polymer PVDF and several magnetostrictive materials such as Metglas and Vitrovac. The materials will be characterized and the physical effects analyzed. Theoretical calculations will be performed in order to optimize/design parameters and coupling conditions.

- Develop a system for the characterization of the ME response.

- Implement a working prototype able to demonstrate the basic principles of a ME harvester. The harvester will be built and characterized. Further, the electronic harvesting circuits will be optimized.

- The developed materials will be also optimized, tested and characterized for sensor and actuator applications.

1.5   Thesis structure

This thesis is divided into eight chapters to provide the logical evolution of the developed work during this research. Five of the eight chapters are based on published/submitted scientific papers. The thesis is divided in two main aspects of the research work, Optimization (chapters 4 and 5) and Applications (chapters 6; 7 and 8).

The chapters 1 and 2 describe the general contextualization of the work. Also in such chapters, the objectives of the study as well as the structure of the thesis are provided. It is to notice that a specific state of the art is provided within each chapter.

Chapter 3 offers a description of the developed system for the characterization of the ME response. In this chapter it is also provided a description of the experimental procedures for each one of the different studies performed in this work, including materials and preparation methods.

The chapters 4 and 5 report the optimization of the ME response of ME laminate composites, including bonding layer, sizes and geometries.

The chapters 6, 7 and 8 report the main applications resulting from this research: the characterization of ME laminates for sensor applications, the development of an energy harvesting device with electronic optimization, and a new tool for the determination of the magnetostrictive coefficient of nanoparticles *via* ME measurements, respectively.

Finally, chapter 9 provides the general conclusions of the study as well as the future work.

1.6 References

[1]   J. Ma, J. Hu, Z. Li, and C.-W. Nan, "Recent Progress in Multiferroic Magnetoelectric Composites: from Bulk to Thin Films," *Advanced Materials,* vol. 23, pp. 1062-1087, Mar 4 2011.

[2]   G. Lawes and G. Srinivasan, "Introduction to magnetoelectric coupling and multiferroic films," *Journal of Physics D: Applied Physics,* vol. 44, 2011.

[3]   D. R. Patil, A. D. Sheikh, C. A. Watve, and B. K. Chougule, "Magnetoelectric properties of ME particulate composites," *Journal of Materials Science,* vol. 43, pp. 2708-2712, 2008.

[4]   W. Prellier, M. P. Singh, and P. Murugavel, "The single-phase multiferroic oxides: From bulk to thin film," *Journal of Physics Condensed Matter,* vol. 17, pp. R803-R832, 2005.

[5]   P. Martins, C. M. Costa, and S. Lanceros-Mendez, "Nucleation of Electroactive β-phase Poly(vinilidene fluoride) with CoFe2O4 and NiFe2O4 Nanofillers: A New Method for the Preparation of Multiferroic Nanocomposites," *Appl. Phys. A Mater. Sci. Process.,* vol. 103, pp. 233-237, 2011.

[6]   P. Martins and S. Lanceros-Méndez, "Polymer-Based Magnetoelectric Materials," *Adv. Funct. Mater.,* vol. 23, pp. 3371-3385, 2013.

[7]   C. W. Nan, "Magnetoelectric Effect in Composites of Piezoelectric and Piezomagnetic Phases," *Phys. Rev. B,* vol. 50, pp. 6082-6088, 1994.

[8]   M. Fiebig, "Revival of the Magnetoelectric Effect," *J. Phys. D: Appl. Phys.,* vol. 38, pp. 123-152, 2005.

[9]   C. W. Nan, M. I. Bichurin, S. Dong, D. Viehland, and G. Srinivasan, "Multiferroic Magnetoelectric Composites: Historical Perspective, Status, and Future Directions," *J. Appl. Phys.,* vol. 103, pp. 1-35, 2008.

[10]   M. Silva, S. Reis, C. S. Lehmann, P. Martins, S. Lanceros-Mendez, A. Lasheras, *et al.*, "Optimization of the Magnetoelectric Response of Poly(vinylidene fluoride)/Epoxy/Vitrovac Laminates.," *ACS Appl. Mater. Interfaces,* vol. 5, pp. 10912-9, 2013.

[11]   P. Martins, R. Gonçalves, S. Lanceros-Mendez, A. Lasheras, J. Gutiérrez, and J. M. Barandiarán, "Effect of filler dispersion and dispersion method on the piezoelectric and magnetoelectric response of CoFe2O4/P(VDF-TrFE) nanocomposites," *Applied Surface Science,* vol. 313, pp. 215-219, 9/15/ 2014.

[12]   J. Ryu, A. V. Carazo, K. Uchino, and H. E. Kim, "Piezoelectric and magnetoelectric properties of lead zirconate titanate/Ni-ferrite particulate composites," *Journal of Electroceramics,* vol. 7, pp. 17-24, 2001.

[13]   R. A. Islam, Y. Ni, A. G. Khachaturyan, and S. Priya, "Giant magnetoelectric effect in sintered multilayered composite structures," *Journal of Applied Physics,* vol. 104, 2008.

[14]   S. Dong, J. Zhai, F. Bai, J. Li, D. Viehland, and T. A. Lograsso, "Magnetostrictive and magnetoelectric behavior of Fe-20 at. % Ga/Pb(Zr,Ti)O 3 laminates," *Journal of Applied Physics,* vol. 97, 2005.

[15]   Y. Jia, H. Luo, X. Zhao, and F. Wang, "Giant magnetoelectric response from a piezoelectric/magnetostrictive laminated composite combined with a piezoelectric transformer," *Advanced Materials,* vol. 20, pp. 4776-4779, 2008.

[16]   K. J. Loh and D. Chang, "Zinc oxide nanoparticle-polymeric thin films for dynamic strain sensing," *Journal of Materials Science,* vol. 46, pp. 228-237, 2011.

[17]   J. F. Scott, "Applications of magnetoelectrics," *Journal of Materials Chemistry,* vol. 22, pp. 4567-4574, 2012 2012.

[18]   P. Martins, A. C. Lopes, and S. Lanceros-Mendez, "Electroactive Phases of Poly(vinylidene fluoride): Determination, Processing and Applications," *Prog. Polym. Sci.,* vol. 39, pp. 683-706, 2013.

[19]   Z. Fang, S. G. Lu, F. Li, S. Datta, Q. M. Zhang, and M. El Tahchi, "Enhancing the Magnetoelectric Response of Metglas/Polyvinylidene Fluoride Laminates By Exploiting the Flux Concentration Effect," *Appl. Phys. Lett. ,* vol. 95, pp. 1-3, 2009.

[20]   J. Jin, S. G. Lu, C. Chanthad, Q. Zhang, M. A. Haque, and Q. Wang, "Multiferroic polymer composites with greatly enhanced magnetoelectric effect under a low magnetic bias," *Advanced Materials,* vol. 23, pp. 3853-3858, 2011.

[21]   S. Ju, S. H. Chae, Y. Choi, S. Lee, H. W. Lee, and C. H. Ji, "A low frequency vibration energy harvester using magnetoelectric laminate composite," *Smart Materials and Structures,* vol. 22, 2013.

[22]   M. Alnassar, A. Alfadhel, Y. P. Ivanov, and J. Kosel, "Magnetoelectric polymer nanocomposite for flexible electronics," *Journal of Applied Physics,* vol. 117, 2015.

[23]   J. Lenz and A. S. Edelstein, "Magnetic sensors and their applications," *IEEE Sensors Journal,* vol. 6, pp. 631-649, 2006.

[24]   Y. Zhao and C. Lu, "Note: Self-biased magnetic field sensor using end-bonding magnetoelectric heterostructure," *Review of Scientific Instruments,* vol. 86, p. 036101, 2015.

[25]   H. Zhang, C. Lu, C. Xu, Y. Xiao, J. Gui, C. Lin*, et al.*, "Improved magnetoelectric effect in magnetostrictive/piezoelectric composite with flux concentration effect for sensitive magnetic sensor," *AIP Advances,* vol. 5, p. 047114, 2015.

[26]   R. J. M. Vullers, R. van Schaijk, I. Doms, C. Van Hoof, and R. Mertens, "Micropower energy harvesting," *Solid-State Electronics,* vol. 53, pp. 684-693, 2009.

[27]   H. S. Kim, J. H. Kim, and J. Kim, "A review of piezoelectric energy harvesting based on vibration," *International Journal of Precision Engineering and Manufacturing,* vol. 12, pp. 1129-1141, 2011.

[28]   J. W. Matiko, N. J. Grabham, S. P. Beeby, and M. J. Tudor, "Review of the application of energy harvesting in buildings," *Measurement Science and Technology,* vol. 25, 2014.

[29]   E. Lage, C. Kirchhof, V. Hrkac, L. Kienle, R. Jahns, R. Knöchel*, et al.*, "Exchange biasing of magnetoelectric composites," *Nat Mater,* vol. 11, pp. 523-529, 06//print 2012.

[30]   D. Fritsch and C. Ederer, "First-principles calculation of magnetoelastic coefficients and magnetostriction in the spinel ferrites CoFe 2O 4 and NiFe 2O 4," *Phys. Rev. B,* vol. 86, p. 014406 2012.

[31]   P. Martins, A. Lasheras, J. Gutierrez, J. M. Barandiaran, I. Orue, and S. Lanceros-Mendez, "Optimizing piezoelectric and magnetoelectric responses on CoFe2O4/P(VDF-TrFE) nanocomposites," *J. Appl. Phys. D,* vol. 44, p. 495303, 2011.

2 Materials and methods

This chapter provides a description of the materials used in this investigation, as well as the experimental details on sample preparation. The development of the ME measurement system is also described.

2.1 Development of a magnetoelectric measurement system.

Due to the particularity of ME measurements, it was necessary to design and develop a system that would allow the reliable and reproducible ME characterization of the samples.

The developed system generates a controlled magnetic field that induces the magnetostrictive element to change dimensions, when this variation occurs, the coupled piezoelectric element also change its dimensions and generates a voltage. The voltage generated by the samples is then analyzed.

In the following, the main components of the developed set-up are described and explained.

2.1.1 Structure, dimensions and operating limits

The ME measurement system are constituted by a two pairs of Helmholtz coils, which generate the magnetic field, these coils are connected to a DC and AC current supply. The sample holder ensures the central position of the sample relatively to the coils, and links the output signal to the Lock in Amplifier.
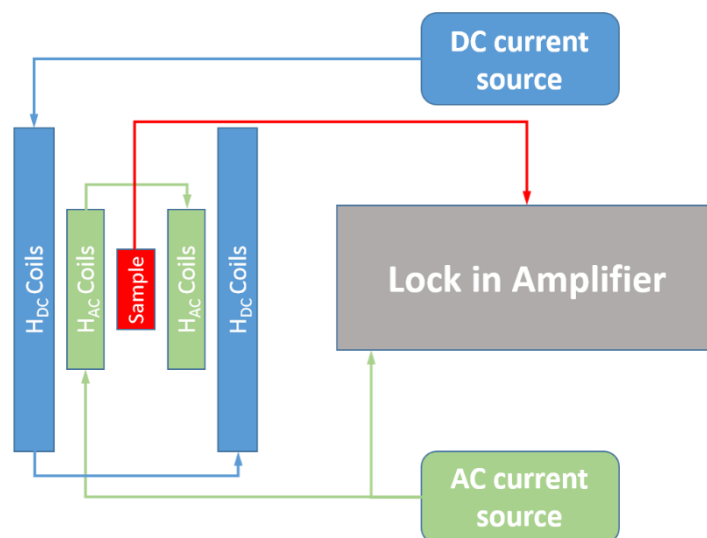
Figure 2.1 – Schematic representation of the ME measurement system.

The ME measurements are carried out by generating two magnetic fields, one AC and one DC, that are applied to the sample. Thus, the constructed structure is composed by

two pairs of Helmholtz coils, being a couple responsible for creating the DC magnetic field and the other for the AC magnetic field.
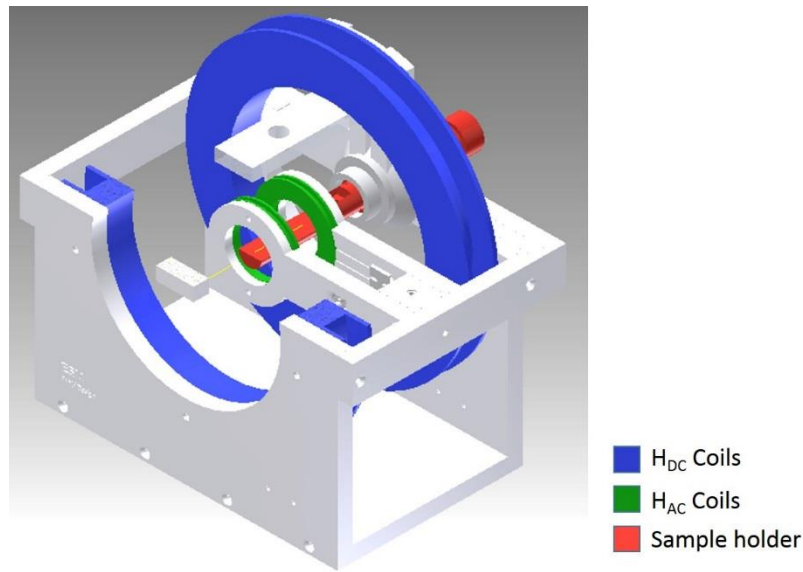
Figure 2.2 – Schematic design of the ME apparatus, constituted by two pairs of Helmholtz coils and a sample holder.

Each pair of coils is connected to two distinct current sources, an AC and a DC. Thus, AC and DC magnetic fields will be generated. The DC coils create magnetic fields in the range 0-22 Oe while the AC coils can generate magnetic fields up to 1.5 Oe with frequencies ranging from 1 mHz to 100 kHz.

The system was designed in the Autodesk Inventor software, which allowed the simulation of the form and dimensions of the system, including the dimensions of the Helmholtz coils, the size of the samples and the size of the sample holder in order to ensure that the samples were always placed at the center of the coils.

The sample holder 10x10 mm, built in nylon, was added to the structure to ensure signal optimization. The sample holder can be removed from the structure allowing to attach the ME samples safer and to achieve a more simple placement of the ME materials for testing. In order to carry out anisotropy tests on composites with different typologies, the sample holder is also allowed to vary the angle between the length of the sample and the direction of the applied magnetic fields.

2.1.2   Helmholtz coils characterization

The concept of Helmholtz coils, developed by the German physicist Hermann von Helmholtz for over a century, is used to perform compatibility and susceptibility testing in electronic devices, magnetic fields measurements, biomagnetic applications and cancellation of the Earth's magnetic field. To create a pair of Helmholtz coils it is required two coils with the same diameter, composed by one or several windings.

In the case of having several windings, these should be wound in the same direction, so that the electric signal can flow in the same direction in both coils, thus ensuring that magnetic fields are all add up.

The distance between the coils must be equal to their radius.[1, 2]

The magnetic field produced by the coils can be static or time-varying, it is perpendicular to the plane of the coils and more uniform in the center. The direction of the magnetic field is determined by the direction of the current and can be easily determined by the right hand rule. [3]

The value of the intensity of the magnetic field generated by the Helmholtz coils is determined by factors such as the current value, coil dimensions and optimal distance between them and number of spires.[1]
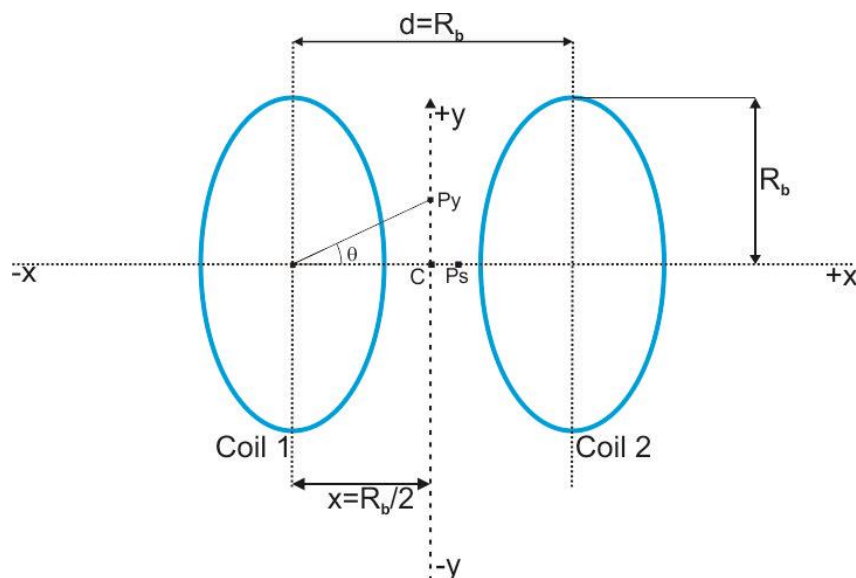
Figure 2.3 – Schematic representation and dimensions for construction of a pair of Helmholtz coils.

In order to predict the electrical and magnetic behavior of Helmholtz coils, and taking into account the magnetism law of Biot-Savart to determine the magnetic field, it is

41

possible to describe the magnetic field at any point P, in the direction of the x-axis, generated by a coil with an electric current I through the equation [4]:

$$B = \frac{1}{2} \frac{\mu_0 R_b^2}{(R_b^2 + x^2)^{3/2}} I \qquad (4)$$

Were, $\mu_0 = 4\pi \times 10^{-7} T \cdot m/A$ it is the magnetic permeability in vacuum. Considering now the magnetic field produced at the center of a coil pair, and that each coil is formed by (N) turns separated by a distance (R_b), the two coils have (N) turns each, multiplying the above equation by $(2N)$ and substituting (x) to a point at the center of the coils $(x = R_b / 2)$ it is obtained the following [4, 5] equation:

$$B = \left(\frac{4}{5}\right)^{\frac{3}{2}} \frac{\mu_0 N}{R_b} I \qquad (5)$$

Through an analyses of the equation, it can be observed that the magnitude of the magnetic field is proportional to (N) and (I) and inversely proportional to (R_b).

Measurements of the ME effect for magnetostrictive alloys used in this work (Vitrovac and Metglas) do not require high intensity DC magnetic fields (<20 Oe).

From equation 5 it is possible to calculate the coils dimensions to the desired values of magnetic field. The AC coils were constructed with a radius of 3 cm and 50 turns and DC coils with a radius of 10 cm and 240 turns. During assembly, the coils were connected in order to ensure that the current flows in the same direction in both coils. Each coil set is connected in series to ensure that current in each coil pair has the same amplitude.

In detail, the magnetic field generated by the Helmholtz coils at a distance (d) from the center of the coils can be obtained from equation 6.

$$B = \frac{v_0 NI}{2R} \left(1/\left(\left(\frac{d}{R}\right)^2 + \frac{d}{R} + \frac{5}{4} \right)^{\frac{3}{2}} + 1/\left(\left(\frac{d}{R}\right)^2 + \frac{d}{R} + \frac{5}{4} \right)^{\frac{3}{2}} \right) \qquad (6)$$

2.1.3 Current sources

Since the ME characterization of samples demands DC and AC magnetic fields, a Keithley 2400 current source was selected to supply the DC coils and a Keithley 6221 current source for the AC coils. The first allows a maximum current of 10 A and the second a maximum current of 100 mA with frequencies ranging from 1 mHz to 100 kHz.

2.1.4 Lock-in Amplifier

For the ME characterization of the composites, as mentioned before, it is needed to apply magnetic fields to the sample and to detect the output voltage signal at the terminals of the ME composite. Due to the small amplitude of the output signal and to the existence of electromagnetic noise, it a lock-in amplifier was used to amplify the signal and separate the output signal from the noise.

The lock-in amplifier (Standford Research SR844) uses a technique called phase-sensitive detection to separate the signal component in a specified phase and frequency. A lock-in amplifier can be viewed as a filter with a very low bandwidth and tuned to the signal frequency that is being measured, thus eliminating part of the noise.
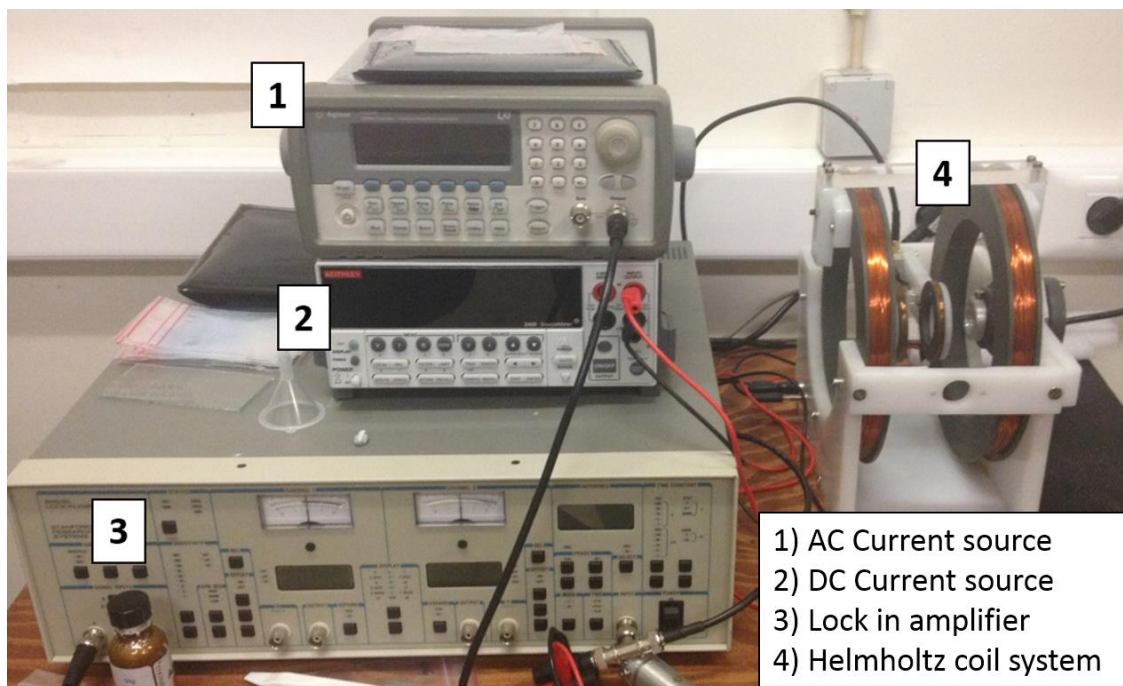
Figure 2.4 - ME measurment system

2.2 Magnetoelectric measurements

Samples were characterized in a ME system composed by two Helmholtz coils (Figure 2.1), one generating the DC magnetic field (H_{DC}) in the range 0 to 20 Oe, and another generating the AC magnetic field (H_{AC}) in the range 0 to 0.2 Oe.

In order to determine the resonance frequency of the composite, the H_{DC} and H_{AC} values were maintained constant (4.75 Oe and 0.1 Oe respectively) and the frequency was

changed from 20 kHz to 100 kHz. The DC magnetic field sensor characterization was performed by keeping the H_{AC} and frequency values constant (0.1 Oe and 48 kHz, respectively). On the other hand, AC magnetic field sensor characterization was carried out by keeping the H_{DC} and frequency values constant (4.75 Oe and 48 kHz, respectively). The voltage induced (δV) in the piezoelectric layer was measured with a lock-in-amplifier.

The ME response of the laminates was determined as:

$$\alpha_{ME} = \frac{dE}{dH} = \frac{1}{t}\left(\frac{\delta V}{\delta H_{AC}}\right) \tag{7}$$

where δH_{AC} is the applied AC magnetic field amplitude, δV is the induced magnetoelectric voltage and t is the thickness of the piezoelectric polymer.

2.3   Sample preparation

2.3.1   Optimization of the magnetoelectric response of poly(vinylidene fluoride)/epoxy/Vitrovac laminates

The following sample preparation procedure applies to the samples investigated in Chapter 3.Commercial poly(vinylidene fluoride), PVDF, with thickness of 28, 52 and 110 µm with Cu-Ni electrodes deposited on both sides was purchased from Measurement Specialties, USA, and used as the piezoelectric phase. All PVDF samples were cut into rectangular shapes with 50 mm x 10 mm size.

Vitrovac 4040® (Fe39Ni39Mo4Si6B12), 30 mm x 6 mm x 25 µm magnetostrictive ribbons were used as magnetostrictive components. With a magnetostrictive coefficient λ_{11} of 8ppm. [6]

To study the effect of each epoxy on the ME response, laminated composites were prepared by gluing the piezoelectric layer to the magnetostrictive layer with three different epoxy resins, chosen due to their distinct mechanical properties (Young Modulus given in the brackets):

- ITW Devcon 5 Minute® Epoxy (7×10^8 Pa),
- Strain Gage Adhesive M-Bond 600 - Vishay Precision Group (2.7×10^8 Pa)
- Stycast 2850 FT blue (9×10^9 Pa).

The Young Modulus of the epoxy resins was determined from the initial slope of strain–stress curves measured using a Shimadzu AG-IS universal testing machine in tensile mode, with a 2 mm min^{-1} loading rate.

Temperature dependent magnetoelectric induced voltage between room temperature and 85 ℃ was performed by introducing the whole experimental set-up (sample, exciting, detecting and bias coils) inside a climatic chamber. Each sample was tested at conditions of resonant frequency and optimized DC field, in order to obtain the maximum ME response.

2.3.2 Size effects on the magnetoelectric response on PVDF/Vitrovac 4040 laminate composites

The following sample preparation procedure applies to the samples investigated in Chapter 4.

Magnetostrictive samples from Vitrovac ($Fe_{39}Ni_{39}Mo_4Si_6B_{12}$) 4040 (25 μm thick) were cut into rectangular shapes using a clean and sharp ceramic scalpel. The rectangular samples of Vitrovac 4040 exhibit a magnetostrictive coefficient λ_{11} of 8ppm.[6]

Poled β-PVDF films 28μm thick with Cu−Ni electrodes deposited on both sides were purchased from Measurement Specialties, USA, and used as provided (d_{33} = −33 pC.N-1 and d_{31} =23 pC.N-1)[7]. All piezoelectric samples were cut into rectangular shapes using a clean and sharp scalpel. The PVDF piezoelectric response (d_{33}) was verified with a wide range d_{33}-meter (model 8000, APC Int. Ltd.) to ensure that the cutting process had no effect on the piezoelectric response of the polymer.

To study the effect of the materials size, structure and geometry on the ME response, various samples were produced as represented Figure 2.5.
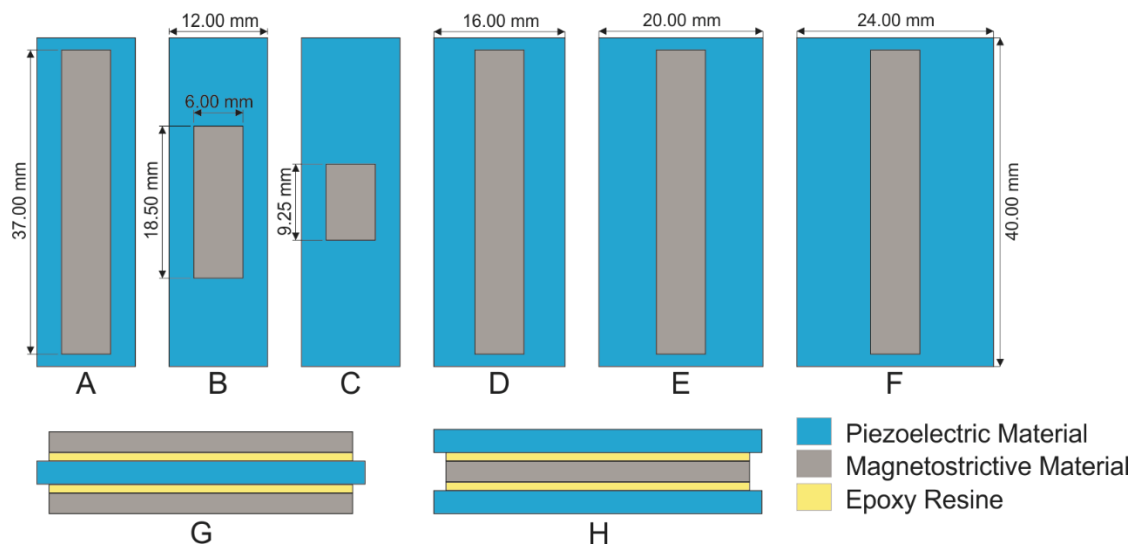
Figure 2.5 - Top view of the Vitrovac/PVDF by-layer composites produced in this study (A-F). Front view of the three-layer composites produced in this study (G-H).

In this way, in samples A-C the longitudinal size aspect ratio (LAR) between the PVDF and the Vitrovac layers was changed between 1.1 and 4.3, in the samples A, D-F the transversal size aspect ratio (TAR) between the PVDF and the Vitrovac layers was changed between 2.0 and 4.0. Samples A-F allowed also to vary the relation between 2.2 and 8.6.

$$\frac{Area_{PVDF}}{Area_{Vitrovac}}(=\frac{A_P}{A_M}) \tag{8}$$

Since the previous study demonstrated the extreme importance of the bonding layer in the ME response of ME laminates [8], special care was taken in the bonding process with the M-Bond epoxy in order to ensure a reproducible bonding and that the inner structure of the interface is the same in all the samples. In this way, it is guaranteed that all the differences in the ME response of the samples is due to the distinct configurations and phase sizes and not a result of heterogeneities induded in the bonding process.

2.3.3 Characterization of Metglas/ Poly(vinylidene fluoride)/ Metglas magnetoelectric laminates for AC/DC magnetic sensor applications

The following sample preparation procedure applies to the samples investigated in Chapter 5. Polymer-based ME laminates were produced by gluing two equal amorphous magnetostrictive ribbons of Metglas with a Devcon 5 minute epoxy (0.7 GPa Young Modulus) to both sides of a commercial poled β-PVDF film (Measurement Specialties, USA) in a (magnetostrictive-piezoelectric-magnetostrictive) MPM configuration, following the optimized conditions presented in subchapter 2.1 [8-10]

The magnetostrictive ribbons (30 mm x 2 mm x 25 μm) were magnetized along the longitudinal direction (magnetostrictive coefficient λ_{11}=25 ppm) and the piezoelectric layer (30 mm x 3 mm x 52 μm) was poled along the thickness direction (piezoelectric coefficient $d_{33} = -33$ pC.N^{-1}).

The voltage induced in the PVDF layer was measured with a lock-in-amplifier (Standford Research SR844).as described in subchapter 2.2
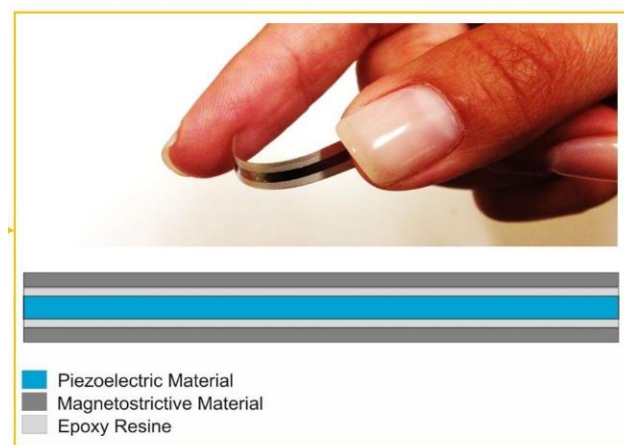
Figure 2.6 - Detail of the ME laminated sample.

2.3.4 Development of an energy harvesting system with optimized circuit design.

The following sample preparation procedure applies to the samples investigated in Chapter 6. For the ME characterization of the composites, the laminates were placed at the centre of Helmholtz coils (Figure 2.7a). The external coils generated the DC magnetic field (H_{DC} 0-20 Oe) and the internal ones generated the AC magnetic field (H_{AC} 0-0.4 Oe). Both magnetic fields were parallel and superimposed to each other.
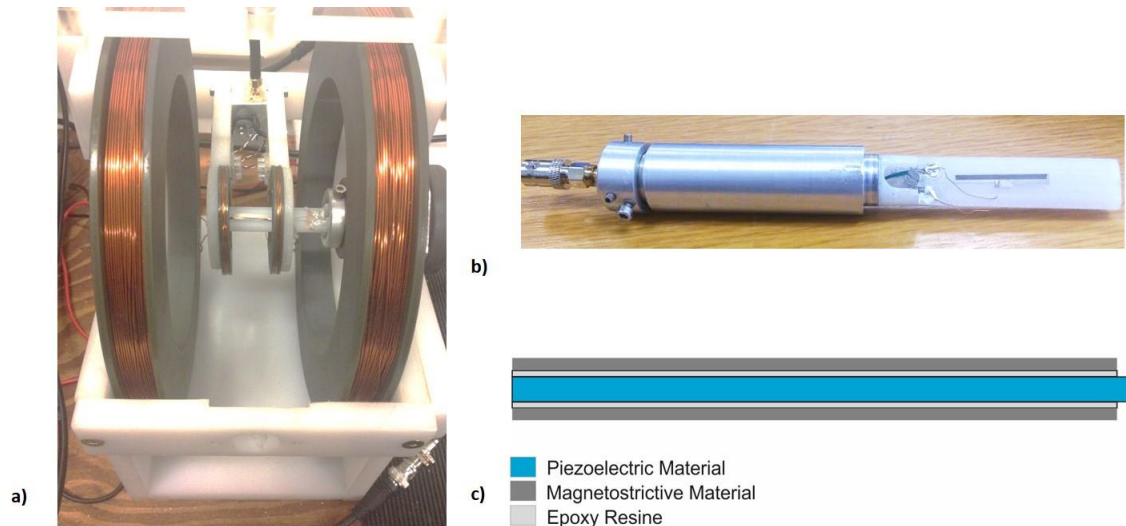
Figure 2.7 - . a) Detail of the ME measurement set-up; b) Home-made ME sample holder; c) Schematic representation of the ME composite produced with one piezoelectric layer and two magnetostrictive layers bonded together with an epoxy resin (MPM configuration).

A home-made sample holder (Figure 2.7b) was used for the measurement of the ME response of the laminates (Figure 2.7c) fabricated by using two equal amorphous magnetostrictive ribbons of Metglas (30 mm $\times$ 5mm $\times$ 0.020 mm) magnetized along the longitudinal direction (magnetostrictive coefficient λ_{11}=30 ppm) bonded with a Devcon 5 minute epoxy (0.7 GPa Young Modulus) to both sides of a piezoelectric layer (30 mm x 5 mm x 52 μm) poled along the thickness direction (piezoelectric coefficient $d_{33} = -33$ pC.N^{-1}) and purchased from Measurement Specialties, USA. A detailed description of the fabrication process is given in chapter 2.1[9]. The ME voltage generated by the composite was then harvested by the collecting circuits.

.

2.4 References

[1] C. F. de Melo, R. L. Araújo, L. M. Ardjomand, N. S. Ramos Quoirin, M. Ikeda, and A. A. Costa, "Calibration of low frequency magnetic field meters using a Helmholtz coil," *Measurement,* vol. 42, pp. 1330-1334, 11// 2009.

[2] J. H. Parry, "Helmholtz Coils and Coil Design," in *Developments in Solid Earth Geophysics*. vol. Volume 3, K. M. C. D.W. Collinson and R. S.K, Eds., ed: Elsevier, 2013, pp. 551-567.

[3] A. Yousaf, F. A. Khan, and L. M. Reindl, "Passive Wireless Sensing of Micro coil parameters in fluidic environments," *Sensors and Actuators A: Physical,* vol. 186, pp. 69-79, 10// 2012.

[4] M. A. Gijs, F. d. r. Lacharme, and U. Lehmann, "Microfluidic applications of magnetic particles for biological analysis and catalysis," *Chemical reviews,* vol. 110, pp. 1518-1563, 2009.

[5] R. P. R. Caldeira, "Controlling superparamagnetic particles with dynamic magnetic fields generated by a Helmholtz-coil system," 2010.

[6] J. Gutiérrez, A. Lasheras, J. M. Barandiarán, J. L. Vilas, A. Maceiras, and L. M. León, "Improving the performance of high temperature piezopolymers for magnetoelectric applications," in *Key Engineering Materials* vol. 543, ed, 2013, pp. 439-442.

[7] P. Martins, A. C. Lopes, and S. Lanceros-Mendez, "Electroactive Phases of Poly(vinylidene fluoride): Determination, Processing and Applications," *Prog. Polym. Sci.,* vol. 39, pp. 683-706, 2013.

[8] M. Silva, S. Reis, C. S. Lehmann, P. Martins, S. Lanceros-Mendez, A. Lasheras*, et al.*, "Optimization of the Magnetoelectric Response of Poly(vinylidene fluoride)/Epoxy/Vitrovac Laminates.," *ACS Appl. Mater. Interfaces,* vol. 5, pp. 10912-9, 2013.

[9] A. Lasheras, J. Gutiérrez, S. Reis, D. Sousa, M. Silva, P. Martins*, et al.*, "Energy harvesting device based on a metallic glass/PVDF magnetoelectric laminated composite," *Smart Materials and Structures,* vol. 24, 2015.

[10] M. P. Silva, P. Martins, A. Lasheras, J. Gutiérrez, J. M. Barandiarán, and S. Lanceros-Mendez, "Size effects on the magnetoelectric response on PVDF/Vitrovac 4040 laminate composites," *Journal of Magnetism and Magnetic Materials,* vol. 377, pp. 29-33, 2015.
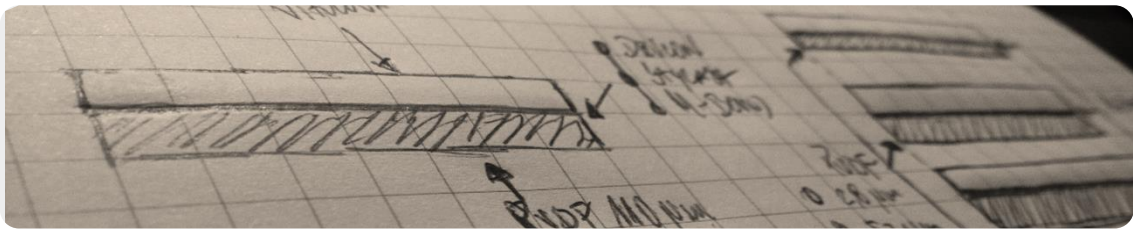
3 Bonding and thickness optimization

This chapter is based on the following publication:

Silva M, Reis S, Lehmann C S, Martins P, Lanceros-Mendez S, Lasheras A, Gutiérrez J and Barandiarán J M 2013 *Optimization of the Magnetoelectric Response of Poly(vinylidene fluoride)/Epoxy/Vitrovac Laminates*. ACS Appl. Mater. Interfaces 5 10912–9

.

3.1 Introduction

Magnetoelectric (ME) materials are being increasingly investigated [1] due to their potential applications as sensors, actuators, energy harvesting devices, memories, transformers, filters, resonators and phase shifters, among others [1-4].

The main characteristic of ME materials is the variation of the electrical polarization (P) in the presence of an applied magnetic field (H);

$$\Delta P = \alpha \Delta H \tag{9}$$

and the variation of the induced magnetization (M) in the presence of an applied electrical field (E):

$$\Delta M = \alpha \Delta E \tag{10}$$

Where α is the E coupling coefficient [3, 5-7] In this way, through the ME effect it can be achieved the cross-correlation between the magnetic and the electric orders of matter.

In multiferroic (MF) single-phase materials this effect is intrinsic and attributed to the coupling of magnetic moments and electric dipoles [3, 5, 6]. Nevertheless, single-phase ME materials, so far, exhibit low Curie temperatures and show weak ME coupling at room temperature, hindering in this way their incorporation in technological applications [7, 8].

In multiple-phase ME materials this effect is extrinsic, emerging in an indirect form, through an elastic mediated coupling between a piezoelectric phase and a magnetostrictive phase [2, 3, 9].

Three main types of non-polymer based ME composites are found in the literature [2, 3]: i) particulate composites of ferrites and piezoelectric ceramics (e.g. lead zirconate titanate (PZT)) [7, 10-12]; ii) laminate composites of ferrites and piezoelectric ceramics [13-15] and iii) laminate composites of magnetic metals/alloys (e.g. Terfenol-D or Metglas) and piezoelectric ceramics [16-19]. The above mentioned composites are thus based on piezoelectric ceramics, being therefore dense and brittle and can lead to fatigue and failure during operation. Moreover those materials have low electrical resistivity and high dielectric losses which can hinder specific applications [20, 21]. The use of piezoelectric polymers, such as poly(vinylidene fluoride), PVDF, and its copolymers can solve some of the problems, found in ceramic composites, since they are flexible, show

large electrical resistivity, small losses and can be easily fabricated by large and small scale low-temperature processing methods into a variety of forms [21-23].

Regarding polymer-based ME materials, three main types of composites can be found in the literature: i) nanocomposites, ii) polymer "as a binder", and iii) laminated composites [4]. Laminated polymer-based ME materials are those with the highest ME response. In particular Fang *et al* [24] reported a magnetoelectric voltage coefficient of 21.46 V.cm^{-1}·Oe^{-1} for a laminate comprising PVDF, Metglas 2605SA1 and Devcon epoxy. Such value was achieved at non-resonance frequencies by taking advantage of the flux concentration effect and is, so far, the highest response among this kind of materials at non-resonance frequencies. At the longitudinal electromechanical resonance, Jin *et al* [25] reported a magnetoelectric voltage coefficient of 383 V.cm^{-1}·Oe^{-1} on cross-linked P(VDF-TrFE)/ Metglas 2605SA1 bonded with an epoxy resin, the highest value reported up to date.

Despite those high values of ME response on polymer based ME laminates, proper description, characterization and optimization of both piezoelectric and magnetostrictive phases, the optimization of the element responsible for the coupling between the phases (usually an epoxy) remains poorly studied [26, 27].

Trying to solve this limitation, in this work, PVDF was bonded to Vitrovac with three epoxys with different elastic modulus in order to study their effect on the ME response.

Vitrovac 4040 was used as magnetostrictive component not for its magnetostriction value (λ=8 ppm), actually modest, but for its high piezomagnetic coefficient (1,3 ppm/Oe) at low magnetic fields ($\approx$15 Oe), and low cost[28]. PVDF was chosen as piezoelectric component since it exhibits the highest piezoelectric response among polymers [23, 29].

In order to theoretically evaluate the experimental results, a Finite Element Method (FEM) based simulation was also performed. Up to date, a wide amount of theoretical approaches have been used to determine the ME response of piezoelectric/magnetoestrictive composites, namely the Green's function technique [30-32], the finite element method [27, 33], the constitutive equations [34] and the effective medium approximation [35]. Nevertheless, considering that both magnetostrictive and piezoelectric behaviors are anisotropic, thus implying that the product effect must be anisotropic and taking into account that in the ME structure reported in this work both layers are separated by an epoxy bonding layer that incorporates specific mechanical

coupling factors into the final ME response, the approach that best fits the evaluation of the macroscopic experimental response is the FEM.

In this way, the ME response of the ME structure was studied as a function of the PVDF thickness and the epoxy properties and the results were theoretically evaluated with final goal to optimize such materials for applications in innovative technological applications such as magnetic sensors (Figure 3.1).
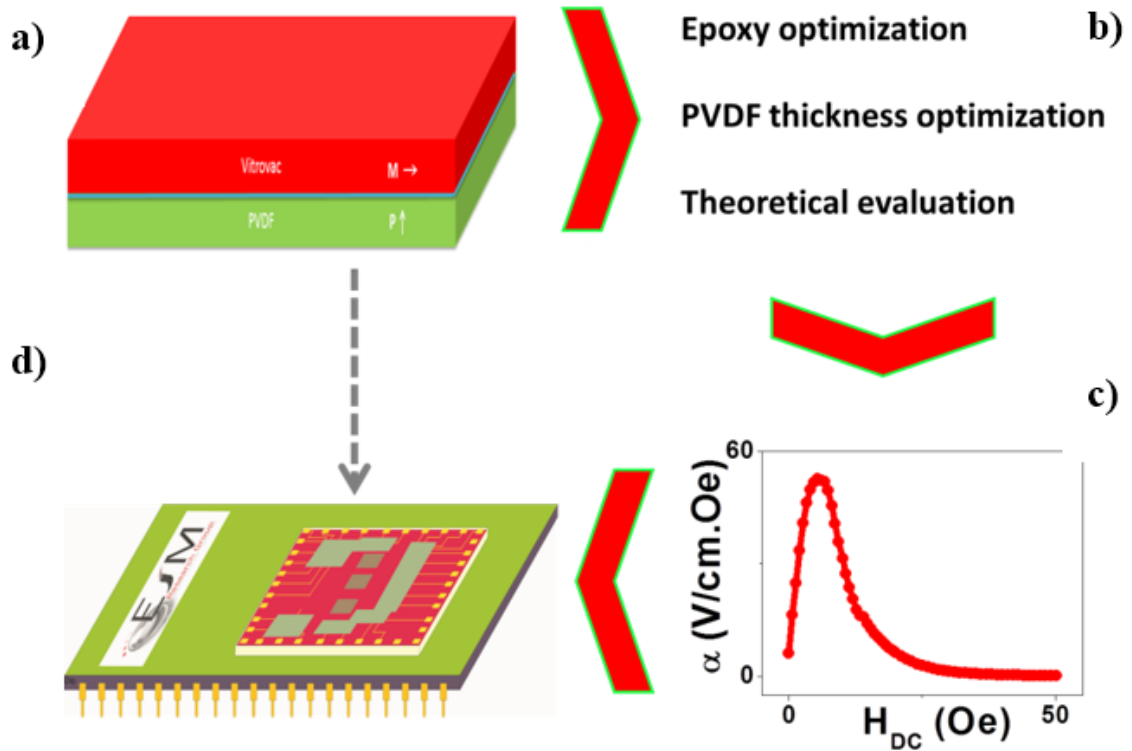
Figure 3.1. Schematic representation of the Vitrovac/Epoxy/PVDF composite (a) and its ME response (c) after optimization (b) that pave the way for its incorporation into technological applications such as magnetic sensors (d).

3.1.1 Theoretical analysis by Finite Element Method

Assuming the linear range of magnetostriction, the electro-mechanical coupling of the 3-layer (piezoelectric+epoxy+magnetostrictive) ME structure –Figure 3.1a- was modeled by Finite Element Method (FEM) in order to obtain the theoretical ME response. A 2D approximation has been considered by establishing the ME response to be constant along the width of the structure. The model additionally considers the ME structure as composed by three flexible films -magnetostrictive layer of Vitrovac, epoxy layer and piezoelectric layer of PVDF- properly glued to each other with an appropriate coupling between the structural and electrical fields. This coupling is fulfilled by the continuity equations on the stationary case, given by:

$$\nabla \cdot D = \rho_V \text{ (Gauss Law, t=0)} \tag{11}$$
$$\nabla \cdot \sigma = f_V \quad \text{(Cauchy Momentum Equation, t=0)} \tag{12}$$

Here "$\nabla \cdot$" represents the divergence, D the electrical displacement field, ρ_v, the free electric charge density, σ, the stress tensor and f_v the force per unit volume.

The constitutive equations for the fully coupled piezoelectric material consist on the direct and indirect piezoelectric effects and are given by [36]

$$T = c_E S - e^T E \tag{13}$$
$$D_A = e_S + \varepsilon_S E \tag{14}$$

where T is the mechanical stress matrix, S the mechanical strain matrix, E the electric field vector and D_A the electric charge vector per unit area.

A coupling coefficient (k) was included to represent the coupling between the epoxy and both Vitrovac and PVDF layers. Such coefficient was set to be between 0 (not coupled) and 1 (ideal coupling).

The input parameter for the calculations will be S=λ(H), which is the magnetically induced magnetostrictive strain in the Vitrovac 4040 constituent.

The material properties of the poled piezoelectric PVDF polymer are described by the mechanical stiffness matrix at constant electric field c_E, the permittivity matrix under constant strain ε_S, and the piezoelectric stress matrix e_S. These properties are shown in Table 1.

Table 3.1 - Material properties of the piezoelectric PVDF polymer [37, 38].

Property	Value
Density (ρ)	1780 kg/m^3
Elasticity matrix, $\mathbf{c}_E$ (Pa)	(xx, yy, zz, yz, xz, xy) $\{\{2.74 \times 10^{09}, 5.21 \times 10^{09}, 4.78 \times 10^{09}, 0, 0, 0\},$ $\{5.21 \times 10^{09}, 2.36 \times 10^{09}, 5.21 \times 10^{09}, 0, 0, 0\},$ $\{4.78 \times 10^{09}, 5.21 \times 10^{09}, 2.12 \times 10^{09}, 0, 0, 0\},$ $\{0, 0, 0, 2.74 \times 10^{09}, 0, 0\},$ $\{0, 0, 0, 0, 2.74 \times 10^{09}, 0\},$ $\{0, 0, 0, 0, 0, 2.74 \times 10^{09}\}\}$
Compliance matrix, $\mathbf{c}_E^{-1}$ (Pa^{-1})	(xx, yy, zz, yz, xz, xy) $\{3.65 \times 10^{-10}, -1.92 \times 10^{-10}, 4.24 \times 10^{-10}, -2.09 \times 10^{-10}, -1.92 \times 10^{-10}, 4.72 \times 10^{-10}, 0, 0, 0, 3.65 \times 10^{-10}, 0, 0, 0, 0, 3.65 \times 10^{-10}, 0, 0, 0, 0, 0, 3.65 \times 10^{-10}\}$
Coupling matrix, $\mathbf{e}$ (C·m^{-1})	(xx, yy, zz, yz, xz, xy) $\{\{0, 0, -4.761, 0, 0, -33.33\},$ $\{0, 0, 3.703, 0, 1.703, 0\},$ $\{1.703, 0, 0, 0, 0, 0\}\}$
Relative permittivity, (ε_S)	$\{\{13, 0, 0\},$ $\{0, 13, 0\},$ $\{0, 0, 13\}\}$

The three layers forming the ME structure are represented in Figure 3.1a together with the polarization and magnetization directions. The size of the ME structure was set to be 30 mm x 10 mm. The thickness of the magnetostrictive layer was fixed to 25 μm and its mechanical properties are shown in Table 2. The experimental cases of piezoelectric layer thickness of 28 μm, 52 μm and 110 μm are studied taken a constant epoxy thickness of 12 μm (determined by scanning electron microscopy (SEM) microscopy).

Table 3.2 - Mechanical properties of Vitrovac 4040.

Property	Value	Unit
Density (ρ)	7900	kg/m^3
Poisson´s Ratio (v)	0.27	-
Young´s Modulus (Y)	1500	MPa

The theoretical evaluation consisted in applying a deformation on the two lateral ends of the magnetostrictive layer consistent with the magnetostrictive response of the material [39, 40] and evaluating the electrical potential obtained across the piezoelectric layer. The applied deformation of the magnetostrictive Vitrovac 4040 will be obtained from the Magnetic Field-Magnetostriction curve of the material [39]. It will be chosen in all cases as the strain corresponding to the maximum deformation experienced by the magnetostrictive layer. Structurally, when the three layers are perfectly bonded, the deformation on the magnetostrictive layer will produce a deformation on the other 2 layers, which will depend on their mechanical properties. The electrical ground was set at the outer surface of the piezoelectric layer, locating also a compliant electrode between the piezoelectric and the bonding layer. The ME structure is set to deform only along the longitudinal direction.

The influence of the bonding layer Young Modulus on the ME performance of the structure was thus simulated together with the ME response of the laminate with varying piezoelectric and bonding layer thickness, in order to optimize the ME response of the fabricated multilayer structures.

3.2 Results and discussion

In this chapter Vitrovac was used as magnetostrictive layer, and PVDF as piezoelectric layer. The bounding layer were composed by three different epoxy resins, M-Bond, Stycast and Devcon. Sample preparation and specifications are described in subchapter 2.3.1.

Figure 3.2 shows the ME response of laminate composites of 110 μm thick PVDF films bonded with Devcon, M-Bond and Stycast to Vitrovac magnetostrictive substrates.
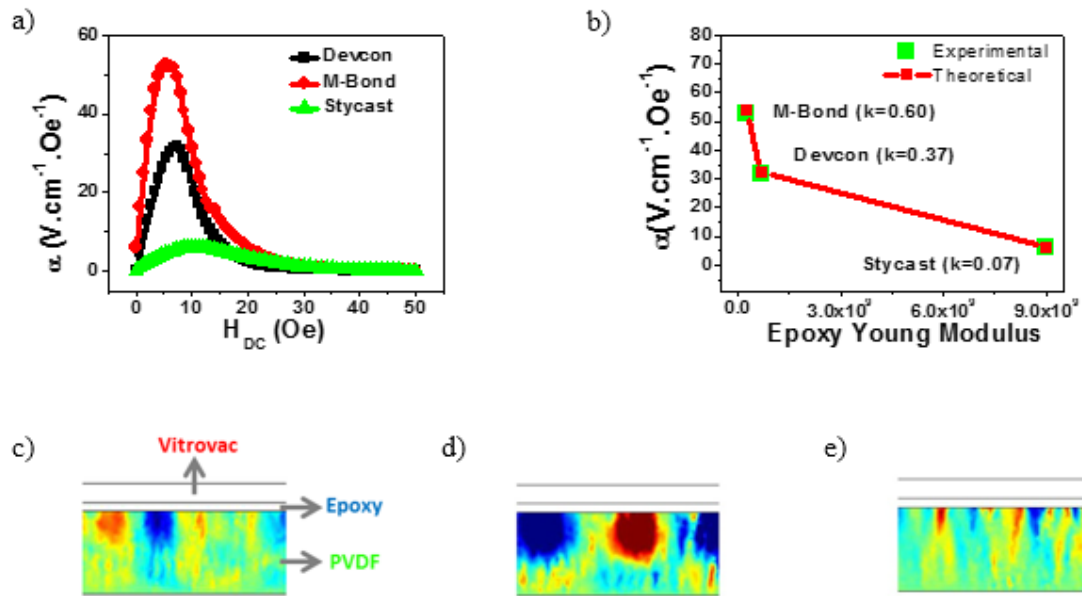
Figure 3.2 - a) Magnetoelectric response, α, at resonance obtained for the PVDF/epoxy/Vitrovac composites for a 110 μm PVDF layer and different epoxy binders; b) Relation between α and the epoxy Young Modulus. Images from the numerical simulation of the ME effect

The obtained results reveal the strong influence of the epoxy layer on the ME response of the composite.

The highest ME response has been obtained for the M-Bond bonded composites, the epoxy with the lowest Young modulus; on the contrary, the lowest response is obtained for Stycast bonded composites, which is the epoxy with the highest Young Modulus and lower k value used [26, 27, 41]. It is observed that with higher Young Modulus the epoxy loses its ability to transmit the deformation from the magnetostrictive layer to the piezoelectric layer due to the increased rigidity, leading to a decreasing in the coupling factor from 0.6 to 0.07 , revealing so an interface detachment between the active layers and the epoxy layer. Further, the highest ME response is obtained at the lowest applied H_{DC} filed by using M-Bond; in correspondence, Stycast shows the lowest ME response at the highest applied H_{DC} field. Devcon containing composites show an

intermediate behavior. This relationship between the ME response and the Young Modulus shows the relevance of the later parameter for the fabrication of devices and indicates the best choice for ME performance optimization. These results are supported by the simulations as the images obtained by FEM (Figure 3.2c, d and e) show a more intense red and blue colors, indicating higher induced voltage values and so higher ME response, for the M-Bond bonded laminates.

As the M-Bond bonded laminates show the highest ME response, this epoxy was used in the study of the effect of the thickness of the PVDF layer on the ME response of PVDF/M-Bond/Vitrovac laminates.

PVDF layers with 28, 52 and 110 μm were used and it was evaluated, both experimentally and through theoretical FEM simulations, the effect of the piezoelectric layer thicknesses on the ME response of the composites. Figure 3.3a shows the ME coefficient as a function of the DC applied field and Figure 3.3b the comparison of experimentally and theoretically obtained values of the ME coefficient for the different piezoelectric layer thickness.
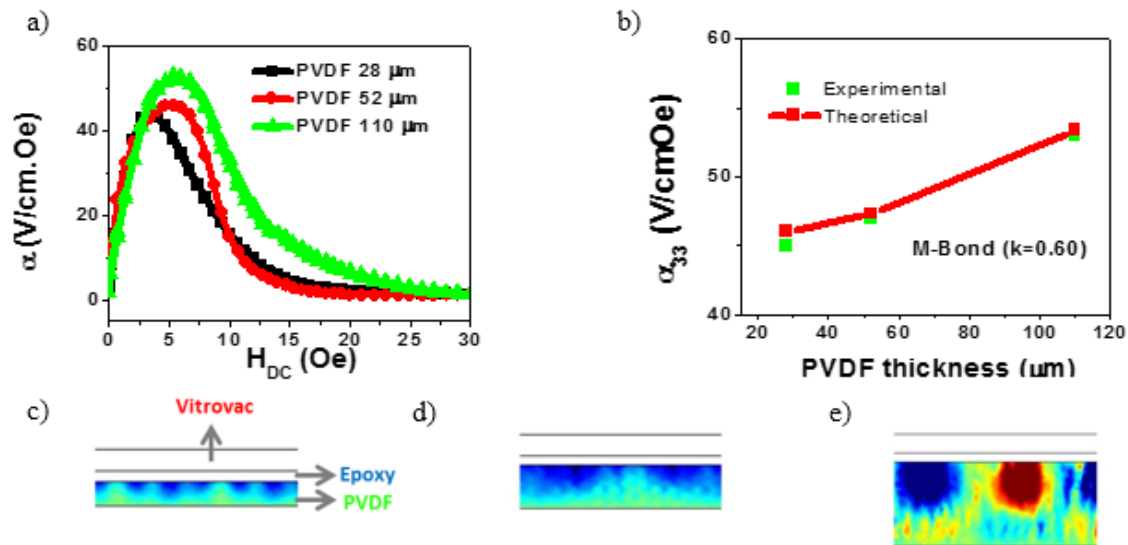
Figure 3.3 - a) Magnetoelectric coefficient, α, measured at the resonance frequency as a function of the DC magnetic field for piezoelectric layer of different thickness and b) comparison between the experimental and theoretical results. Images from the FEM simula

As previously reported, Figure 3.3 shows that the ME response of PVDF based ME laminated composites increases with increasing thickness of PVDF layer [42]. Nevertheless, an increase of 300% in the thickness of PVDF (from 28μm to 110μm) has, as a consequence, just an increase of 20% in the ME response (from 45 V.cm^{-1}.Oe^{-1} to 53 V.cm^{-1}.Oe^{-1}).

In the images obtained by the FEM simulations (Figure 3.3 c, d and e) it can be observed that the intensity of the red and blue colors increases with increasing thickness of PVDF. With increasing the PVDF layer thickness a larger number of dielectric moments suffer variation under the applied stress, resulting in a higher ME response [41]. However it should be noted that it must exist a maximum value for the PVDF thickness at which the ME response is maximized as a larger thicknesses will lead to inhomogeneous deformations of the material, with more deformation at the boundary layer with the binder and lower deformation at the down side, thus decreasing its ME response [41], as shown in the simulation represented in Figure 3.4.
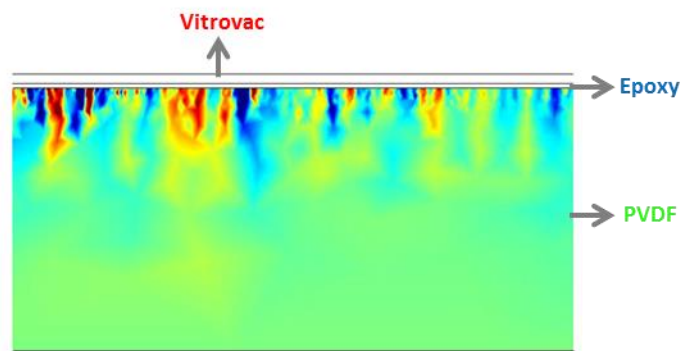
Figure 3.4 - Numerical simulation of a thick PVDF layer (750 µm) bonded to a Vitrovac layer with M-Bond epoxy (12 µm).

Figure 3.4 shows that for a very thick layer of PVDF (750 µm) the deformation generated by Vitrovac is only transmitted to a volume fraction of the PVDF layer close to the epoxy layer, causing the observed decrease of the magnitude of the ME effect.

Another important parameter for practical applications is the thermal stability of the device. Figure 3.5 shows the variation of the ME response with temperature in the temperature range 20-85 °C for a PVDF 110µm/M-Bond/Vitrovac laminate. The maximum temperature of 85 ºC was chosen as around that temperature, PVDF undergoes the α-relaxation leading to strong shrinking of the material [43].
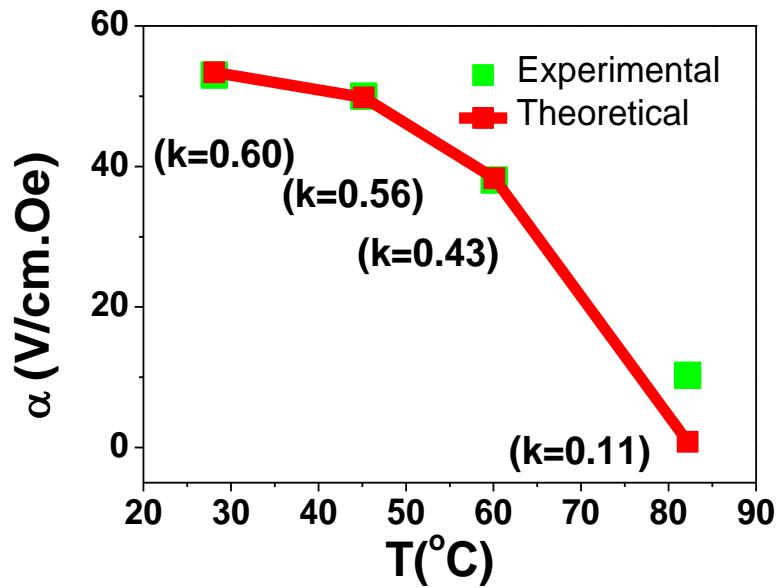
Figure 3.5 - Temperature dependence of the magnetoelectric coefficient, α, measured at the resonance frequency for the composites PVDF (110μm)/M-Bond/Vitrovac.

As previously reported [28] the ME response of PVDF based materials decreases with increasing temperature. This decrease is not mainly explained by the depoling effects (related to increased molecular mobility with increasing temperature) which leads to a decreased piezoelectric response, since it is reported just a decrease of 20% in the PVDF piezoelectric coefficient when the temperature increases until 100ºC [44]. Figure 3.5 demonstrates a decrease of more than 80% in the ME response of the laminate which is related with a decrease of the coupling, defined as k, between the epoxy and the active layers of the laminate. The coupling factor k varies from 0.6 at room temperature to 0.11 at 80 ºC, and reflects a weaker coupling between the layers due to a softening of the materials leading to a smaller k. Results on Figure 3.2 suggest that softer materials possess higher k value. In this way, the k values decrease revealed in Figure 3.5 should be related with the temperature dependent deformations that lead to interface detachment (due to the different thermal expansion coefficients of the material) and therefore reduced transduction capability.

Despite the temperature effect on the ME response, the ME coupling coefficient still remains at suitable values up to temperatures of 80 ºC, which allows widespread use for sensor and actuator applications. In a similar way, it has been reported that PVDF still retains stable piezoelectric response after temperature annealing at 140 ºC, with a value of ~ -4 pC/N, which is still high for polymer systems [44], making this polymer an

appropriate choice for the development of the flexible, low cost and easy shaping ME materials with large potential for device fabrication [4].

Finally, the ME response of the laminates was theoretically optimized regarding the epoxy properties (Young Modulus and thickness) and the thickness of the PVDF piezoelectric layer (Figure 3.6).
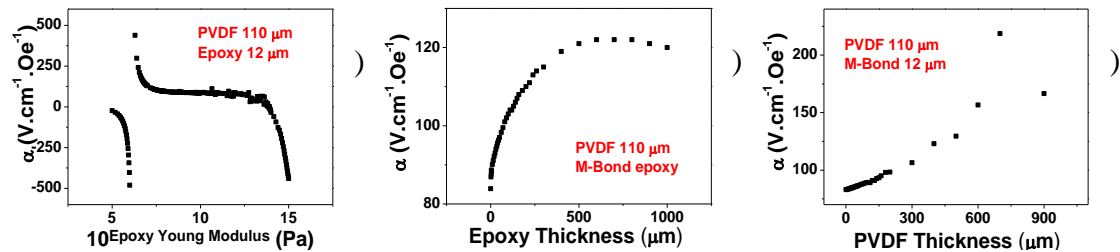
Figure 3.6 - Theoretical ME response as a function of a) epoxy Young modulus; b) epoxy thickness and c) PVDF layer thickness.

Figure 3.6a reveals that at the 10^6 Pa Young Modulus value occurs an abrupt change in the epoxy behavior. For lower values the epoxy behaves as a rubber, stretching in the vicinity of the magnetostrictive material and cringing in the vicinity of the PVDF layer. For higher values of the Young Modulus, the epoxy loses its ability to transmit the deformation from the magnetostrictive layer to the piezoelectric layer due to the increased rigidity, having as a consequence a decrease in the ME response.

Increasing the epoxy thickness leads to an increase of the ME voltage coefficient explained by a better coupling between the epoxy layer and the other two layers, as represented on Figure 3.6b. From a certain value of epoxy thickness, the glue loses the ability to transmit the deformation between the layers, the decrease being is explained by the high distance between the layer in which the deformation occurs (Vitrovac) and the layer on which the deformation has to be transmitted (PVDF), as a consequence part of the deformation is damped along the thick epoxy layer. Thicker epoxy layers will also limit the ME response due to low mechanical strength and contributes towards increasing noise level and aging [45].

Figure 3.6c shows an increased ME as a response to the increase of the PVDF layer thickness until it reaches the value of 700 μm.

As previously mentioned, increasing the PVDF layer thickness gives as a first consequence that a larger number of dielectric moments will suffer variation under the applied stress, resulting in a higher ME response [41], nevertheless above 700 μm thick layers, inhomogeneous deformations of the material will be obtained, with larger

62

deformations at the boundary layer with the binder and lower deformation far from that layer, thus decreasing the ME response [41].

3.3 Conclusions

The effect of the bonding layer type and piezoelectric layer thickness on the ME response of layered poly(vinylidene fluoride) (PVDF)/epoxy/Vitrovac composites is reported. The materials have been experimentally and theoretically studied through FEM model, including the magnetoelastic and piezoelectric laws. It is verified an increase of the ME voltage coefficient from 45 $V.cm^{-1}.Oe^{-1}$ to 53 $V.cm^{-1}.Oe^{-1}$ with increasing PVDF thickness from 28 μm to 110 μm and a reduction of the ME voltage coefficient from 53 $V.cm^{-1}.Oe^{-1}$ to 6 $V.cm^{-1}.Oe^{-1}$ with increasing Young Modulus from 9.0×10^9 Pa to 2.7×10^8 Pa.

The k value, indicative of the quality of the bonding between the active layers and the epoxy layer is the highest for the M-Bond laminates (0.60) and lowest for the Stycast laminates (0.07). Stycast laminates exhibits an intermediate behaviour. Also regarding the k values, it is found that it decreases with increasing temperatures due to interface detachment and leading to reduced transduction.

Good agreement between the FEM model and the experimental results were obtained for PVDF/epoxy/Vitrovac tri-layer composites allowing the model to be used for optimizing the epoxy properties (Young modulus and thickness) and the thickness of PVDF in order to obtain the highest ME coupling on the laminates.

The highest ME response of 53 $V.cm^{-1}.Oe^{-1}$ obtained for a PVDF (100μm thick)/M-Bond epoxy/Vitrovac laminate as well as the possibility to optimize such value taking into account the Young Modulus and thickness of the epoxy and the the PVDF thickness, make this laminate an excellent candidate to be used in applications such as sensors, actuators, energy harvesting devices and memories.

3.4   References

[1]   M. Fiebig, "Revival of the magnetoelectric effect," *Journal of Physics D: Applied Physics,* vol. 38, pp. R123-R152, 2005.

[2]   C. W. Nan, M. I. Bichurin, S. Dong, D. Viehland, and G. Srinivasan, "Multiferroic magnetoelectric composites: Historical perspective, status, and future directions," *Journal of Applied Physics,* vol. 103, 2008.

[3]   J. Ma, J. Hu, Z. Li, and C.-W. Nan, "Recent Progress in Multiferroic Magnetoelectric Composites: from Bulk to Thin Films," *Advanced Materials,* vol. 23, pp. 1062-1087, Mar 4 2011.

[4]   P. Martins and S. Lanceros-Méndez, "Polymer-Based Magnetoelectric Materials," *Advanced Functional Materials,* pp. n/a-n/a, 2013.

[5]   W. Prellier, M. P. Singh, and P. Murugavel, "The single-phase multiferroic oxides: From bulk to thin film," *Journal of Physics Condensed Matter,* vol. 17, pp. R803-R832, 2005.

[6]   G. Lawes and G. Srinivasan, "Introduction to magnetoelectric coupling and multiferroic films," *Journal of Physics D: Applied Physics,* vol. 44, 2011.

[7]   D. R. Patil, A. D. Sheikh, C. A. Watve, and B. K. Chougule, "Magnetoelectric properties of ME particulate composites," *Journal of Materials Science,* vol. 43, pp. 2708-2712, 2008.

[8]   P. Martins, C. M. Costa, and S. Lanceros-Mendez, "Nucleation of electroactive β-phase poly(vinilidene fluoride) with CoFe2O4 and NiFe2O4 nanofillers: A new method for the preparation of multiferroic nanocomposites," *Applied Physics A: Materials Science and Processing,* vol. 103, pp. 233-237, 2011.

[9]   S. Priya, R. Islam, S. Dong, and D. Viehland, "Recent advancements in magnetoelectric particulate and laminate composites," *Journal of Electroceramics,* vol. 19, pp. 147-164, 2007.

[10]   J. Ryu, A. V. Carazo, K. Uchino, and H. E. Kim, "Piezoelectric and magnetoelectric properties of lead zirconate titanate/Ni-ferrite particulate composites," *Journal of Electroceramics,* vol. 7, pp. 17-24, 2001.

[11]   J. Zhai, N. Cai, Z. Shi, Y. Lin, and C. W. Nan, "Magnetic-dielectric properties of NiFe2O4/PZT particulate composites," *Journal of Physics D: Applied Physics,* vol. 37, pp. 823-827, 2004.

[12]   R. A. Islam and S. Priya, "Effect of piezoelectric grain size on magnetoelectric coefficient of Pb(Zr0.52Ti0.48)O3-Ni0.8Zn 0.2Fe2O4 particulate composites," *Journal of Materials Science,* vol. 43, pp. 3560-3568, 2008.

[13]   G. Srinivasan, E. T. Rasmussen, J. Gallegos, R. Srinivasan, Y. I. Bokhan, and V. M. Laletin, "Magnetoelectric bilayer and multilayer structures of magnetostrictive

and piezoelectric oxides," *Physical Review B - Condensed Matter and Materials Physics,* vol. 64, pp. 2144081-2144086, 2001.

[14]   G. Srinivasan, E. T. Rasmussen, and R. Hayes, "Magnetoelectric effects in ferrite-lead zirconate titanate layered composites: The influence of zinc substitution in ferrites," *Physical Review B - Condensed Matter and Materials Physics,* vol. 67, pp. 144181-1441810, 2003.

[15]   R. A. Islam, Y. Ni, A. G. Khachaturyan, and S. Priya, "Giant magnetoelectric effect in sintered multilayered composite structures," *Journal of Applied Physics,* vol. 104, 2008.

[16]   J. Ryu, S. Priya, K. Uchino, and H. E. Kim, "Magnetoelectric effect in composites of magnetostrictive and piezoelectric materials," *Journal of Electroceramics,* vol. 8, pp. 107-119, 2002.

[17]   S. Dong, J. F. Li, and D. Viehland, "Characterization of magnetoelectric laminate composites operated in longitudinal-transverse and transverse-transverse modes," *Journal of Applied Physics,* vol. 95, pp. 2625-2630, 2004.

[18]   S. Dong, J. Zhai, F. Bai, J. Li, D. Viehland, and T. A. Lograsso, "Magnetostrictive and magnetoelectric behavior of Fe-20 at. % Ga/Pb(Zr,Ti)O 3 laminates," *Journal of Applied Physics,* vol. 97, 2005.

[19]   Y. Jia, H. Luo, X. Zhao, and F. Wang, "Giant magnetoelectric response from a piezoelectric/magnetostrictive laminated composite combined with a piezoelectric transformer," *Advanced Materials,* vol. 20, pp. 4776-4779, 2008.

[20]   S. Jiansirisomboon, K. Songsiri, A. Watcharapasorn, and T. Tunkasiri, "Mechanical properties and crack growth behavior in poled ferroelectric PMN-PZT ceramics," *Current Applied Physics,* vol. 6, pp. 299-302, 2006.

[21]   K. J. Loh and D. Chang, "Zinc oxide nanoparticle-polymeric thin films for dynamic strain sensing," *Journal of Materials Science,* vol. 46, pp. 228-237, 2011.

[22]   J. F. Scott, "Applications of magnetoelectrics," *Journal of Materials Chemistry,* vol. 22, pp. 4567-4574, 2012 2012.

[23]   P. Martins, A. C. Lopes, and S. Lanceros-Mendez, "Electroactive phases of poly(vinylidene fluoride): Determination, processing and applications," *Progress in Polymer Science.*

[24]   Z. Fang, S. G. Lu, F. Li, S. Datta, Q. M. Zhang, and M. El Tahchi, "Enhancing the magnetoelectric response of Metglas/polyvinylidene fluoride laminates by exploiting the flux concentration effect," *Applied Physics Letters,* vol. 95, 2009.

[25]   J. Jin, S. G. Lu, C. Chanthad, Q. Zhang, M. A. Haque, and Q. Wang, "Multiferroic polymer composites with greatly enhanced magnetoelectric effect under a low magnetic bias," *Advanced Materials,* vol. 23, pp. 3853-3858, 2011.

[26] C. W. Nan, G. Liu, and Y. Lin, "Influence of interfacial bonding on giant magnetoelectric response of multiferroic laminated composites of Tb1-xDyxFe2 and PbZrxTi1-xO3," *Applied Physics Letters,* vol. 83, pp. 4366-4368, 2003.

[27] G. Liu, C. W. Nan, N. Cai, and Y. Lin, "Dependence of giant magnetoelectric effect on interfacial bonding for multiferroic laminated composites of rare-earth-iron alloys and lead-zirconate-tltanate," *Journal of Applied Physics,* vol. 95, pp. 2660-2664, 2004.

[28] J. Gutierrez, A. Lasheras, J. M. Barandiaran, J. L. Vilas, M. S. Sebastian, and L. M. Leon, "Temperature Response of Magnetostrictive/Piezoelectric Polymer Magnetoelectric Laminates," in *Materials and Applications for Sensors and Transducers.* vol. 495, E. Hristoforou and D. S. Vlachos, Eds., ed, 2012, pp. 351-354.

[29] P. Martins, A. Lasheras, J. Gutierrez, J. M. Barandiaran, I. Orue, and S. Lanceros-Mendez, "Optimizing piezoelectric and magnetoelectric responses on CoFe 2O 4/P(VDF-TrFE) nanocomposites," *Journal of Physics D: Applied Physics,* vol. 44, 2011.

[30] C. W. Nan, "Magnetoelectric effect in composites of piezoelectric and piezomagnetic phases," *Physical Review B,* vol. 50, pp. 6082-6088, 1994.

[31] N. Ce Wen, M. Li, and J. H. Huang, "Calculations of giant magnetoelectric effects in ferroic composites of rare-earth-iron alloys and ferroelectric polymers," *Physical Review B - Condensed Matter and Materials Physics,* vol. 63, pp. 1444151-1444159, 2001.

[32] N. Cai, J. Zhai, C. W. Nan, Y. Lin, and Z. Shi, "Dielectric, ferroelectric, magnetic, and magnetoelectric properties of multiferroic laminated composites," *Physical Review B - Condensed Matter and Materials Physics,* vol. 68, pp. 2241031-2241037, 2003.

[33] G. Liu, C. W. Nan, N. Cai, and Y. Lin, "Calculations of giant magnetoelectric effect in multiferroic composites of rare-earth-iron alloys and PZT by finite element method," *International Journal of Solids and Structures,* vol. 41, pp. 4423-4434, 2004.

[34] B. Bao and Y. Luo, "Theory of magnetoelectric effect in laminate composites considering two-dimensional internal stresses and equivalent circuit," *Journal of Applied Physics,* vol. 109, pp. 094503-5, 2011.

[35] S. Srinivas and J. Y. Li, "The effective magnetoelectric coefficients of polycrystalline multiferroic composites," *Acta Materialia,* vol. 53, pp. 4135-4142, 2005.

[36] A. Preumont and F. Bossens, "Active tendon control of vibration of truss structures: theory and experiments," *Journal of Intelligent Material Systems and Structures,* vol. 11, pp. 91-99, 2000.

[37] D. Esterly, "Manufacturing of Poly(vinylidene fluoride) and Evaluation of its Mechanical Properties," Master of Science, Virginia Polytechnic Institute and State University, Blacksburg, Virginia, 2002.

[38] M. Martins, V. Correia, J. M. Cabral, S. Lanceros-Mendez, and J. G. Rocha, "Optimization of piezoelectric ultrasound emitter transducers for underwater communications," *Sensors and Actuators, A: Physical,* vol. 184, pp. 141-148, 2012.

[39] A. Grunwald and A. G. Olabi, "Design of a magnetostrictive (MS) actuator," *Sensors and Actuators, A: Physical,* vol. 144, pp. 161-175, 2008.

[40] K. Fonteyn, A. Belahcen, R. Kouhia, P. Rasilo, and A. Arkkio, "FEM for directly coupled magneto-mechanical phenomena in electrical machines," *IEEE Transactions on Magnetics,* vol. 46, pp. 2923-2926, 2010.

[41] M. Li, D. Hasanyan, Y. Wang, J. Gao, J. Li, and D. Viehland, "Theoretical modelling of magnetoelectric effects in multi-push-pull mode Metglas/piezo-fibre laminates," *Journal of Physics D-Applied Physics,* vol. 45, Sep 5 2012.

[42] J. Carvell, R. Cheng, and Q. Yang, "Induced magneto-electric coupling at ferroelectric/ferromagnetic interface," *Journal of Applied Physics,* vol. 113, pp. 17C715-3, 2013.

[43] V. Sencadas, S. Lanceros-Méndez, R. Sabater I Serra, A. Andrio Balado, and J. L. Gómez Ribelles, "Relaxation dynamics of poly(vinylidene fluoride) studied by dynamical mechanical measurements and dielectric spectroscopy," *European Physical Journal E,* vol. 35, 2012.

[44] M. P. Silva, C. M. Costa, V. Sencadas, A. J. Paleo, and S. Lanceros-Méndez, "Degradation of the dielectric and piezoelectric response of β-poly(vinylidene fluoride) after temperature annealing," *Journal of Polymer Research,* vol. 18, pp. 1451-1457, 2011.

[45] Y. Yan, Y. Zhou, and S. Priya, "Giant self-biased magnetoelectric coupling in co-fired textured layered composites," *Applied Physics Letters,* vol. 102, Feb 4 2013.
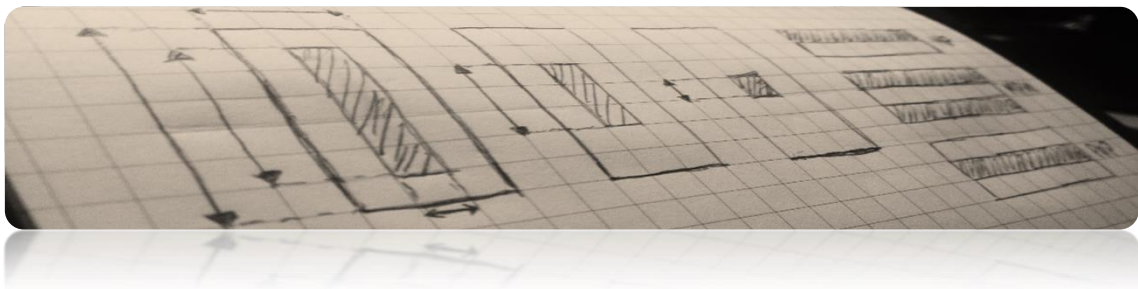
4 Size and geometry optimization

This chapter is based on the following publication:

Silva M P, Martins P, Lasheras A, Gutiérrez J, Barandiarán J M and Lanceros-Mendez S 2014 *Size effects on the magnetoelectric response on PVDF/Vitrovac 4040 laminate composites* J. Magn. Magn. Mater. 377 29–33

4.1 Introduction

Magnetoelectric materials (ME) are characterized by the variation of the electric polarization (P) in the presence of an applied magnetic field (H) (equation 1),

$$\Delta P = \alpha \Delta H \tag{15}$$

where α is the ME coupling coefficient [1-4]. In single-phase materials this effect is intrinsic and corresponds to the coupling between magnetic moments and electric dipoles [1-3]. Low Curie temperatures and weak ME coupling at room temperature difficult their introduction in technological applications [4-6].

Due to those limitations, the research interest began to focus in the ME effect of multiple-phase materials, in which such effect is a result of the product of the magnetostrictive effect (magnetic/mechanical) within the magnetostrictive phase and the piezoelectric effect (mechanical/electrical) within the piezoelectric phase (equation 2).

$$ME_H effect = \frac{electric}{mechanical} \times \frac{mechanical}{magnetic} = \frac{\partial E}{\partial \lambda} \times \frac{\partial \lambda}{\partial B} \tag{16}$$

where $\partial \lambda / \partial B$ and $\partial E / \partial \lambda$ are the piezomagnetic coefficient and piezoelectric coefficients respectively. Thus, the ME effect in multiple-phase materials is extrinsic, strongly depending on the microstructure and coupling interaction across the magnetic-piezoelectric interfaces [6-8].

This ME-product property leads to output signals at room temperature that are many orders of magnitude higher than the ones in single phase materials, being therefore very attractive for innovative applications in areas such as such as brain activity sensors and magnetic sensors (Figure 4.1), among others [1, 6, 7, 9].
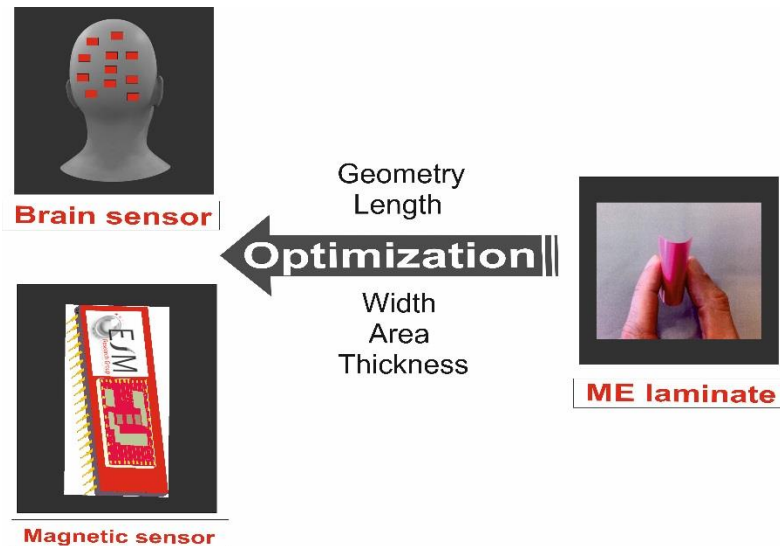
Figure 4.1 - Possible applications of ME materials: Monitoring brain activity and magnetic sensors.

Additionally, the multiferroic composite approach offers a large potential for technological optimization because of the degrees of freedom in sensor design, including the choice of the piezoelectric and magnetostrictive materials, their deposition process and/or binding and their three dimensional arrangement [10]. In the last decade, different approaches for the development of ME-sensors have been reported, all of them based on one of two fundamental type of piezoelectric materials: either are constituted by piezoelectric ceramics or piezoelectric polymers [6], together with the magnetostrictive element.

Piezoelectric ceramics have low electrical resistivity, high dielectric losses and moreover are dense and brittle, which can lead to fatigue and failure.[6, 11, 12] In order to improve and solve some problems related to ceramic composites, piezoelectric polymers such as poly(vinylidene fluoride), PVDF, and its copolymers have been used since they are flexible, show large electrical resistivity and low losses, and can be processed in different shapes at low processing temperatures [6, 12-14]. Three main types of polymer-based ME composites can be found in the literature: (a) nanocomposites, (b) polymer "*as a binder*", and (c) laminated composites [6]. Within those materials, the highest ME response is obtained in laminated polymer based ME materials, being the highest value (21.46 $V.cm^{-1}.Oe^{-1}$) at non resonance frequencies reported for a three layer laminate comprising PVDF, Metglas and a Devcon epoxy [15]. On the other hand , the highest ME value reported at electromechanical resonance was $383 V.cm^{-1}.Oe^{-1}$ using P(VDF-TrFE)/Metglas 2605SA1 bonded with an epoxy resin, [16].

70

For sensor applications, the optimization of the element responsible for the coupling between magnetostrictive and piezoelectric components plays a crucial role [17-19]. A study on PVDF bonded to Vitrovac 4040 with epoxies with different elastic moduli show a decrease in the ME voltage coefficient from 53 to 6 V.cm^{-1}.Oe^{-1} with increasing epoxy Young Modulus from 2.7×10^8 to 9.0×10^9 Pa, the highest ME response of 53 V.cm^{-1}.Oe^{-1} being obtained for a PVDF/M-Bond epoxy/Vitrovac laminate. [17]

A different approach for the coupling of the piezoelectric and magnetostrictive elements was recently presented by direct spin coating of a PVDF layer onto a Metglas substrate. By eliminating the usage of an adhesive epoxy for the mechanical coupling between the layers and using a clamping effect a giant ME voltage coefficient of 850 V.cm^{-1}.Oe^{-1} was obtained at the bending mode resonance frequency of 27.8 Hz [10].

However, coupling between the different phases is not the only parameter that requires optimization prior to their incorporation into technological applications: characteristics such as size, structure and relative geometry of the components may allow tailoring the applicability of ME composite materials [20].

In this way, this work shows the influence of the relative size of the magnetostrictive and piezoelectric elements on the ME response. Additionally the effect of distinct geometries in the ME response will be also addressed. Vitrovac (Fe$_{39}$Ni$_{39}$Mo$_4$Si$_6$B$_{12}$) 4040 was used as the magnetostrictive element due to its large piezomagnetic coefficient (1.3 ppm.Oe^{-1}) at low magnetic fields, [21] and PVDF was chosen as the piezoelectric element, due to its highest piezoelectric response among polymers [13, 22]. M-Bond epoxy was used as coupling agent since it has proved obtain higher ME coefficients in ME laminates when compared to other epoxy resins [17].

4.2   Results and discussion

In this chapter Vitrovac was used as magnetostrictive layer and PVDF as piezoelectric layer. The bonding layer is composed by M-Bond epoxy resin.

Sample preparation and sample design are described in subchapter 2.3.2

The influence of the magnetostrictive layer length on the ME response of the laminate was studied by varying the longitudinal aspect ratio (LAR) between 1.1 mm and 4.3 (Figure 4.2).
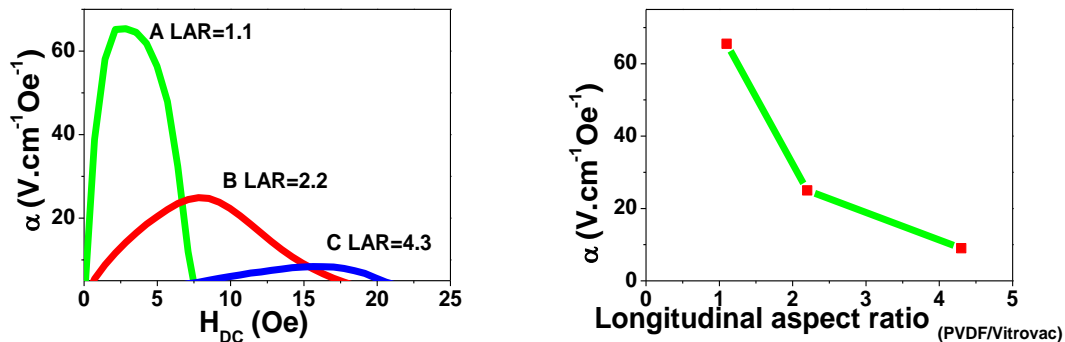
Figure 4.2 - a) ME response of laminates with different LAR; b) Variation of the ME response with increasing LAR.

Results reveal the strong influence of the LAR on the ME response of the composite. The highest ME response has been obtained for the Vitrovac with the LAR value close to 1 (Laminate A), and the lowest response was obtained for the highest LAR (Laminate C) (Figure 4.2a). It can be observed on Figure 4.2 that the ME response varies almost linearly with LAR, since with higher magnetostrictive area, more strain will be transmitted to the piezoelectric layer, thereby producing a higher voltage.

Figure 4.2 also shows that the magnetic field at which the maximum ME response is obtained increases with increasing LAR, behavior which is related to the demagnetizing field, which is stronger for smaller samples [24].

Figure 4.3 demonstrates the behavior of ME laminate composites with the variation of TAR.
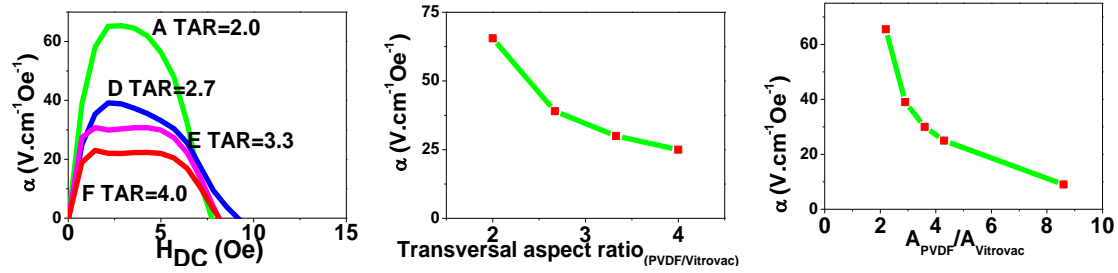
Figure 4.3 - a) ME response obtained with different TAR; b) Variation of the ME response with increasing TAR; c) ME response obtained with distinct Ap∕Am ratios.

The obtained results indicate the strong influence of TAR on the ME response. The highest response was obtained for the composite with the TAR closest to 1 (2.0), and the lowest response was obtained for the sample with the highest TAR (4.0).

With increasing PVDF surface area not directly bonded to the magnetostrictive Vitrovac, A_{NB}, relative to the PVDF area directly bonded to Vitrovac, A_B, clamping effects will arise, since the A_{NB} will attenuate the strain variations of the A_B. In this way, stress clamping of the A_{NB} hinders polarization switching on the A_B, reducing the piezoelectric response [25] and, as a consequence, decreasing the ME response.

Such effect is further evidenced when the shape of the ME peaks of Figure 4.3a is analyzed together with Figure 4.3b. When the width of PVDF is close to the width of Vitrovac, A_B is much higher than A_{NB} and the PVDF layer is free to strain as a response of the deformation of the Vitrovac layer. When the magnetic field increases, the magnetostrictive strain variation of Vitrovac ranges from zero to its maximum value and consequently the piezomagnetic coefficient achieves is maximum value. In this situation, the deformation variation increases with increasing DC magnetic field and, as a result, the ME coefficient also increases and reaches its maximum when the magnetostrictive strain variation also reaches the maximum value.

As the external magnetic field continues to increase, the magnetostrictive strain variation starts to decrease together with the deformation variation values leading to a decrease of the ME field coefficient [26]. When A_{NB} is much higher than A_B, the PVDF not directly bonded to Vitrovac will mitigate the strain of PVDF directly bonded to Vitrovac when the applied DC magnetic field is between 1 and 5 Oe In this situation, the increase of the magnetostrictive strain is not accompanied by an increase in the ME response [25].

Additionally the A_p/A_m ratio was changed between 2.2 and 8.6 and the effect of this variation in the ME response of the composites has been studied (Figure 4.3c). It is

verified that when the A_p/A_m ratio approach 1, the ME response is optimized. This behaviour is consistent with the results shown in Figure 4.2 and Figure 4.3.

Finally, the effect of the laminate configuration in the ME response was analyzed by measuring a by-layer composite (a), a three-layer magnetostrictive-piezoelectric-magnetostrictive (MPM) composite (g) and a three-layer piezoelectric-magnetostrictive-piezoelectric (PMP) composite (Figure 4.4).
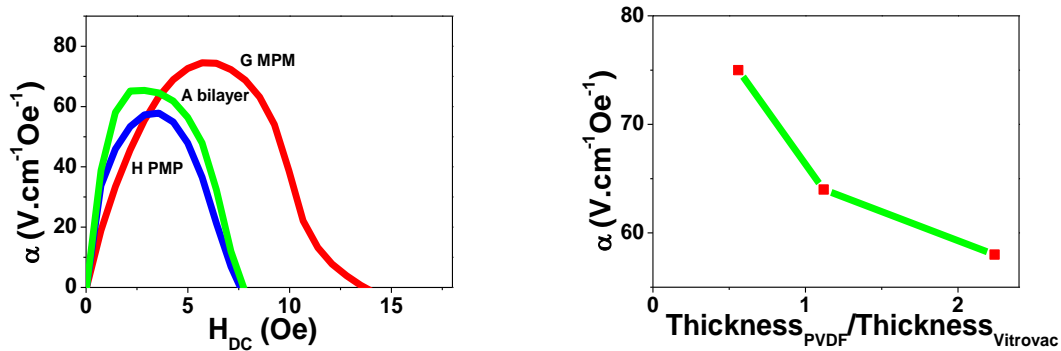
Figure 4.4 - a) ME response obtained on laminates with bilayer composite (Sample A), three-layer magnetostrictive-piezoelectric-magnetostrictive (MPM) (Sample G) composite, and three-layer piezoelectric-magnetostrictive-piezoelectric composite (PMP) (Sample H) configurations. b) ME response obtained with distinct ratios.

Figure 4.4a shows that the laminate configuration with the highest ME response is the Vitrovac-PVDF-Vitrovac (MPM) since the two magnetostrictive layers deliver more deformation to the piezoelectric layer and, as result, a higher ME response is obtained. On the other hand, the PMP configuration achieves the lowest ME response due to larger clamping effect between the two layers of PVDF and the Vitrovac layer.

In terms of the inner structure of the bilayer laminates and under the H_{AC} field excitation applied along the length axis, the Vitrovac layer will elongate and shrink along that direction (Metglas4040λ_{11}=8ppm [23]). This deformation will be transmitted to the epoxy which in turn will make the PVDF film to undergo a longitudinal strain, inducing a dielectric polarization in its transverse direction (PVDFd$_{31}$=23 pC.N^{-1} [13]). Such transfer process is optimized in the MPM configuration weakened in the PMP configuration.

Figure 4.4b allows to study the effect of the $Thickness_{PVDF}/Thickness_{Vitrovac}$ ratio in the ME response of the composites. The decrease in the ME coefficient with increasing $Thickness_{PVDF}/Thickness_{Vitrovac}$ ratio being explained in terms of the decreased compressive stress in the piezoelectric layer [27].

74

Note that the ME peak of the sample G, is slightly shifted to higher ME fields as a result of the demagnetizing effect of the Vitrovac layers [28, 29]. These results indicate that as the number of Vitrovac layers increases, a higher DC magnetic field is required to reach the maximum ME coefficient. This implies that it is possible to control the ME output value and saturation point by changing the number of Vitrovac layers [30].

4.3 Conclusions

Thin, flexible, low-weight and low-cost ME laminates with simple fabrication and tunable properties, consisting of Metglas/PVDF unimorph and three-layer sandwich configurations have been produced with the objective to study the influence of the size of magnetostrictive and piezoelectric elements on the ME response as well as the effect of distinct geometries in the ME response will be also addressed.

It is concluded that the ME voltage coefficient increases with decreasing LAR (from 4.3 to 1.1), reaching a maximum ME voltage coefficient of 66 V.cm^{-1}.Oe^{-1}. Multiferroic laminates with lowest TAR resulted in better ME performance when compared with higher TAR. It was further demonstrated an intimate relation between the A_p/A_m ratio and the ME response of the composites. When such ratio values approach 1, the ME response is optimized.

Tri-layered composites configurations (magnetostrictive-piezoelectric-magnetostrictive type), have a higher ME response (75 V.cm-1.Oe-1) than the bi-layer configuration (66 V.cm-1.Oe-1).

Additionally it was observed a decrease in the ME coefficient with increasing *Thickness$_{PVDF}$*/*Thickness$_{Vitrovac}$* ratio.

Furthermore the ME output voltage and optimum magnetic field can be controlled by changing the number of Vitrovac layers, which makes this composite a promising candidate for magnetic sensors and energy harvesting applications.

4.4 References

[1]   J. Ma, J. Hu, Z. Li, and C.-W. Nan, "Recent Progress in Multiferroic Magnetoelectric Composites: from Bulk to Thin Films," *Adv. Mater. ,* vol. 23, pp. 1062-1087, Mar 4 2011.

[2]   W. Prellier, M. P. Singh, and P. Murugavel, "The Single-phase Multiferroic Oxides: From Bulk to Thin Film," *J. Phys.: Condens. Matter,* vol. 17, pp. 803-832, 2005.

[3]   G. Lawes and G. Srinivasan, "Introduction to Magnetoelectric Coupling and Multiferroic Films," *J. Phys. D: Appl. Phys.,* vol. 44, 2011.

[4]   D. R. Patil, A. D. Sheikh, C. A. Watve, and B. K. Chougule, "Magnetoelectric Properties of ME Particulate Composites," *J. Mater. Sci.,* vol. 43, pp. 2708-2712, 2008.

[5]   P. Martins, C. M. Costa, and S. Lanceros-Mendez, "Nucleation of Electroactive β-phase Poly(vinilidene fluoride) with CoFe2O4 and NiFe2O4 Nanofillers: A New Method for the Preparation of Multiferroic Nanocomposites," *Appl. Phys. A Mater. Sci. Process.,* vol. 103, pp. 233-237, 2011.

[6]   P. Martins and S. Lanceros-Méndez, "Polymer-Based Magnetoelectric Materials," *Adv. Funct. Mater.,* vol. 23, pp. 3371-3385, 2013.

[7]   C. W. Nan, M. I. Bichurin, S. Dong, D. Viehland, and G. Srinivasan, "Multiferroic Magnetoelectric Composites: Historical Perspective, Status, and Future Directions," *J. Appl. Phys.,* vol. 103, pp. 1-35, 2008.

[8]   C. W. Nan, "Magnetoelectric Effect in Composites of Piezoelectric and Piezomagnetic Phases," *Phys. Rev. B,* vol. 50, pp. 6082-6088, 1994.

[9]   M. Fiebig, "Revival of the Magnetoelectric Effect," *J. Phys. D: Appl. Phys.,* vol. 38, pp. 123-152, 2005.

[10]   A. Kulkarni, K. Meurisch, I. Teliban, R. Jahns, T. Strunskus, A. Piorra, *et al.*, "Giant Magnetoelectric Effect at Low Frequencies in Polymer-based Thin Film Composites," *Appl. Phys. Lett. ,* vol. 104, pp. 1-5, 2014.

[11]   S. Jiansirisomboon, K. Songsiri, A. Watcharapasorn, and T. Tunkasiri, "Mechanical Properties and Crack Growth Behavior in Poled Ferroelectric PMN-PZT Ceramics," *Curr. Appl. Phys. ,* vol. 6, pp. 299-302, 2006.

[12]   K. J. Loh and D. Chang, "Zinc Oxide Nanoparticle-Polymeric Thin Films for Dynamic Strain Sensing," *J. Mater. Sci.,* vol. 46, pp. 228-237, 2011.

[13]   P. Martins, A. C. Lopes, and S. Lanceros-Mendez, "Electroactive Phases of Poly(vinylidene fluoride): Determination, Processing and Applications," *Prog. Polym. Sci.,* vol. 39, pp. 683-706, 2013.

[14]   J. F. Scott, "Applications of Magnetoelectrics," *J. Mat. Chem.,* vol. 22, pp. 4567-4574, 2012 2012.

[15]   Z. Fang, S. G. Lu, F. Li, S. Datta, Q. M. Zhang, and M. El Tahchi, "Enhancing the Magnetoelectric Response of Metglas/Polyvinylidene Fluoride Laminates By

Exploiting the Flux Concentration Effect," *Appl. Phys. Lett.*, vol. 95, pp. 1-3, 2009.

[16]   J. Jin, S. G. Lu, C. Chanthad, Q. Zhang, M. A. Haque, and Q. Wang, "Multiferroic Polymer Composites With Greatly Enhanced Magnetoelectric Effect Under a Low Magnetic Bias," *Adv. Mater.*, vol. 23, pp. 3853-3858, 2011.

[17]   M. Silva, S. Reis, C. S. Lehmann, P. Martins, S. Lanceros-Mendez, A. Lasheras, *et al.*, "Optimization of the Magnetoelectric Response of Poly(vinylidene fluoride)/Epoxy/Vitrovac Laminates.," *ACS Appl. Mater. Interfaces,* vol. 5, pp. 10912-9, 2013.

[18]   G. Liu, C. W. Nan, N. Cai, and Y. Lin, "Dependence of Giant Magnetoelectric Effect on Interfacial Bonding for Multiferroic Laminated Composites of Rare-Earth-Iron Alloys and Lead-Zirconate-Titanate," *J. Appl. Phys.,* vol. 95, pp. 2660-2664, 2004.

[19]   C. W. Nan, G. Liu, and Y. Lin, "Influence of Interfacial Bonding on Giant Magnetoelectric Response of Multiferroic Laminated Composites of Tb1-xDyxFe2 and PbZrxTi1-xO3," *Appl. Phys. Lett.*, vol. 83, pp. 4366-4368, 2003.

[20]   Y. Huang and C. L. Zhang, "Magnetoelectric Effect in a Circumferentially Polarized Composite Cylinder," *Smart Mater. Struct.,* vol. 22, p. 105018, 2013.

[21]   J. Gutierrez, A. Lasheras, J. M. Barandiaran, J. L. Vilas, M. S. Sebastian, and L. M. Leon, "Temperature Response of Magnetostrictive/Piezoelectric Polymer Magnetoelectric Laminates," *Materials and Applications for Sensors and Transducers,* vol. 495, pp. 351-354, 2012.

[22]   P. Martins, A. Lasheras, J. Gutierrez, J. M. Barandiaran, I. Orue, and S. Lanceros-Mendez, "Optimizing Piezoelectric and Magnetoelectric Responses on CoFe2O4/P(VDF-TrFE) Nanocomposites," *J. Phys. D: Appl. Phys.,* vol. 44, p. 495303, 2011.

[23]   J. Gutiérrez, A. Lasheras, J. M. Barandiarán, J. L. Vilas, A. Maceiras, and L. M. León, "Improving the performance of high temperature piezopolymers for magnetoelectric applications," in *Key Engineering Materials* vol. 543, ed, 2013, pp. 439-442.

[24]   V. Zhukova, A. Zhukov, J. Gonzalez, and J. M. Blanco, "Length Effect in a Negative Magnetostrictive Co-Si-B Amorphous Wire With Rectangular Hysteresis Loop," *J Magn. Magn. Mater.,* vol. 254, pp. 182-184, Jan 2003.

[25]   T. A. Berfield, R. J. Ong, D. A. Payne, and N. R. Sottos, "Residual Stress Effects on Piezoelectric Response of Sol-gel Derived Lead Zirconate Titanate Thin Films," *J. Appl. Phys.,* vol. 101, 2007.

[26]   H. M. Zhou, L. M. Xuan, C. Li, and J. Wei, "Numerical Simulation of Nonlinear Magnetic-Mechanical-Electric Coupling Effect in Laminated Magnetoelectric Composites," *J. Magn. Magn. Mater.,* vol. 323, pp. 2802-2807, 2011.

[27]   R. A. Islam, Y. Ni, A. G. Khachaturyan, and S. Priya, "Giant Magnetoelectric Effect in Sintered Multilayered Composite Structures," *J. Appl. Phys.,* vol. 104, 2008.

[28]   F. Kreitmeier, D. V. Chashin, Y. K. Fetisov, L. Y. Fetisov, I. Schulz, G. J. Monkman*, et al.*, "Nonlinear Magnetoelectric Response of Planar Ferromagnetic-Piezoelectric Structures to Sub-millisecond Magnetic Pulses," *Sensors,* vol. 12, pp. 14821-14837, 2012.

[29]   E. Liverts, A. Grosz, B. Zadov, M. I. Bichurin, Y. J. Pukinskiy, S. Priya*, et al.*, "Demagnetizing Factors for Two Parallel Ferromagnetic Plates and Their Applications to Magnetoelectric Laminated Sensors," *J. Appl. Phys.,* vol. 109, 2011.

[30]   C.-S. Park and S. Priya, "Broadband/Wideband Magnetoelectric Response," *Adv. Cond. Mat. Phys.,* vol. 2012, p. 12, 2012.
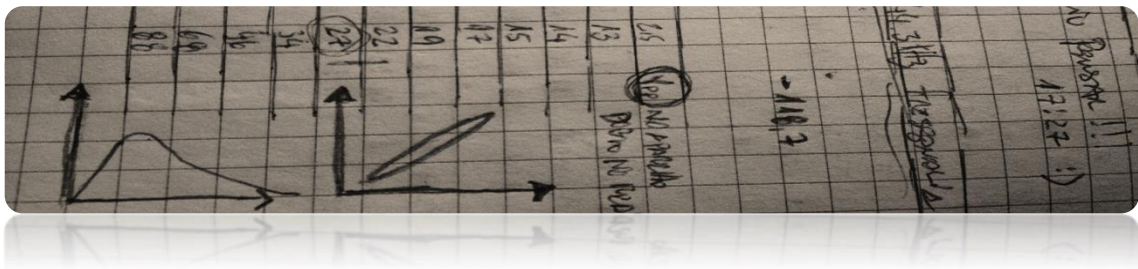
5 Characterization of magnetoelectric laminates for sensor applications

This chapter is based on the following publication:

S. Reis*, M.P.Silva*, N. Castro, V. Correia, P. Martins, A. Lasheras, J. Gutierrez, J. M. Barandiarán, J. G. Rocha and S. Lanceros-Mendez. *Characterization of Metglas/Poly(vinylidene fluoride)/Metglas magnetoelectric laminates for AC/DC magnetic sensor applications*. Submited to Smart Materials and Structures – IOPscience.

*equal contribution

5.1   Introduction

The magnetoelectric (ME) effect is defined as the variation of the electric polarization in the presence of an applied magnetic field (direct ME effect) or as the variation of the magnetization in the presence of an applied electrical field (converse ME effect) [1, 2].

This effect is present in materials through different principles: by the coupling of magnetic moments and electric dipoles in single-phase multiferroic materials [3] or by the elastic coupling between electroactive and magnetic phases in composites [2, 4-7]. Single-phase ME materials are not suitable for technological applications due to their low ME response ($\approx$ 1-20 mV.cm^{-1}.Oe^{-1}) at very low temperatures ($\approx$ 10 K)[5].

From the different composite structures, laminated ME composites, comprising bonded piezoelectric and magnetostrictive layers, are the ones with the highest ME response, thus being the most studied materials for their implementation into technological applications [5, 8, 9]. The piezoelectric element in such laminated composite structures can be ceramic or polymeric[5, 10]. Despite the higher ME response found in ceramic ME composites, their low electrical resistivity, high dielectric losses, fragility and fatigue [5, 11, 12] are the main drawbacks that impair their widespread applicability [5]. Without the problems found in ceramic based ME materials and with high ME coupling, easy fabrication, large scale production ability, low-temperature processing into a variety of forms and, in some cases, biocompatibility, polymer based ME materials emerged as an appropriate solution [5, 13]. The ME coefficients values found in polymer-based ME laminates as well as the broad range of the magnetic fields at which they respond, allow a large range of applications, in particular in the fields of magnetic sensors and actuators [5, 14, 15].

Due to the limitations found in some of the conventional magnetic field sensors, including low operational temperatures and high operational power [5, 16], self-powered polymer-based ME sensors are of increasing interest and applicability due to their novel working principle [5, 17, 18].

Sensor essential characteristics determining the applicability of ME magnetic sensors include sensibility, linearity, hysteresis, accuracy and resolution [19-21], but there are just a few studies dedicated partially to this issue [22-24].

In this way, this works focus on the determination of such characteristics on an optimized polymer-based ME laminate composed of Fe$_{64}$Co$_{17}$Si$_7$B$_{12}$ (Metglas) and

poly(vinylidene fluoride), PVDF. Such selection is related with the highest sensitivity and lowest noise of Metglas [18, 25]. Further, Metglas shows a high magnetic permeability and piezomagnetic coefficient [26]. PVDF is selected as piezoelectric component due to its highest piezoelectric coefficient among all polymers, stability, flexibility, large electrical resistivity, low losses and for the possibility of being processed in different shapes at low processing temperatures[13]. Additionally, PVDF/Metglas composites exhibit the highest ME response among all polymer-based ME materials, being in this way the best composite for the present study [5].

5.2 Results and discussion

In this chapter Metglas was used as magnetostrictive layer, and PVDF as piezoelectric layer. The bonding layer is composed by Devcon epoxy resin. Sample preparation is described in subchapter 2.3.3

Figure 5.1 shows the ME voltage response of the Metglas/PVDF/Metglas composite that will serve as the basis for the material characterization for sensor applications.
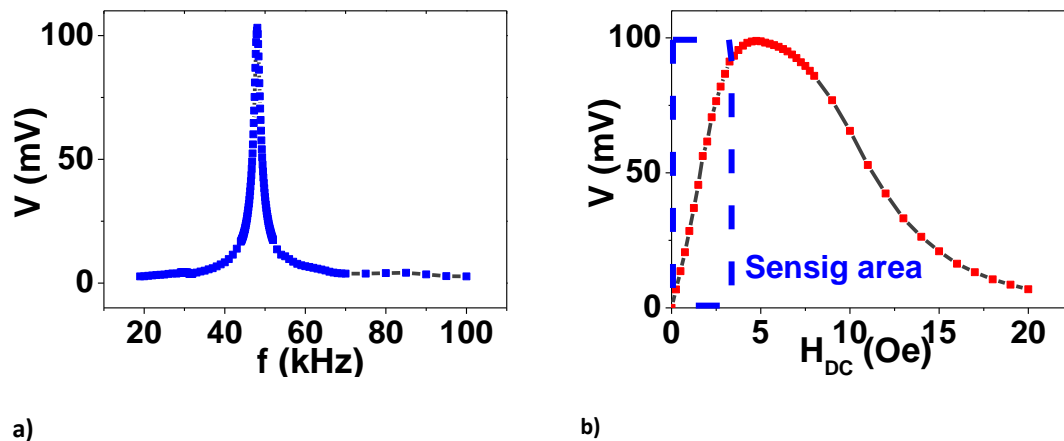
Figure 5.1 - Magnetoelectric voltage response (V) as a function of: (a) frequency and (b) DC magnetic field.

Figure 5.1a shows that the highest ME voltage response is obtained for the 48 kHz resonance frequency. When the laminated composite operates in such resonance mode, its ME effect is largely enhanced, generating an ME voltage output of nearly two orders of magnitude higher than for non-resonant conditions [27].

Further, the ME voltage increases with the H_{DC} magnetic field until 4.75 Oe when the maximum ME voltage of 100mV is reached (Figure 5.1b). A maximum ME coefficient (α_{33}) of 190 $V.cm^{-1}.Oe^{-1}$ is determined for such DC magnetic field after equation 1,

$$\alpha_{33} = \frac{\Delta V}{t.H_{AC}}$$
(17)

where ΔV, t and H_{AC} are the induced ME voltage, the PVDF thickness and the AC magnetic field, respectively.

Such behaviour is related with the increase of the piezomagnetic coefficient until the optimum DC magnetic field is reached. With further increase of the DC magnetic

field, a decrease in the induced voltage is observed, resulting from the saturation of the magnetostriction response [28-30].

DC linearity, sensibility, resolution and accuracy tests were performed in order to validate the use of the Metglas/PVDF/Metglas as a DC magnetic field sensor by applying a 0.1 Oe AC field (Figure 5.2).
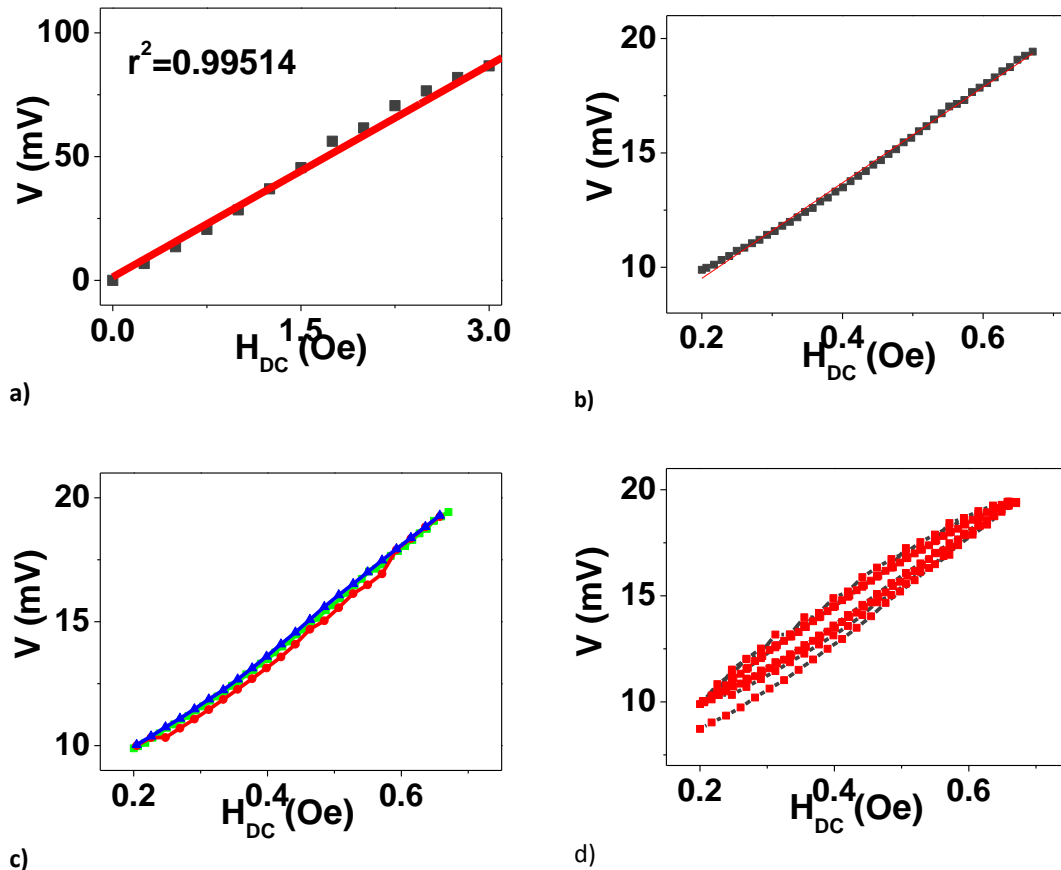
Figure 5.2. DC magnetic field sensor characterization: (a) linearity, (b) resolution and sensibility (c) accuracy and (d) hysteresis.

The linearity value was obtained in the 0-3 Oe DC magnetic field range (Figure 5.2a), since after the 3 Oe value, the ME response starts to reach the saturation, resulting in a linearity loss. Resolution and sensibility (Figure 5.2b), accuracy (Figure 5.2c) and hysteresis (Figure 5.2d) were determined at low DC magnetic fields (0.2 Oe-0.7 Oe) since for such small DC magnetic fields, the electromagnetic noise will have more influence on the data, thus ensuring that the sensor will be tested in the worst possible conditions for low field signal detection with large application potential in compasses, navigation, location, magnetic anomaly detection and in the medical/biological field[5, 16, 31].

Linearity, hysteresis and accuracy of a sensor is typically expressed as a percentage of Full-Scale Output (FSO), i.e., the ratio of the maximum output deviation

84

(Δ) divided by the full-scale output, specified as a percentage (Equation 2)[32]. Being the full-scale output (difference between the electrical output signals measured with maximum input stimulus and the lowest applied input stimulus) of 86.7 mV for the DC characterization, 200 mV for the AC characterization at resonance and 2 mV for the AC characterization at non-resonance frequencies.

$$\%FSO = \frac{\Delta}{FSO} \times 100\% \qquad (18)$$

From the linear fit of Figure 5.2a a coefficient of determination r^2 of 0.995 was obtained and the obtained linearity value is 95.9% FSO.

The accuracy, hysteresis, sensibility and resolution were found to be 99.4% FSO and 1.2% FSO, 30 mV.Oe^{-1} and 8 µOe respectively. The observed ME hysteresis (Figure 5.2d) is related with the magnetic hysteresis of the Metglas alloy, that is more pronounced in the vicinity of maximum permeability $\approx$0.55 Oe[33].

In order to further evaluate the behaviour as AC magnetic field sensor, the ME composite was tested and characterized at resonance (Figure 5.3 (a) and (b)) and non-resonance frequencies (Figure 5.3 (c)) and (d)) with and applied DC field of 4.7Oe.
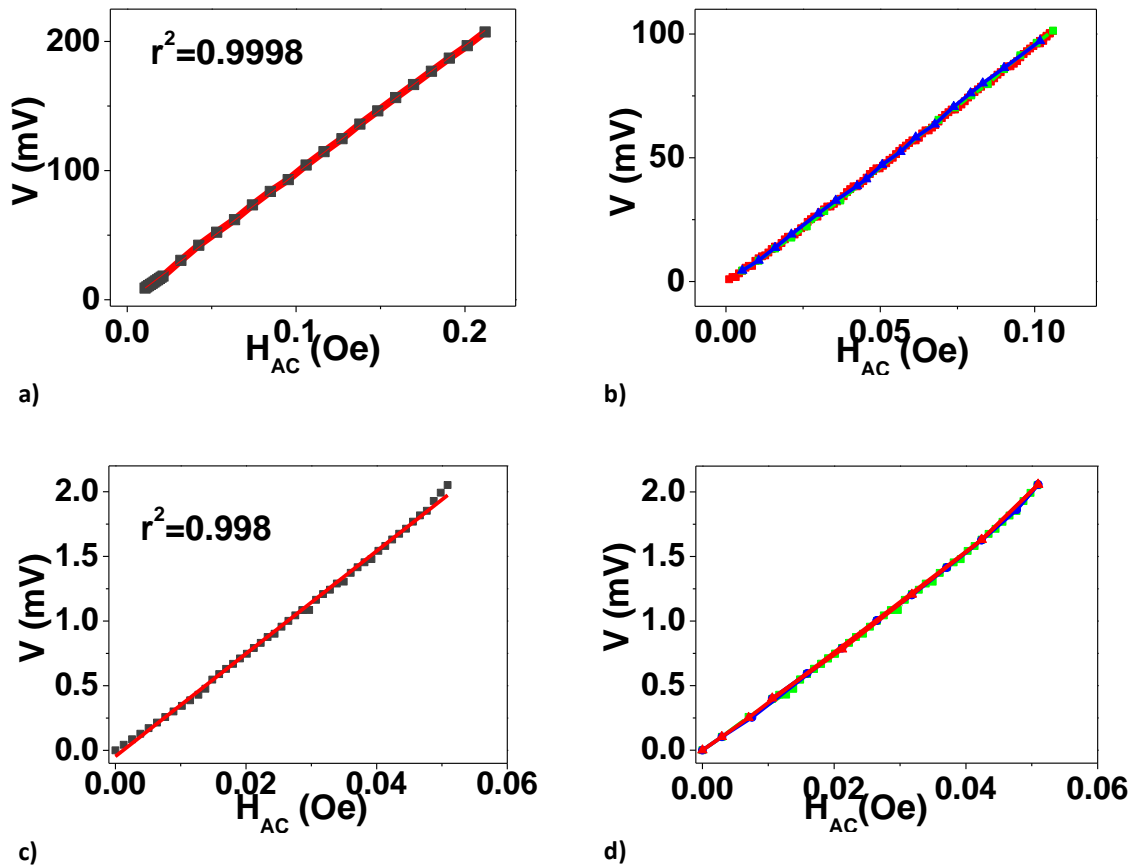
Figure 5.3. AC field magnetic field sensor characterization at resonance frequencies: (a) linearity, sensibility and resolution;   (b) accuracy/hysteresis. AC field magnetic field sensor characterization at resonance frequencies: (c) linearity, sensibility and resolution;   (d) accuracy /hysteresis.

From the linear fit of the data presented in Figure 5.3a it was obtained a coefficient of determination r^2 of 0.9998 and the obtained linearity value was 99.4% FSO for the AC magnetic field sensor working at the resonance frequency of 48 kHz. Additionally, the accuracy (Figure 5.3b), sensibility and resolution of such sensor were found to be 97.9% FSO, 992 mV.Oe^{-1} and 300 nOe respectively.

For non-resonance frequencies the r^2, linearity, accuracy, sensibility and resolution values were 0.998, 98.6%, 2.3%, 40 mV.Oe^{-1}, 1 µOe, respectively.

Further, both for resonance and non-resonance conditions no hysteresis has been detected (Figure 5.3 b and d, respectively).

The ME sensor parameters are summarized in Table 5.1. The sensibility and resolution values were additionally compared with latest high-sensitivity polymer-based ME materials reported on the literature.

Table 5.1 - Metglas/poly(vinylidene fluoride)/Metglas magnetic field sensor parameters

Parameter	DC magnetic field sensor		AC magnetic field sensor		
	Our Work	Literature	Our Work resonance	Our Work non resonance	Literature
Sensibility ($mV.Oe^{-1}$)	30	≈10 ref[22]	992	40	10 ref[23]
Linearity (r^2/FSO%)	0.995/95.9	-	0.9998/99.43	0.998/98.6	-
Accuracy (%FSO)	99.4	-	99.2	97.7	-
Resolution (μOe)	8	70 ref[24]	0.3	1	10 ref[23]
Hysteresis (FSO%)	1.22	-	-	-	-

Data from Table 5.1 reveal that the parameter values obtained for the AC/DC magnetic field sensor reported in this study are favourably comparable with the best ones found in the literature in terms of DC sensibility and AC accuracy.

Additionally, it is the first time that sensibility, linearity, accuracy, resolution and hysteresis values are reported all together to the same polymer-based ME magnetic sensor. Features reported in this study, are suitable for the applicability of the material, thus validating its use as innovative magnetic field sensors[5].

5.3 Conclusions

A Metglas/poly(vinylidene fluoride)/Metglas ME laminate composite has been developed in order to validate its use as AC/DC magnetic field sensors.

Sensibility and resolution values were found to be 30 mV.Oe-1 and 8 μOe for the DC magnetic field sensor and 992 mV.Oe-1 and 0.3 μOe for the AC magnetic field sensor. Such values are positively comparable with the ones reported in the most recent and sensitive polymer-based ME sensors.

Additionally, it was reported the correlation coefficient, linearity and accuracy values for the DC (0.995, 95.9% and 99.4%) and AC (0.9998, 99.4% and 99.2%) magnetic field, certifying the applicability of polymer-based ME materials as innovative AC/DC magnetic field sensors.

5.4 References

[1] W. Eerenstein, N. D. Mathur, and J. F. Scott, "Multiferroic and magnetoelectric materials," *Nature,* vol. 442, pp. 759-65, 2006.

[2] G. Srinivasan, "Magnetoelectric Composites," *Annual Review of Materials Research,* vol. 40, pp. 153-178, 2010.

[3] G. Lawes and G. Srinivasan, "Introduction to magnetoelectric coupling and multiferroic films," *Journal of Physics D: Applied Physics,* vol. 44, pp. 243001-243001, 2011.

[4] C.-w. W. Nan, M. I. Bichurin, S. Dong, D. Viehland, and G. Srinivasan, "Multiferroic magnetoelectric composites: Historical perspective, status, and future directions," *Journal of Applied Physics,* vol. 103, pp. 031101-031101, 2008.

[5] P. Martins and S. Lanceros-Méndez, "Polymer-Based Magnetoelectric Materials," *Advanced Functional Materials,* vol. 23, pp. 3371-3385, 2013.

[6] J. Ma, J. Hu, Z. Li, and C.-W. Nan, "Recent progress in multiferroic magnetoelectric composites: from bulk to thin films," *Advanced materials (Deerfield Beach, Fla.),* vol. 23, pp. 1062-87, 2011.

[7] Y. Z. Wang, "Influences of imperfect interface on effective magnetoelectric properties in multiferroic composites with elliptical fibers," *Smart Materials and Structures,* vol. 24, 2015.

[8] S. Priya, R. Islam, S. Dong, and D. Viehland, "Recent advancements in magnetoelectric particulate and laminate composites," *Journal of Electroceramics,* vol. 19, pp. 149-166, 2007.

[9] G. Yu and H. Zhang, "Surface effect on the magnetoelectric response of magnetoelectric layered composite with nanoscale thickness," *Smart Materials and Structures,* vol. 24, 2015.

[10] M. Rawat and K. L. Yadav, "Dielectric, ferroelectric and magnetoelectric response in Ba0.92 (Bi0.5Na0.5)0.08TiO3-Ni 0.65Zn0.35Fe2O4 composite ceramics," *Smart Materials and Structures,* vol. 23, 2014.

[11] S. Jiansirisomboon, K. Songsiri, a. Watcharapasorn, and T. Tunkasiri, "Mechanical properties and crack growth behavior in poled ferroelectric PMN–PZT ceramics," *Current Applied Physics,* vol. 6, pp. 299-302, 2006.

[12] K. J. Loh and D. Chang, "Zinc oxide nanoparticle-polymeric thin films for dynamic strain sensing," *Journal of Materials Science,* vol. 46, pp. 228-237, 2011.

[13] P. Martins, a. C. C. Lopes, and S. Lanceros-Mendez, "Electroactive phases of poly(vinylidene fluoride): Determination, processing and applications," *Progress in Polymer Science,* vol. 39, pp. 683-706, 2014.

[14] M. Alnassar, A. Alfadhel, Y. P. Ivanov, and J. Kosel, "Magnetoelectric polymer nanocomposite for flexible electronics," *Journal of Applied Physics,* vol. 117, 2015.

[15] S. Ju, S. H. Chae, Y. Choi, S. Lee, H. W. Lee, and C. H. Ji, "A low frequency vibration energy harvester using magnetoelectric laminate composite," *Smart Materials and Structures,* vol. 22, 2013.

[16] J. Lenz and A. S. Edelstein, "Magnetic sensors and their applications," *IEEE Sensors Journal,* vol. 6, pp. 631-649, 2006.

[17] Y. Zhao and C. Lu, "Note: Self-biased magnetic field sensor using end-bonding magnetoelectric heterostructure," *Review of Scientific Instruments,* vol. 86, p. 036101, 2015.

[18] H. Zhang, C. Lu, C. Xu, Y. Xiao, J. Gui, C. Lin*, et al.*, "Improved magnetoelectric effect in magnetostrictive/piezoelectric composite with flux concentration effect for sensitive magnetic sensor," *AIP Advances,* vol. 5, p. 047114, 2015.

[19] R. Boll and K. J. Overshott, *Sensors, Magnetic Sensors*: Wiley, 2008.

[20] F. Chen, Y. Jiang, and L. Jiang, "3 x 3 coupler based interferometric magnetic field sensor using a TbDyFe rod," *Applied Optics,* vol. 54, pp. 2085-2090, Mar 10 2015.

[21] T. Liu, Y. Chen, Q. Han, and X. Lu, "Magnetic Field Sensor Based on U-Bent Single-Mode Fiber and Magnetic Fluid," *Ieee Photonics Journal,* vol. 6, Dec 2014.

[22] C. S. Park, D. Avirovik, S. Bressers, and S. Priya, "Low-frequency nanotesla sensitivity in Metglas/piezoelectric/carbon fiber/piezoelectric composites with active tip mass," *Applied Physics Letters,* vol. 98, 2011.

[23] Y. K. Fetisov, D. A. Burdin, D. V. Chashin, and N. A. Ekonomov, "High-sensitivity wideband magnetic field sensor using nonlinear resonance magnetoelectric effect," *IEEE Sensors Journal,* vol. 14, pp. 2252-2256, 2014.

[24] J. G. Tao, Y. Y. Jia, H. Wu, and J. G. Yang, "Low-frequency nanotesla resolution of magnetic field detection in Metglas/magnetostrictive/piezoelectric laminates," in *Advanced Materials Research* vol. 960-961, ed, 2014, pp. 695-699.

[25] J. Jin, S. G. Lu, C. Chanthad, Q. Zhang, M. A. Haque, and Q. Wang, "Multiferroic polymer composites with greatly enhanced magnetoelectric effect under a low magnetic bias," *Advanced Materials,* vol. 23, pp. 3853-3858, 2011.

[26] J. Zhai, S. Dong, Z. Xing, J. Li, and D. Viehland, "Giant magnetoelectric effect in Metglas/polyvinylidene-fluoride laminates," *Applied Physics Letters,* vol. 89, p. 083507, 2006.

[27] M. Guo and S. Dong, "A resonance-bending mode magnetoelectric-coupling equivalent circuit," *IEEE Transactions on Ultrasonics, Ferroelectrics, and Frequency Control,* vol. 56, pp. 2578-2586, 2009.

[28] X. W. Dong, B. Wang, K. F. Wang, J. G. Wan, and J. M. Liu, "Ultra-sensitive detection of magnetic field and its direction using bilayer PVDF/Metglas laminate," *Sensors and Actuators, A: Physical,* vol. 153, pp. 64-68, 2009.

[29] Y. S. Koo, K. M. Song, N. Hur, J. H. Jung, T. H. Jang, H. J. Lee*, et al.*, "Strain-induced magnetoelectric coupling in BaTiO3 / Fe 3 O4 core/shell nanoparticles," *Applied Physics Letters,* vol. 94, 2009.

[30]   Y. X. Zheng, Q. Q. Cao, C. L. Zhang, H. C. Xuan, L. Y. Wang, D. H. Wang*, et al.*, "Study of uniaxial magnetism and enhanced magnetostriction in magnetic-annealed polycrystalline CoFe2O4," *Journal of Applied Physics,* vol. 110, 2011.

[31]   S. Taghvaeeyan and R. Rajamani, "Magnetic sensor-based large distance position estimation with disturbance compensation," *IEEE Sensors Journal,* vol. 15, pp. 4249-4258, 2015.

[32]   G. Singh, O. Guyon, P. Baudoz, N. Jovanovich, F. Martinache, T. Kudo*, et al.*, "Lyot-based low order wavefront sensor: Implementation on the Subaru Coronagraphic Extreme Adaptive Optics System and its laboratory performance," *Proceedings of SPIE - The International Society for Optical Engineering,* vol. 9148, pp. 1-9, 2014.

[33]   Z. Turgut, H. Kosai, T. Bixel, J. Scofield, S. L. Semiatin, and J. Horwath, "Hysteresis loss analysis of soft magnetic materials under direct current bias conditions," *Journal of Applied Physics,* vol. 117, 2015.
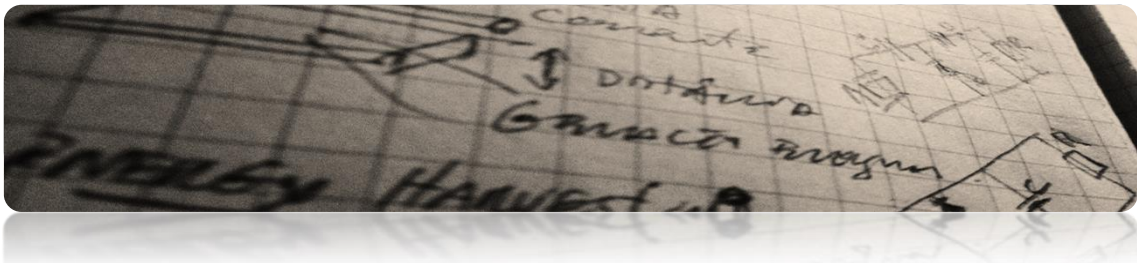
6 Development of an energy harvesting system with optimized circuit design

This chapter is based on the following publication:

S. Reis*, M.P.Silva*, N. Castro, V. Correia, J.G. Rocha, P. Martins, A. Lasheras, J. Gutierrez, J.M. Barandiarán and S. Lanceros-Mendez. *Development of an energy harvesting system with optimized circuit design based on magnetoelectric Metglas/poly(vinylidene fluoride)/Metglas composites*. Submmited to Applied Energy, Elsevier.

*Equal contribution

6.1 Introduction

Low power portable electronic devices and wireless sensors networks used for environmental, building, military and industrial process monitoring, agriculture management and implantable biomedical sensors are typically powered by batteries, with a finite supply of energy [1, 2]. Furthermore, some of such devices are located in remote locations, thus making battery change/recharge complex, inefficient, highly costly or even impossible [3-5].

Therefore, energy harvesting as self-power source of portable devices or wireless sensor network systems is an increasingly interesting issue, with strong impact and application potential [4, 6]. The combination of such energy harvesting devices with small-sized rechargeable batteries (or any other energy storage system) is the best approach to enable energy autonomy of devices over their entire lifetime [6].

Most energy harvesting systems convert into electrical energy other forms of energy such as solar, thermal, mechanical or electromagnetic [1, 3, 7, 8].

Solar energy harvesting offers excellent power densities from direct sunlight, however it is inadequate for areas with a deficit of light. Thermal harvesting is also of interest when the necessary thermal gradients are available, however, it is difficult to reach useful thermal gradients larger than 10 ºC in volumes of 1 cm^3 [1]. Mechanical energy harvesting is particularly attractive due to its universality; however, power and amplitude of the harvested signals are highly dependent on vibration conditions [9, 10]. Furthermore, usually mechanical harvesters are systems with a relatively large size, difficult to be miniaturized without decreasing the output power. Further, it shows strong power losses, thereby limiting the interest of the industry in such technologies [11].

Thus, when compared to the previous energy harvesting possibilities, energy harvesting from electromagnetic energy offers potential advantages such as being a renewable and inexhaustible power source, ubiquitous and, therefore, present in difficult to access locations [10-12] . Electromagnetic energy sources result from radiation emitting devices such as mobile base stations, Wi-Fi routers, satellite communications, radio and TV transmitters, as well as from magnetic and electric fields generated in power distribution lines. From all these sources electrical energy can be extracted [13].

The magnetoelectric (ME) effect provides an innovative highly flexible solution for the realization of such energy conversion [14]. As the next generation of innovative

energy-harvesting applications require flexibility, large area potential, lightweight and even biocompatibility [15-17], ME materials based on piezoelectric polymers may be an interesting approach to meet these requirements [16, 18].

Recently the ME coefficients obtained on polymer-based ME materials are on the same order of magnitude as the best ones obtained in inorganic ME materials, already being used/researched as energy harvesters, encouraging the emergence of polymer-based ME energy harvesting systems [16]. On the other hand, only a few studies have been devoted yet to energy harvesting from polymer-based ME materials [19].

In the reported harvesters, the generated alternating current (AC) voltages are typically processed using a classical extraction circuit composed by a rectifier and a direct current (DC)-DC converter with matching impedance strategies [20, 21]. Moreover, since the voltage level produced by a classical electromagnetic generator is usually low, it has to be specially optimized when designing the transducer in order to be useful for powering electronic devices [12, 20] .

In this work $Fe_{61.6}Co_{16.4}Si_{10.8}B_{11.2}$ (Metglas)/polyvinylidene fluoride (PVDF)/Metglas ME [16, 19] optimized energy harvester system [12, 22] is presented with five possible harvesting circuits: full-wave bridge rectifier, and four voltage multipliers with three different number of stages and two distinct configurations (Cockcroft-Walton and Dicksovoltagen).

The ME composite composed by PVDF and Metglas was chosen as basic material due to its stability, flexibility, large electrical resistivity, low losses and to the possibility of the polymer to be processed in different shapes at low processing temperatures [23, 24] as well as due to the high magnetic permeability and piezomagnetic coefficient of Metglas [25, 26]. Additionally Metglas/PVDF composites have previously shown their potential for energy harvesting devices due to their large ME response [16].

6.1.1 Circuit Desing

In order to optimize the output power as a function of load resistance (R_{Load}), five circuits were tested: a full-wave bridge voltage rectifier (R), two Cockcroft-Walton voltage multipliers with one (CW1) and two (CW2) stages and a Dickson voltage multiplier with two and three stages (D2 and D3) (Figure 6.1).

$$V_{Load} \approx \sqrt{2}V_{MErms} - 2V_D$$

$$V_{Load} \approx \left(\sqrt{2}V_{MErms} \cdot 2\right) - 2V_D$$

$$V_{Load} \approx \left(\sqrt{2}V_{MErms} \cdot 4\right) - 4V_D$$

$$V_{Load} \approx \left(\sqrt{2}V_{MErms} \cdot 4\right) - 4V_D$$

$$V_{Load} \approx \left(\sqrt{2}V_{MErms} \cdot 6\right) - 6V_D$$
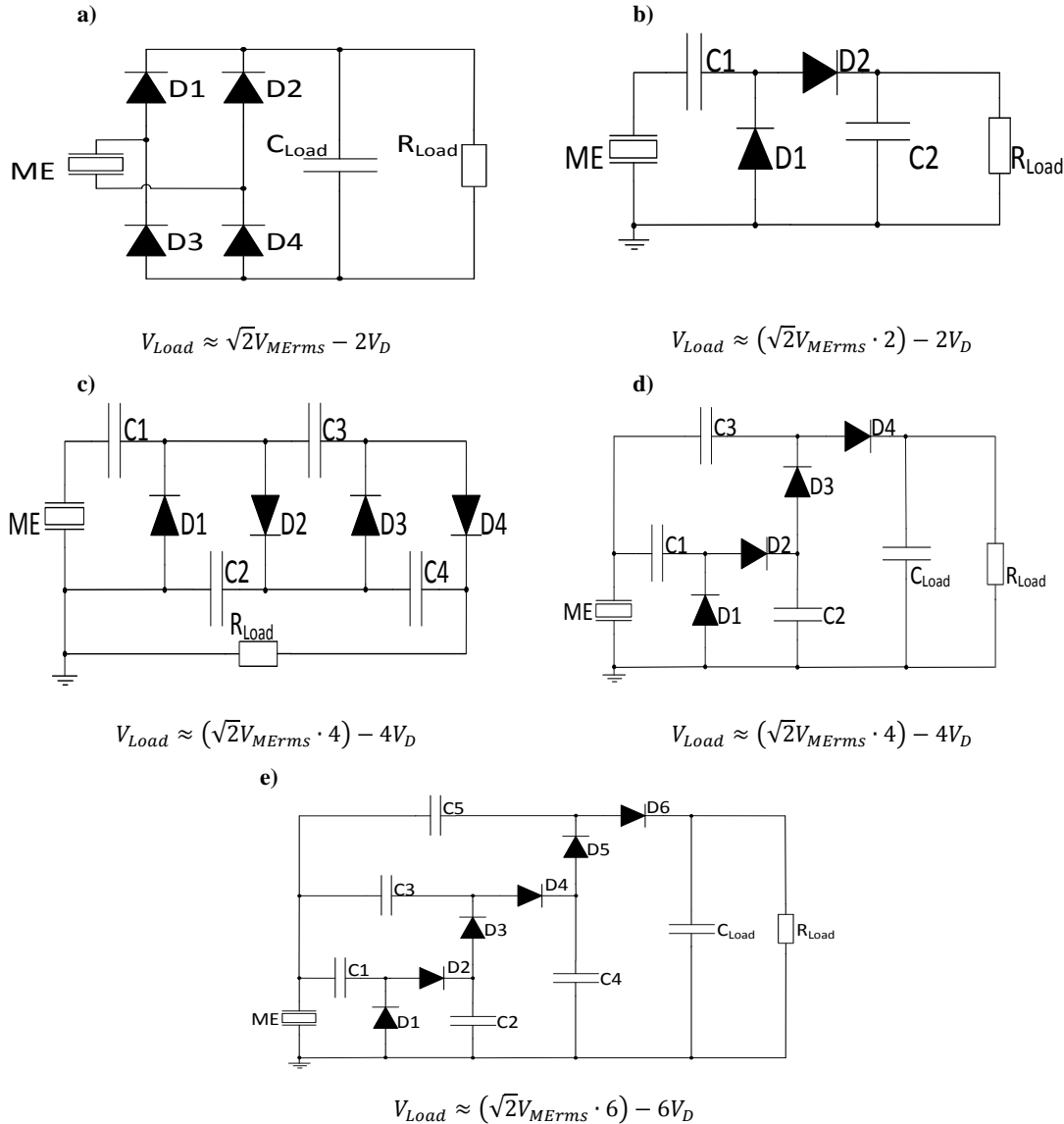
Figure 6.1 - Schematic representation of: a) Full-wave bridge voltage rectifier; b) Cockcroft-Walton voltage multiplier with one stage; c) Cockcroft-Walton voltage multiplier with two stages: d) Dickson voltage multiplier with two stages and e) Dickson voltage multiplier with three stages. VMErms represents the induced voltage in the ME sample, VD represents the forward voltage drop across each diode and VLoad represents the theoretical load voltage.

Schottky diodes (BAT15-03W) and Polyphenylene Sulfide film capacitors (220-680nF) with a surface-mounted device (SMD) package were used for the development of the circuits. These diodes were chosen due to their low forward voltage of ≈100 mV for

a forward current of 10 μA and the capacitors were selected due to its high charge/discharge rate and their low equivalent series resistance[19, 27].

The full-wave bridge voltage rectifier circuit is widely used in energy harvesting systems that converts AC voltage to DC voltage [12, 22]. It shows low energy loss, low complexity and high efficiency. This circuit consists in four Schottky diodes (Figure 6.1a) that convert an AC voltage into a DC voltage [28, 29] using the two half cycles (positive and negative) from the ME composite AC wave output. In the positive half cycle of the AC wave, diodes D1 and D2 are forward biased. In the negative half cycle, diodes D3 and D4 are forward biased [28, 30], converting all negative components into positive ones. In this way, the voltage of the two half-cycles at the end of the bridge are positive and the rectified signal completes a period twice as fast as the input frequency, thus the period is halved and the frequency is doubled.

The smoothing capacitor, at the end of the bridge, should be high enough to reduce the output voltage ripple according to the frequency and the output current as shown in equation.

$$\delta V = \frac{I}{2fC} \tag{19}$$

In this particular case, to provide a continuous wave, it is suitable to use 270 nF capacitance or higher in order to obtain a suitable ripple at the output voltage [31].

The voltage multipliers are an efficient way to convert from AC to DC and simultaneously boost the output voltage [3]. The Cockcroft-Walton circuit is a half-wave rectifier constituted by n stages, each stage formed by two diodes and two capacitors (Figure 6.1b and Figure 6.1c). The even capacitors are called smoothing capacitors and the odd ones, called transfer capacitors [32]. The one stage Cockcroft-Walton voltage multiplier, presented in Figure 6.1b, consists on a clamper constituted by the capacitor C1 and the diode D1 and a peak detector constituted by the capacitor C2 and the diode D2. The clamper signal is measured in the diode D1 and corresponds to the wave input shifted from the negative peak to zero. The peak detector assigns a DC voltage with approximately twice the input peak voltage value. The two stages Cockcroft-Walton voltage multiplier, presented in Figure 6.1c, has a similar behaviour than the previous one but the input signal is increased four times by adding another multiplier level. In order to

calculate the capacitor values it is necessary to define a maximum ripple voltage according to the frequency, the output current and the number of multiplier stages [32].

$$\delta V = \frac{I}{fC} \frac{n(n+1)}{2} \qquad (20)$$

For a ripple below 1 mV, capacitors of 330 nF or higher should be used in the one stage and 560 nF or higher in the two stage Cockcroft-Walton voltage multiplier.

The Dickson voltage multiplier circuit is also a half-wave rectifier, which can be developed with n stages, wherein each stage is formed by two diodes and two capacitors. This circuit is based in the original Dickson charge pump, which is a DC-DC converter. In this circuit the original DC input is shunted to the ground level and the logic control is replaced by the AC input signal to be harvested [33]. In the two stages Dickson voltage multiplier, presented in Figure 6.1d, at the first positive half cycle of the AC wave, C1 is charged with V_{ME}. In the negative half cycle, C1 is pushed to $2V_{ME}$, turning D2 and charging C2 to $2V_{ME}$. Thereafter C3 is charged to $3V_{ME}$. In the last negative half cycle, C3 is pushed to $4V_{ME}$, turning D4 and charging Cload to $4V_{ME}$[34].

In order to calculate the load capacitors it is necessary to define a maximum ripple voltage according to the frequency and the output current [34].

$$\delta V = \frac{I}{fC} \qquad (21)$$

For a ripple below 1 mV, capacitors of 220 nF or higher should be used. The other capacitors are assumed to be equal to the load capacitor.

6.2 Results and Discussion

In this chapter Metglas was used as magnetostrictive layer, and PVDF as piezoelectric layer. The bonding layer is composed by Devcon epoxy resin. Sample preparation is described in subchapter 2.3.4

Prior to the evaluation of the circuit performance, Figure 6.2 shows the ME voltage response of the Metglas/PVDF/Metglas composite that will serve as the basis for the energy harvesting device measured at 0.1 Oe AC field.
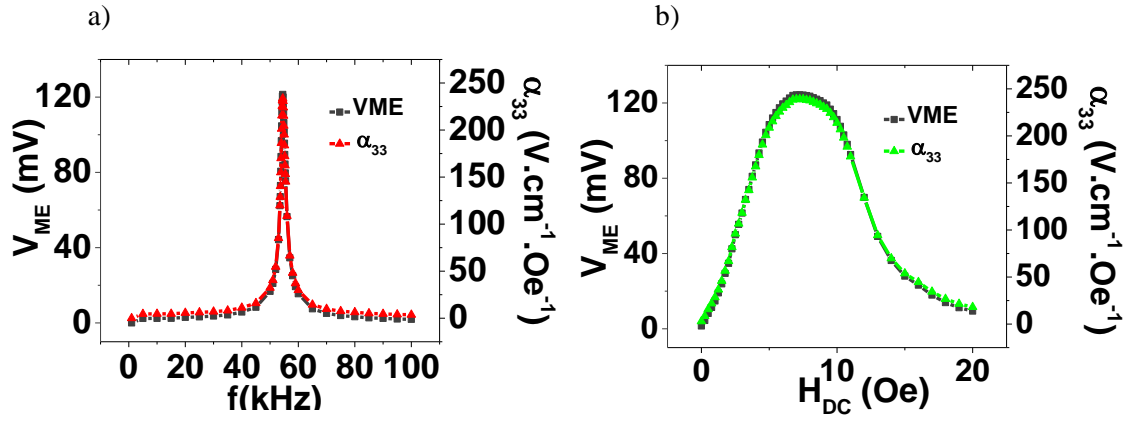
Figure 6.2 - Magnetoelectric voltage response (VME) and ME coefficient α33) as a function of: a) frequency (f) and b) DC magnetic field (HDC).

Figure 6.2 shows that the highest ME voltage response of 125mV is obtained at the 54.5 kHz resonance frequency (3a). Further, the ME voltage increases with the H_{DC} magnetic field up to 7 Oe when the maximum ME voltage is reached (Figure 6.2b). A maximum ME coefficient (α_{33}) of 250 V.cm^{-1}.Oe^{-1} was determined for such DC magnetic field after equation 4,

$$\alpha_{33} = \frac{\Delta V}{t.H_{AC}} \tag{22}$$

where ΔV, t and H_{AC} are the induced ME voltage, the PVDF thickness and the AC magnetic field respectively.

To maximize the load voltage, the ME laminate composite should work at such optimum H_{DC} and at the resonance frequency.

The ME energy harvesting voltage, current and power were then recorded at the highest H_{AC} (0.4 Oe) as a function of the load resistance value, as shown in Figure 6.2.

Figure 6.3 shows the load voltage, current and power versus the load resistance. As expected, the output voltage increases, whereas the output current decreases with increasing load resistance (Figure 6.3 a-b).

98
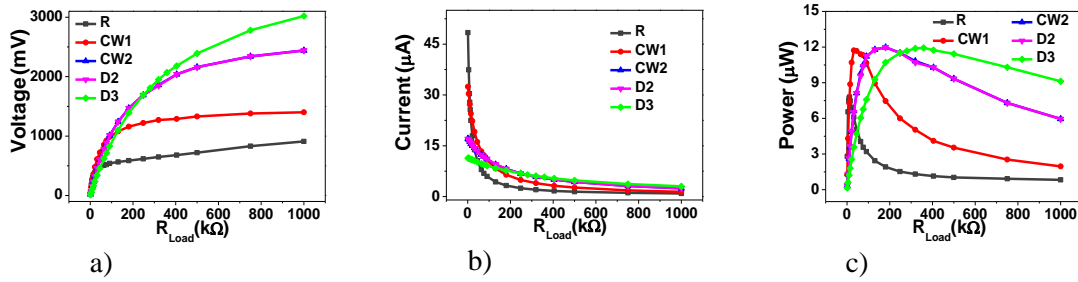
Figure 6.3 - Voltage (a), current (b) and power (c) as a function of the load resistance (R).

The maximum output power is 12 µW for a load resistance of 180 kΩ, obtained on circuits with 2 stages (CW2 and D2). Decreasing the number of stages to 1 (CW1) results in a decrease on the optimal load resistance to 35 kΩ, whereas increasing the number of stages to 3 (D3) results in an increase on the optimal load resistance to 320 kΩ, without substantial changes on the maximum output power (≈12 µW). All features of the Metglas/PVDF/Metglas harvester with the distinct circuits ate summarized on Table I.

Table 6.1 - Maximum theoretical voltage ($V_{DC}T$, from the equations in Figure 6.1), maximum measured voltage ($V_{DC}R$); maximum power generated by the harvester (P_{MAX}) at the optimal load resistance (R_{OPTIM}), current (I_{DC}) and voltage (V_{DC}) values at R_{OPTIM}

Circuit	V_{DCT} [V]	V_{DCR} [V]	P_{max} [µW]	R_{OPTIM} [kΩ]	I_{DC} [µA]	V_{DC} [V]
R	1.28	0.91	7.79	12	25.64	0.30
CW1	1.46	1.40	11.72	32	19.16	0.61
CW2	2.92	2.43	12.15	180	8.21	1.48
D2	2.92	2.44	12.31	180	8.26	1.49
D3	4.38	3.02	11.94	359	5.77	2.07

The average 20% difference found between the V_{DCT} and V_{DCR} values is attributed to the voltage loss in the capacitors, impedance matching problems between the output signal from ME sample and the input of the circuits and ripple issues [35].

The circuit D3 with the highest R_{OPTIM} (359 kΩ) reached the highest V_{DC} (2.07 V) and the lowest I_{DC} (5.77 µA). In turn, the circuit R with the lowest R_{OPTIM} (12 kΩ) led to the lowest V_{DC} (0.30 mV) and the highest I_{DC} (25.64 µA).

Despite the power harvested with CW2 and D2 circuits being almost the same (≈12 µW), the capacitors used in the D2 circuit show the lowest capacity, small size and are cheaper than the ones used on CW2, for such reason, the D2 multiplier circuit was used to study the influence of the AC and DC magnetic fields on the generated power by the harvesting device (Figure 6.4a-b).
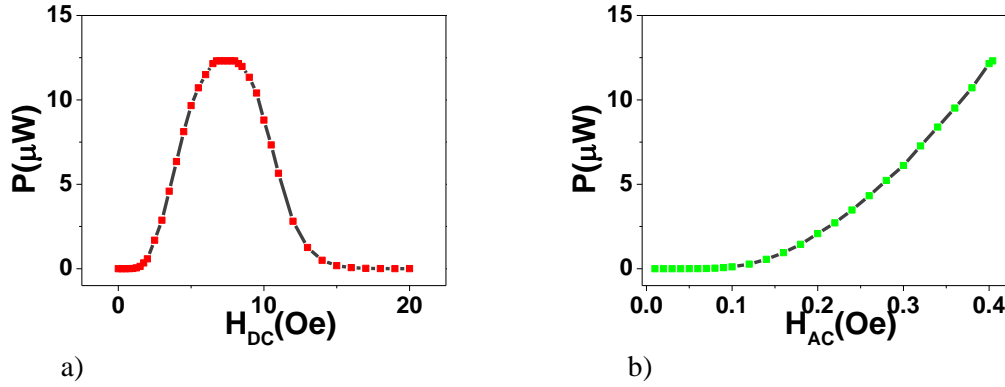
Figure 6.4 - Output power of the ME energy device as a function of the: a) DC magnetic field and b) AC magnetic field.

Increasing DC magnetic field leads to a power generation saturation at 12μW, value that is the highest reported on polymer-based ME materials [19]. This increase up to 7 Oe is due to the increase of the piezomagnetic coefficient. For lager magnetic fields, the power decreases since the Metglas magnetostriction coefficient reaches its saturation value (Figure 6.4 a) [36].

It is observed that increasing AC magnetic fields (Figure 6.4b) leads to an increase of the power output of the device, as increasing AC magnetic field increases the voltage generated by the device following equation 5 [37, 38]:

$$\Delta V = \alpha_{33} \times t \times H_{AC} \qquad (23)$$

In order to compare the obtained values with the ones from the literature, taking into account the generated power (P=12 μW) and volume of the ME laminate (V=1.38×10^{-2} cm^3), the power density (P$_{density}$) was calculated [39, 40]:

$$P_{density} = \frac{P}{V} \qquad (24)$$

It was detemined a P$_{density}$=0.9 mW.cm^{-3} value which is in the same order of magnitude of the highest values reported in the literature on ME energy harvesting materials $\approx$ 1.5 mW.cm^{-3} [19, 40, 41] usefull for applications on microdevices for hard-to-reach locations such as remote/hazardous industrial environments or medically implantable devices. Additionally Metglas/PVDF/Metglas harvesters can find application in more traditional devices including electric window opener, door locking, mirror (optical) and light adjustment systems and tire pressure monitoring [42].

6.3   Conclusions

It has been successfully demonstrated the development of an innovative magnetic harvester based on Metglas/PVDF/Metglas ME laminate composite with optimized harvesting circuits, including full-wave bridge voltage rectifier, Cockcroft-Walton voltage multiplier circuit with 1 and 2 stages, and Dickson voltage multiplier circuit with 2 and 3 stages.

The circuit a Dickson voltage multiplier with three stages and the highest R_{OPTIM} (359 $k\Omega$) leads to the highest V_{DC} (2.07 V) and the lowest I_{DC} (5.77 µA), on the opposite, the full-wave bridge voltage rectifier circuit with the lowest R_{OPTIM} (12 $k\Omega$) generated the lowest V_{DC} (0.30 V) and the highest I_{DC} (25.64 µA).

The highest $Power_{density}$=0.9 mW.cm^{-3} and Power=12 µW values were found for the harvester with a Dickson voltage multiplier with two stages, for a load resistance of 180 $k\Omega$, at 7 Oe DC magnetic field and a 54.5 kHz resonance frequency. The developed system shows this a high application potential in the environmental, building, monitoring, agriculture management and biomedical areas.

6.4 References

[1] S. Roundy, P. K. Wright, and J. Rabaey, "A study of low level vibrations as a power source for wireless sensor nodes," *Computer Communications,* vol. 26, pp. 1131-1144, 2003.

[2] J. Dayou, J. Kim, J. Im, L. Zhai, A. T. C. How, and W. Y. H. Liew, "The effects of width reduction on the damping of a cantilever beam and its application in increasing the harvesting power of piezoelectric energy harvester," *Smart Materials and Structures,* vol. 24, 2015.

[3] N. M. Roscoe and M. D. Judd, "Harvesting energy from magnetic fields to power condition monitoring sensors," *IEEE Sensors Journal,* vol. 13, pp. 2263-2270, 2013.

[4] H. S. Kim, J. H. Kim, and J. Kim, "A review of piezoelectric energy harvesting based on vibration," *International Journal of Precision Engineering and Manufacturing,* vol. 12, pp. 1129-1141, 2011.

[5] G. Kyriakarakos, A. I. Dounis, S. Rozakis, K. G. Arvanitis, and G. Papadakis, "Polygeneration microgrids: A viable solution in remote areas for supplying power, potable water and hydrogen as transportation fuel," *Applied Energy,* vol. 88, pp. 4517-4526, 2011.

[6] R. J. M. Vullers, R. van Schaijk, I. Doms, C. Van Hoof, and R. Mertens, "Micropower energy harvesting," *Solid-State Electronics,* vol. 53, pp. 684-693, 2009.

[7] A. Chiarelli, A. R. Dawson, and A. García, "Parametric analysis of energy harvesting pavements operated by air convection," *Applied Energy,* vol. 154, pp. 951-958, 2015.

[8] A. Bakhshandeh Rostami and A. C. Fernandes, "The effect of inertia and flap on autorotation applied for hydrokinetic energy harvesting," *Applied Energy,* vol. 143, pp. 312-323, 2015.

[9] H. Uluşan, K. Gharehbaghi, O. Zorlu, A. Muhtaroǧlu, and H. Külah, "A fully integrated and battery-free interface for low-voltage electromagnetic energy harvesters," *IEEE Transactions on Power Electronics,* vol. 30, pp. 3712-3719, 2015.

[10] S. Zhou, J. Cao, D. J. Inman, J. Lin, S. Liu, and Z. Wang, "Broadband tristable energy harvester: Modeling and experiment verification," *Applied Energy,* vol. 133, pp. 33-39, 2014.

[11] G. Zhou, L. Huang, W. Li, and Z. Zhu, "Harvesting ambient environmental energy for wireless sensor networks: A survey," *Journal of Sensors,* vol. 2014, pp. 1-20, 2014.

[12] P. Li, Y. Wen, P. Liu, X. Li, and C. Jia, "A magnetoelectric energy harvester and management circuit for wireless sensor network," *Sensors and Actuators, A: Physical,* vol. 157, pp. 100-106, 2010.

[13]   J. W. Matiko, N. J. Grabham, S. P. Beeby, and M. J. Tudor, "Review of the application of energy harvesting in buildings," *Measurement Science and Technology,* vol. 25, 2014.

[14]   J. Han, J. Hu, S. X. Wang, and J. He, "Magnetic energy harvesting properties of piezofiber bimorph/NdFeB composites," *Applied Physics Letters,* vol. 104, 2014.

[15]   Y. Qi, N. T. Jafferis, K. Lyons Jr, C. M. Lee, H. Ahmad, and M. C. McAlpine, "Piezoelectric ribbons printed onto rubber for flexible energy conversion," *Nano Letters,* vol. 10, pp. 524-525, 2010.

[16]   P. Martins and S. Lanceros-Méndez, "Polymer-Based Magnetoelectric Materials," *Advanced Functional Materials,* vol. 23, pp. 3371-3385, 2013.

[17]   C. Y. Sue and N. C. Tsai, "Human powered MEMS-based energy harvest devices," *Applied Energy,* vol. 93, pp. 390-403, 2012.

[18]   S. Ducharme, T. J. Reece, C. M. Othon, and R. K. Rannow, "Ferroelectric polymer Langmuir-Blodgett films for a nonvolatile memory applications," *IEEE Transactions on Device and Materials Reliability,* vol. 5, pp. 720-735, 2005.

[19]   A. Lasheras, J. Gutiérrez, S. Reis, D. Sousa, M. Silva, P. Martins*, et al.*, "Energy harvesting device based on a metallic glass/PVDF magnetoelectric laminated composite," *Smart Materials and Structures,* vol. 24, 2015.

[20]   E. Arroyo, A. Badel, and F. Formosa, "Energy harvesting from ambient vibrations: Electromagnetic device and synchronous extraction circuit," *Journal of Intelligent Material Systems and Structures,* vol. 24, pp. 2023-2035, 2013.

[21]   T. C. Huang, M. J. Du, Y. C. Kang, R. H. Peng, K. H. Chen, Y. H. Lin*, et al.*, "120% Harvesting energy improvement by maximum power extracting control for high sustainability magnetic power monitoring and harvesting system," *IEEE Transactions on Power Electronics,* vol. 30, pp. 2262-2274, 2015.

[22]   A. Tabesh and L. G. Fréchette, "A low-power stand-alone adaptive circuit for harvesting energy from a piezoelectric micropower generator," *IEEE Transactions on Industrial Electronics,* vol. 57, pp. 840-849, 2010.

[23]   M. Silva, S. Reis, C. S. Lehmann, P. Martins, S. Lanceros-Mendez, A. Lasheras*, et al.*, "Optimization of the magnetoelectric response of poly(vinylidene fluoride)/epoxy/vitrovac laminates," *ACS Appl. Mater. Interfaces,* vol. 5, pp. 10912-10919, 2013.

[24]   P. Martins, A. C. Lopes, and S. Lanceros-Mendez, "Electroactive phases of poly(vinylidene fluoride): Determination, processing and applications," *Progress in Polymer Science,* vol. 39, pp. 683-706, 2014.

[25]   J. Zhai, S. Dong, Z. Xing, J. Li, and D. Viehland, "Giant magnetoelectric effect in Metglas/polyvinylidene-fluoride laminates," *Applied Physics Letters,* vol. 89, 2006.

[26]   A. Lasheras, J. Gutiérrez, J. M. Barandiarán, D. Shishkin, and A. Potapov, "Parameters Affecting the Magnetoelectric Response of Magnetostrictive/Piezoelectric Polymer Laminates," in *Key Engineering Materials*, 2015, pp. 40-44.

[27] J. Liu, P. Fei, J. Song, X. Wang, C. Lao, R. Tummala, *et al.*, "Carrier density and schottky barrier on the performance of DC nanogenerator," *Nano Letters,* vol. 8, pp. 328-332, 2008.

[28] L. Karthikeyan and B. Amrutur, "Signal-powered low-drop-diode equivalent circuit for full-wave bridge rectifier," *IEEE Transactions on Power Electronics,* vol. 27, pp. 4192-4201, 2012.

[29] G. D. Szarka, B. H. Stark, and S. G. Burrow, "Review of power conditioning for kinetic energy harvesting systems," *IEEE Transactions on Power Electronics,* vol. 27, pp. 803-815, 2012.

[30] H. Kim, S. Priya, H. Stephanou, and K. Uchino, "Consideration of impedance matching techniques for efficient piezoelectric energy harvesting," *IEEE Transactions on Ultrasonics, Ferroelectrics, and Frequency Control,* vol. 54, pp. 1851-1858, 2007.

[31] A. Bayrashev, W. P. Robbins, and B. Ziaie, "Low frequency wireless powering of microsystems using piezoelectric- magnetostrictive laminate composites," *Sensors and Actuators, A: Physical,* vol. 114, pp. 244-249, 2004.

[32] C. G. H. Maennel, "Improvement in the modelling of a half-wave Cockroft-Walton voltage multiplier," *Review of Scientific Instruments,* vol. 84, 2013.

[33] R. E. Barnett, J. Liu, and S. Lazar, "A RF to DC voltage conversion model for multi-stage rectifiers in UHF RFID transponders," *IEEE Journal of Solid-State Circuits,* vol. 44, pp. 354-370, 2009.

[34] J. Yi, W. H. Ki, and C. Y. Tsui, "Analysis and design strategy of UHF micro-power CMOS rectifiers for micro-sensor and RFID applications," *IEEE Transactions on Circuits and Systems I: Regular Papers,* vol. 54, pp. 153-166, 2007.

[35] C. T. Pan, M. C. Cheng, C. M. Lai, and P. Y. Chen, "Current-ripple-free module integrated converter with more precise maximum power tracking control for PV energy harvesting," *IEEE Transactions on Industry Applications,* vol. 51, pp. 271-278, 2015.

[36] X. W. Dong, B. Wang, K. F. Wang, J. G. Wan, and J. M. Liu, "Ultra-sensitive detection of magnetic field and its direction using bilayer PVDF/Metglas laminate," *Sensors and Actuators A: Physical,* vol. 153, pp. 64-68, 6/25/ 2009.

[37] S. Dong, J. F. Li, and D. Viehland, "Longitudinal and transverse magnetoelectric voltage coefficients of magnetostrictive/piezoelectric laminate composite: Theory," *IEEE Transactions on Ultrasonics, Ferroelectrics, and Frequency Control,* vol. 50, pp. 1253-1261, 2003.

[38] P. Martins, A. Lasheras, J. Gutierrez, J. M. Barandiaran, I. Orue, and S. Lanceros-Mendez, "Optimizing piezoelectric and magnetoelectric responses on CoFe 2O4/P(VDF-TrFE) nanocomposites," *J. Phys. D: Appl. Phys.,* vol. 44, p. 495303, 2011.

[39] X. Wang, S. Wang, Y. Yang, and Z. L. Wang, "Hybridized Electromagnetic–Triboelectric Nanogenerator for Scavenging Air-Flow Energy to Sustainably Power Temperature Sensors," *ACS Nano,* vol. 9, pp. 4553-4562, 2015/04/28 2015.

[40] S. D. Moss, O. R. Payne, G. A. Hart, and C. Ung, "Scaling and power density metrics of electromagnetic vibration energy harvesting devices," *Smart Materials and Structures,* vol. 24, 2015.

[41] Y. Zhou, D. J. Apo, and S. Priya, "Dual-phase self-biased magnetoelectric energy harvester," *Applied Physics Letters,* vol. 103, 2013.

[42] V. Bhatnagar and P. Owende, "Energy harvesting for assistive and mobile applications," *Energy Science & Engineering,* vol. 3, pp. 153-173, 2015.
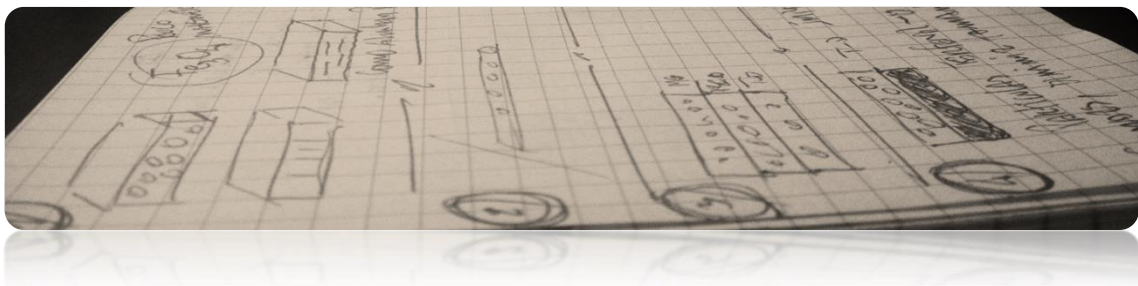
7 Determination of the magnetostrictive response of nanoparticles via magnetoelectric measurements

7.1 Introduction

The coupling between the magnetic and electrical orders of matter in multiferroic or magnetoelectric (ME) materials holds promise for conceptually novel electronic devices [1-4].

Due to the high room temperature ME response, the possibility of using conventional low-temperature processing into a variety of forms, such as thin sheets or molded shapes, and improved mechanical properties, polymer-based ME nanocomposites, constituted by piezoelectric polymers and magnetostrictive nanoparticles are attracting increased attention when compared with single-phase ME materials or ceramic-based ME materials[5-7].

Additionally, after the macroscopic characterization of the ME composites and supported by the theoretical description of the ME response as a function of both piezoelectric and magnetostrictive properties of the polymer-based ME nanocomposites, a new, powerful and innovative tool can be developed for the determination of the magnetostriction nanoparticles. Since such determination achieved in the nano-size scale of the particles, it represents an obvious advantage over the currently used techniques, showing therefore large application potential in areas such as energy, sensor and actuator development or in the biomedical field [8, 9].

Magnetostriction is defined as the phenomenon where the dimensions or shape of a material change in response to an external applied magnetic field [10, 11]. It is quantified as the fractional change in the length (l), $\lambda = \Delta l/l$, when a field is applied along the easy axis of magnetization and is typically in the order of 10^{-6} [12, 13].

Materials with large magnetostriction, λ, are extensively used in sensors, actuators, micro-electromechanical systems and energy-harvesters, among others[13]. In this way, the magnitude of the magnetostrictive strain of a magnetic material is of great concern for the development and application on innovative technological devices[8]. The magnetostriction of a material can be measured by direct or indirect methods. Direct methods enable the magnetostrictive strain to be measured as a function of the applied field, whereas indirect methods are suitable only for measuring the saturation magnetostriction λsat[14].

Direct methods involve measurements performed with strain gauges [15, 16], capacitance transducers[17, 18] or interferometers[19, 20], being the capacitance method

one of the most sensitive techniques [17, 21]. Nevertheless all these methods have the disadvantage that they require a specific and difficult sample preparation, relaying in confidence coupling. Further, those methods have limited sensitivity ($\Delta\lambda/\lambda o \approx 1\times10^{-6}$) and λ needs to be determined from measurements performed parallel and perpendicular to the applied magnetic external field[17].

On the other hand, indirect measurements are techniques based on the Villari effect, which is the inverse of the Joule magnetostriction (the stress applied to the sample will produce a change in the magnetic permeability of the sample)[14]. These techniques are designed as indirect measurements of the magnetostriction as they do not produce a direct measure of the sample length change. Several techniques based on this effect have been used in the measurement of magnetostriction such as the ferromagnetic resonance[22, 23], the Becker-Kersten method[24], the Small angle magnetization rotation (SAMR) method[14, 25] and the cantilever deflection method[10]. However, the above mentioned indirect methods are limited by the maximum strain and anisotropy of the samples[26].

Although some sensitive techniques have been developed to determine the bulk material's magnetostriction , for some applications that require nanoscale materials such as such as cancer research, neurology, brain functions, pain treatment, magnetologic gates , memory devices or nano-actuators is very important to know the magnetostrictive properties of material in the nano-size scale[8, 27]. Until now, the magnetostrictive properties of such nanomaterials were mainly determined by compacting the nanoparticles into pellets or pastilles and measuring the deformation of the resulting agglomerate [28, 29]. Nevertheless it is well known that such compression has a large influence on the magnetostrictive properties of the material, hindering the quality of the obtained results since at the nanoscale regime, the particles are typically single domain and their properties are mainly governed by particle size, size distribution, shape, surface effects and dipolar interactions [17, 29].

7.1.1 Theoretical background

In this study a new method is proposed for the determination of the magnetostriction of magnetic nanoparticles. The method is based on the Van den Boomgaard *et al.* [30] theory and the magnetoelectric (ME) measurements of polymer-based ME composites. Due to the soft matrix of the resulting composite, no hindering on the nanofiller deformation is expected[31].

The ME effect, at the basis of this new magnetostriction determination method, is defined as the variation of the electrical polarization (*P*) of a material in the presence of an applied magnetic field (*H*);

$$\Delta P = \alpha \times \Delta H \qquad (25)$$

where α is the ME coupling coefficient[32].

In multiferroic (MF) single-phase materials this effect is intrinsic and attributed to the coupling of magnetic moments and electric dipoles[33]. In multiple-phase ME materials, as the ones that will be used in this study, this effect is extrinsic, emerging in an indirect form, through an elastic mediated coupling between a piezoelectric phase and a magnetostrictive phase [1, 5].

In such multiferroic ME composites, α can be determined by:

$$\alpha = \frac{\Delta V}{B_{AC} \times t} \qquad (26)$$

where ΔV is the ME voltage generated in the composite, B_{AC} the AC magnetic field and *t* the thickness of the ME composite[5, 32].

Van den Boomgaard *et al.* [30] assuming the existence of perfect coupling between the phases, proposed that ME voltage coefficient can be determined by:

$$(\alpha)_{composite} = \left(\frac{dx}{dH}\right)_{composite} \times \left(\frac{dE}{dx}\right)_{composite} =$$
$$m_V \times \left(\frac{dE}{dx}\right)_{magnetostrictive} \times \left(\frac{dE}{dx}\right)_{piezoelectric} \qquad (27)$$

Where (dx/dH) is the change in dimension per unit magnetic field, (dE/dx) is the change in dimension per unit electric field and m_V is the volume fraction of the magnetostrictive material.

Five years later, Zubkov *et al.* [34] provided a modified version of equation 1, in which included the strain derivative (dS/dH) parameter in the quantification of α :

$$(\alpha)_{composite} = m_V \times \left(\frac{dS}{dH}\right)_{magnetostrictive} \times (1-m_V)\left(\frac{dE}{dS}\right)_{piezoelectric} \qquad (28)$$

Based on equations 3 and 4 and knowing that $dE = dE_3 = g_{33}dT_3$ and $dS = (dT_3)/C_{33}$ (where g_{33} and C_{33} are the piezoelectric voltage and stiffness coefficients respectively of the piezoelectric phase, T is the stress and S is the strain) Ryu *et al.*[35] related the ME voltage coefficient α with the strain derivative by the following formula:

$$\alpha = m_V \times \left(\frac{dS}{dH}\right)_{magnetostrictive} \times (1-m_V)\left(g_{33} \times C_{33}\right)_{piezoelectric} \qquad (29)$$

Knowing that $g_{33} = d_{33}/(\varepsilon_0 \times \varepsilon)$ (where d_{33}, ε_0 and ε are the piezoelectric voltage coefficient, the vacuum permittivity and the relative permittivity of the material, respectively) and that $C_{33} = (E_Y \times l \times w)/t$ (where E_Y, l, w and t are the Young's modulus, length, width and thickness of the composite, respectively) the strain derivative (dS/dH) can be determined by:

$$\left(\frac{dS}{dH}\right) = \frac{\alpha}{m_V \times (1-m_V) \times \left(\frac{d_{33}}{\varepsilon_0 \times \varepsilon} \times \frac{E_Y \times l \times w}{t}\right)_{piezoelectric}} \qquad (30)$$

Assuming that λ increases almost linearly with increasing magnetic field, until saturation was reached [10, 36, 37], λs can be calculated by:

$$\lambda_S = \left(\frac{dS}{dH}\right) \times B_S \qquad (31)$$

where B_S is the magnetic field at which the saturation is achieved.

In this way, after experimental determination of α, m_V, d_{33}, ε, E_Y, l, w, and t, it is possible to accurately calculate λs and dS/dH.

7.2 Sample preparation and composite parameter determination

The proposed method is based on the simple preparation method and characterization of polymer-based ME nanocomposites [5, 38] (Figure 7.1). In these composites, the desired content of magnetostrictive nanoparticles whose magnetostrictive coefficient is intended to be determined, is mixed with an efficient solvent and a piezoelectric polymer (Step 1). After the polymer dissolution in the solvent and proper mixing with the magnetostrictive nanoparticles, a magnetoelectric film is obtained by depositing the solution in a clean glass substrate and through the solvent evaporation (Step 2). The ME film is then poled by corona in order to improve the piezoelectric response and, as a consequence, the ME response (Step 3). Examples in which this procedure has been applied can be found in [39] and[40] for the first step, [41] and [42] for the second and [43] and [44] for the last step.
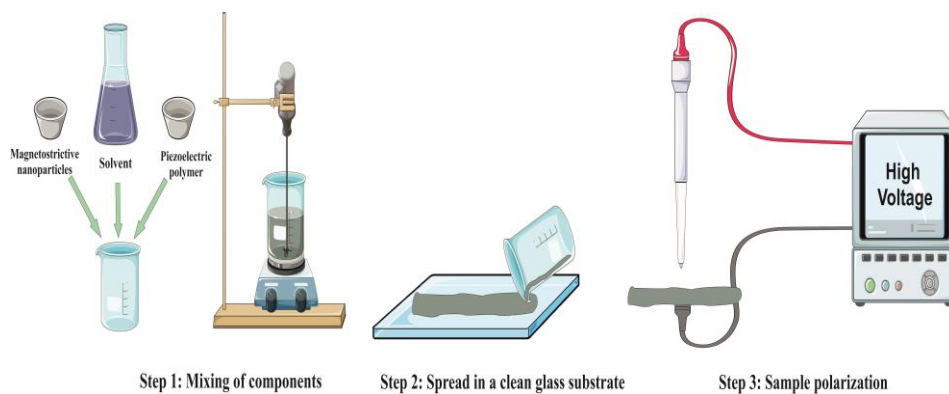
Figure 7.1 - Three-step method to obtain the ME nanocomposite film. Step1-Mixing; Step2-Film processing; Step3-Poling.

This careful, simple and easily reproducible experimental procedure ensures that the magnetostriction will be determined with well-dispersed nanoparticles, eliminating undesirable factors such as the ones related with the agglomeration of nanoparticles.

After obtaining the ME film, the ME response of the sample, $\alpha,$ can be obtained following the procedure indicated in [38, 45].

The ME response of the composite is typically studied as a function of the frequency [36, 38], filler content [5, 46] and DC magnetic field [35, 36]. Together with the ME characterization, such the one schematically shown in Figure 7.2a, it is also necessary to determine the piezoelectric response (d_{33} – Figure 7.2b), the dielectric constant (ε' – Figure 7.2c) and the Young's modulus (E_Y – Figure 7.2d) of the polymer nanocomposite.

113
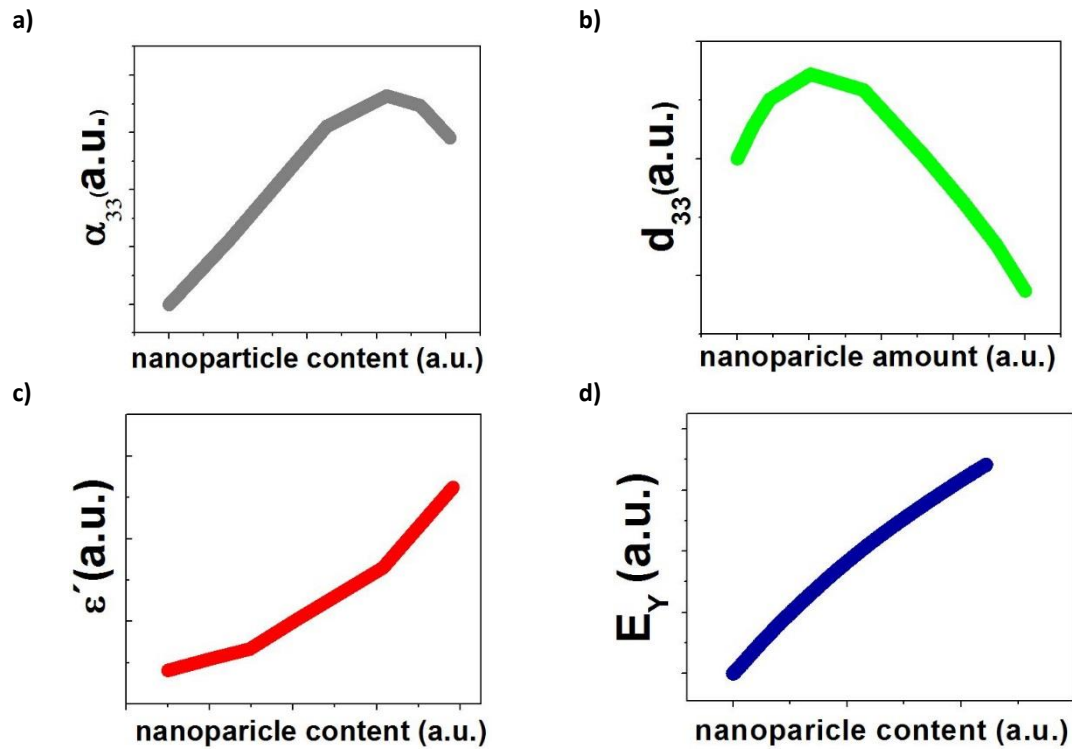
Figure 7.2 - Measurements needed to determine the λ of nanoparticles. Typical ME (a), piezoelectric (b) and dielectric (c) responses for ME nanocomposites as a function of the magnetostrictive nanoparticle content. d) Typical dependence of the ME nanocomposite Young's Modulus on the magnetostrictive nanoparticle content.

As represented in Figure 7.2, the above mentioned parameters depend on the magnetostrictive nanoparticle content within the polymer matrix. In this way, the method can be validated also by evaluating the magnetostriction at different filler contents.

After α, d_{33}, ε and E_Y are obtained and knowing m_V, l, w, and t it is possible to precisely determine λs and dS/dH by using equations 5-7.

7.3 Validation of the proposed methodology

To validate the novel proposed method, data from literature corresponding to Poly(vinylidene fluoride-trifluoroethylene) (P(VDF-TrFE)) composites with CoFe2O4 (CFO)[38] and Ni0.5Zn0.5 Fe2O4 (NZO)[45] magnetostrictive nanoparticles were used to ensure that this method is compatible to a wide range of magnetostrictive coefficients. P(VDF-TrFE) was chosen since it shows one of the highest piezoelectric responses among the small class of polymers that exhibits piezoelectricity, it is chemically inert, always crystallizes in the piezoelectric phase for specific copolymer contents between 50 and 80%, provides a soft matrix to the magnetostrictive nanoparticles and is the most widely used polymer for ME nanocomposite preparation[5, 47, 48].

Data from Bis-2-cyano-3-(3-aminophenoxy)phenoxybenzene (diamine 2CN)/1,3-Bis(3-aminophenoxy)benzene (diamine 0CN)/CFO multiferroic composite with 10 wt.% of CFO were also used in order to validate the method for a distinct piezoelectric polymer matrix[49].

Additionally, for all nanocomposites indicated above, α, mV, d33, ε, EY, l, w, and t values used to determine λs and dS/dH (Table 7.1) are available on the literature.

Table 7.1 - α, m_V, d_{33}, ε, E_Y, l, w, and t values used to determine λs and dS/dH. The reference of the used data is provided, together with the piezoelectric matrix, the magnetostrictive nanoparticle, the comparison with the λ obtained in bulk or in pellets and the difference between those values.

Piezo matrix	Nanoparticle	α	m_V	Ref	d_{33} pC.N^{-1}	ε	E_Y GPa	$w \times l \times t$ (mm×mm×µm)	ds/dH ×10^{-9}	λ ppm	$\overline{\lambda}$ bulk/pellet	Difference %
PVDF-TrFE	CFO	31.0	0.26	[38]	15	22	1.55	6.5×12.5×50	1.05	208	169[50]	19
		17.0	0.08		15	13	1.14	6.5×12.5×50	1.06	212		20
		3.25	0.02		23	11	0.50	6.5×12.5×50	1.09	217		22
	NZO	1.25	0.08	[45]	15	12	1.14	9.0×21.0×50	0.04	14	11[51]	21
0CN/2CN	CFO	0.90	0.06	[49]	11	12	1.16	5×5×150	1.00	200	169[50]	16

Table 7.1 reveals that the obtained magnetostriction is ($\approx$20%) higher for nanoparticles than their bulk sized counterparts pellets or pastilles obtained from the literature. It is to notice that the effect of the magnetostriction being larger in nanoparticles has been already reported [12, 52]. Such differences are explained by the surface effects and dipolar interactions between the particles as well as the clamping on pellets or pastilles. The ME coupling determination of the magnetostriction, contrary to previous techniques, is not affected by those effects, since the magnetostriction is determined when the nanoparticles are well distributed in a soft polymer matrix and it is not influenced by factors related to the nanoparticles compression [52].

Additionally, Table 1 allows to plot the determined λ as a function of weight percentage (wt.%) of CFO (Figure 7.3).
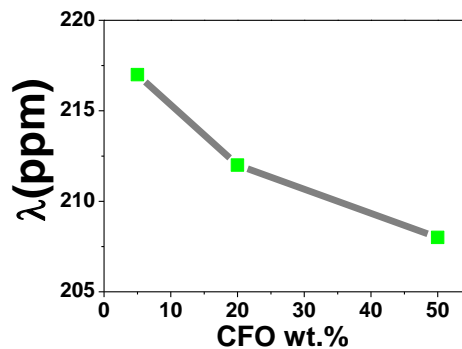

Figure 7.3 - λ as a function of CFO wt.%. Influence of the CFO wt% on the determined CFO nanoparticle magnetostrictive properties.

Figure 7.3 reveals a small decrease in λ with increasing wt% of CFO, such behavior can be related with a small agglomeration of nanoparticles causing a decrease in the determined magnetostriction. In this way, in order to obtain reliable λ values and to avoid undesired effects such as the disruption of the polymer matrix, clusters, agglomerations and nanoparticles compression, which will decrease the determined λ value, the proposed method should be ideally used on polymer nanocomposites with nanoparticles $m_v \leq 0.08$[38, 45, 52, 53].

7.4   Conclusions

In summary, this work successfully demonstrates that the magnetostriction of nanoparticles can be accurately determined based on the ME effect measured on polymer-based ME composite materials. Further, this simple and versatile method allows the λ determination on several piezoelectric matrixes and magnetostrictive fillers, matching the latest industry and science demands since it determines the magnetostrictive properties of particles on their nano-sized and dispersed state.

7.5 References

[1] Y. Geng, H. Das, A. L. Wysocki, X. Wang, S. W. Cheong, M. Mostovoy*, et al.*, "Direct visualization of magnetoelectric domains," *Nat Mater,* vol. 13, pp. 163-167, 02//print 2014.

[2] J. M. Hu, T. Yang, J. Wang, H. Huang, J. Zhang, L. Q. Chen*, et al.*, "Purely electric-field-driven perpendicular magnetization reversal," *Nano Letters,* vol. 15, pp. 616-622, 2015.

[3] H. K. D. Kim, L. T. Schelhas, S. Keller, J. L. Hockel, S. H. Tolbert, and G. P. Carman, "Magnetoelectric control of superparamagnetism," *Nano Letters,* vol. 13, pp. 884-888, 2013.

[4] Y. Y. Liu, R. K. Vasudevan, K. Pan, S. H. Xie, W. I. Liang, A. Kumar*, et al.*, "Controlling magnetoelectric coupling by nanoscale phase transformation in strain engineered bismuth ferrite," *Nanoscale,* vol. 4, pp. 3175-3183, 2012.

[5] P. Martins and S. Lanceros-Méndez, "Polymer-Based Magnetoelectric Materials," *Advanced Functional Materials,* vol. 23, pp. 3371-3385, 2013.

[6] H. Miao, X. Zhou, S. Dong, H. Luo, and F. Li, "Magnetic-field-induced ferroelectric polarization reversal in magnetoelectric composites revealed by piezoresponse force microscopy," *Nanoscale,* vol. 6, pp. 8515-8520, 2014.

[7] G. Caruntu, A. Yourdkhani, M. Vopsaroiu, and G. Srinivasan, "Probing the local strain-mediated magnetoelectric coupling in multiferroic nanocomposites by magnetic field-assisted piezoresponse force microscopy," *Nanoscale,* vol. 4, pp. 3218-3227, 2012.

[8] R. Adhikari, A. Sarkar, M. V. Limaye, S. K. Kulkarni, and A. K. Das, "Variation and sign change of magnetostrictive strain as a function of Ni concentration in Ni-substituted ZnFe 2O 4 sintered nanoparticles," *J. Appl. Phys.,* vol. 111, p. 073903 2012.

[9] X. Liu, S. Liu, M. G. Han, L. Zhao, H. Deng, J. Li*, et al.*, "Magnetoelectricity in CoFe2O4 nanocrystal-P(VDF-HFP) thin films," *Nanoscale Research Letters,* vol. 8, pp. 1-10, 2013.

[10] D. Hunter, W. Osborn, K. Wang, N. Kazantseva, J. Hattrick-Simpers, R. Suchoski*, et al.*, "Giant magnetostriction in annealed Co1-xFex thin-films," *Nat. Commun.,* vol. 2, p. 518, 2011.

[11] M. Rotter, Z. S. Wang, A. T. Boothroyd, D. Prabhakaran, A. Tanaka, and M. Doerr, "Mechanism of spin crossover in LaCoO3 resolved by shape magnetostriction in pulsed magnetic fields," *Sci. Rep.,* vol. 4, p. 7003, 11/11/online 2014.

[12] G. Balaji, R. A. Narayanan, A. Weber, F. Mohammad, and C. S. S. R. Kumar, "Giant magnetostriction in magnetite nanoparticles," *Mater. Sci. Eng. R,* vol. 177, pp. 14-18, 1/25/ 2012.

[13]   H. Wang, Y. N. Zhang, R. Q. Wu, L. Z. Sun, D. S. Xu, and Z. D. Zhang, "Understanding strong magnetostriction in Fe100−xGax alloys," *Sci. Rep.,* vol. 3, p. 3521, 12/17/online 2013.

[14]   N. B. Ekreem, A. G. Olabi, T. Prescott, A. Rafferty, and M. S. J. Hashmi, "An overview of magnetostriction, its use and methods to measure these properties," *J. Mater. Eng. Perform.,* vol. 191, pp. 96-101, 8/1/ 2007.

[15]   G. S. N. Rao, O. E. Caltun, K. R. Rao, P. S. V. Subba Rao, and B. Parvatheeswara Rao, "Improved magnetostrictive properties of Co-Mn ferrites for automobile torque sensor applications," *J. Magn. Magn. Mater.,* vol. 341, pp. 60-64, 2013.

[16]   G. Shilyashki, H. Pfützner, F. Hofbauer, D. Sabic, and V. Galabov, "Magnetostriction distribution in a model transformer core," *J. Elec. Eng. ,* vol. 61, pp. 130-132, 2013.

[17]   R. Grössinger, H. Sassik, D. Holzer, and N. Pillmayr, "Magnetic characterization of soft magnetic materials—experiments and analysis," *J Magn Magn Mater* vol. 254–255, pp. 7-13, 1// 2003.

[18]   R. S. Turtelli, C. Grijalva, F. Kubel, D. Geist, R. Grössinger, M. Kriegisch, *et al.,* "Low magnetostriction in Fe100-xMnx (x 45, 48, 50, 52, 55) alloys," *IOP Conf. Ser., Mater. Sci. Eng.,* vol. 60, p. 012006, 2014.

[19]   Y. G. Xu and X. G. Chen, "On relationship between annealing treatment and magnetostriction behavior of Fe-16Cr-2.5Mo damping alloy," *J. Alloy. Comp.,* vol. 582, pp. 364-368, 2014.

[20]   S. G. Ghalamestani, T. G. D. Hilgert, L. Vandevelde, J. J. J. Dirckx, and J. A. A. Melkebeek, "Magnetostriction measurement by using dual heterodyne laser interferometers," *IEEE Trans. Magn.,* vol. 46, pp. 505-508, 2010.

[21]   A. Devishvili, M. Rotter, A. Lindbaum, A. Barcza, A. Hiess, W. Schmidt, *et al.,* "Measuring magnetostriction with neutrons," *J. Phys. Condens. Matter,* vol. 20, p. 104218, 2008.

[22]   K. Nesteruk, R. Zuberek, S. Piechota, M. W. Gutowski, and H. Szymczak, "Thin film's magnetostriction investigated by strain modulated ferromagnetic resonance at low temperature," *Meas. Sci. Technol,* vol. 25, p. 075502, 2014.

[23]   J. Lou, R. E. Insignares, Z. Cai, K. S. Ziemer, M. Liu, and N. X. Sun, "Soft magnetism, magnetostriction, and microwave properties of FeGaB thin films," *Appl. Phys. Lett.,* vol. 91, p. 182504, 2007.

[24]   T. H. O'Dell, "Magnetostriction measurements on amorphous ribbons by the Becker-Kersten method," *Phys. Status Solidi A,* vol. 68, pp. 221-226, 1981.

[25]   S. Kaloshkin, A. Talaat, M. Ipatov, V. Zhukova, J. M. Blanco, M. Churyukanova, *et al.,* "Correlation between the magnetostriction constant and thermal properties of soft magnetic microwires," *Phys. Status Solidi A,* vol. 211, pp. 1083-1086, 2014.

[26]   J. P. Jay, F. Le Berre, S. P. Pogossian, and M. V. Indenbom, "Direct and inverse measurement of thin films magnetostriction," *J Magn Magn Mater,* vol. 322, pp. 2203-2214, 2010.

118

[27]   L. M. a. G. C. Armin Kargol, *Biomedical Applications of Multiferroic Nanoparticles*. L.A.: InTech, 2012.

[28]   R. Adhikari, A. Sarkar, and A. K. Das, "A versatile cantilever beam magnetometer for ex situ characterization of magnetic materials," *Rev. Sci. Instrum.,* vol. 83, p. 013903, 2012.

[29]   A. Muhammad, R. Sato-Turtelli, M. Kriegisch, R. Grössinger, F. Kubel, and T. Konegger, "Large enhancement of magnetostriction due to compaction hydrostatic pressure and magnetic annealing in CoFe2O4," *J. Appl. Phys.,* vol. 111, p. 013918, 2012.

[30]   J. Van Den Boomgaard, A. M. J. G. Van Run, and J. Van Suchtelen, "Magnetoelectricity in piezoelectric-magnetostrictive composites," *Ferroelectrics,* vol. 10, pp. 295-298, 1975.

[31]   L. Dobrzański, A. Tomiczek, and A. Pacyna, "Properties of the magnetostrictive composite materials with the polyurethane matrix reinforced with Terfenol-D particles," *Manuf. Eng.,* vol. 55, pp. 316-322, 2012.

[32]   W. Eerenstein, N. D. Mathur, and J. F. Scott, "Multiferroic and magnetoelectric materials," *Nature,* vol. 442, pp. 759-65, 2006.

[33]   I. Kézsmárki, D. Szaller, S. Bordács, V. Kocsis, Y. Tokunaga, Y. Taguchi, *et al.*, "One-way transparency of four-coloured spin-wave excitations in multiferroic materials," *Nat Commun,* vol. 5, p. 3203, 02/03/online 2014.

[34]   A. S. Zubkov, "Impulsive Piezoceramic Generators With Magnetostrictive Drive," *Elec. Tech. USSR,* vol. 00134155, pp. 59-78, 1978.

[35]   J. Ryu, S. Priya, K. Uchino, and H. E. Kim, "Magnetoelectric effect in composites of magnetostrictive and piezoelectric materials," *J. Electroceram.,* vol. 8, pp. 107-119, 2002.

[36]   E. Lage, C. Kirchhof, V. Hrkac, L. Kienle, R. Jahns, R. Knöchel, *et al.*, "Exchange biasing of magnetoelectric composites," *Nat Mater,* vol. 11, pp. 523-529, 06//print 2012.

[37]   D. Fritsch and C. Ederer, "First-principles calculation of magnetoelastic coefficients and magnetostriction in the spinel ferrites CoFe 2O 4 and NiFe 2O 4," *Phys. Rev. B,* vol. 86, p. 014406 2012.

[38]   P. Martins, A. Lasheras, J. Gutierrez, J. M. Barandiaran, I. Orue, and S. Lanceros-Mendez, "Optimizing piezoelectric and magnetoelectric responses on CoFe2O4/P(VDF-TrFE) nanocomposites," *J. Appl. Phys. D,* vol. 44, p. 495303, 2011.

[39]   L. Ourry, S. Marchesini, M. Bibani, S. Mercone, S. Ammar, and F. Mammeri, "Influence of nanoparticle size and concentration on the electroactive phase content of PVDF in PVDF-CoFe2O4-based hybrid films," *Phys. Status Solidi A,* vol. 212, pp. 252–258, 2014.

[40]   V. Revathi, S. Dinesh Kumar, P. Chithra Lekha, V. Subramanian, T. S. Natarajan, and C. Muthamizhchelvan, "Structural, dielectric, and magnetic studies on

electrospun magnesium ferrite-polyvinylidene fluoride core-shell composite fibers," *Acta Metall. Sin.,* vol. 27, pp. 557-562, 2014.

[41]   T. Prabhakaran and J. Hemalatha, "Ferroelectric and magnetic studies on unpoled Poly (vinylidine Fluoride)/Fe3O4 magnetoelectric nanocomposite structures," *Mater. Chem. Phys.,* vol. 137, pp. 781-787, 1/15/ 2013.

[42]   J. X. Zhang, J. Y. Dai, L. C. So, C. L. Sun, C. Y. Lo, S. W. Or*, et al.*, "The effect of magnetic nanoparticles on the morphology, ferroelectric, and magnetoelectric behaviors of CFO/P(VDF-TrFE) 0-3 nanocomposites," *J. Appl. Phys.,* vol. 105, p. 054102 2009.

[43]   Y. Jiang, Y. Ye, J. Yu, Z. Wu, W. Li, J. Xu*, et al.*, "Study of thermally poled and corona charged poly(vinylidene fluoride) films," *Polym. Eng. Sci.,* vol. 47, pp. 1344-1350, 2007.

[44]   J. W. Zhang, R. Belouadah, L. Lebrun, and D. Guyomar, "Magnetoelectric phenomena of insulator polymers after corona poling: Procedure and experiments," *Sens. Actuator A-Phys.,* vol. 220, pp. 112-117, 2014.

[45]   P. Martins, X. Moya, L. C. Phillips, S. Kar-Narayan, N. D. Mathur, and S. Lanceros-Mendez, "Linear anhysteretic direct magnetoelectric effect in Ni 0.5Zn0.5Fe2O4/poly(vinylidene fluoride-trifluoroethylene) 0-3 nanocomposites," *J. Phys. D: Appl. Phys.,* vol. 44, p. 482001, 2011.

[46]   M. Kumar and K. L. Yadav, "Magnetoelectric characterization of xNi0.75Co0.25Fe2O4–(1−x)BiFeO3 nanocomposites," *J. Phys. Chem. Solids,* vol. 68, pp. 1791-1795, 9// 2007.

[47]   M. Li, H. J. Wondergem, M. J. Spijkman, K. Asadi, I. Katsouras, P. W. M. Blom*, et al.*, "Revisiting the δ-phase of poly(vinylidene fluoride) for solution-processed ferroelectric thin films," *Nat. Mater.,* vol. 12, pp. 433-438, 2013.

[48]   P. Martins, A. C. Lopes, and S. Lanceros-Mendez, "Electroactive phases of poly(vinylidene fluoride): Determination, processing and applications," *Prog. Polym. Sci.,* vol. 39, pp. 683-706, 2014.

[49]   P. M. A. Maceiras, R. Gonçalves,G. Botelho, E. Venkata Ramana, S.K.Mendiratta, M. San Sebastián, J.L. Vilas, S. Lanceros-Mendez2 and L.M. León, "High-temperature polymer based magnetoelectric nanocomposites," *Eur. Polym. J.,* vol. 64, pp. 224–228, 2015.

[50]   S. D. Bhame and P. A. Joy, "Enhanced magnetostrictive properties of CoFe2O4 synthesized by an autocombustion method," *Sens. Actuator A-Phys.,* vol. 137, pp. 256-261, 2007.

[51]   M. Atif, M. Nadeem, R. Grössinger, and R. S. Turtelli, "Studies on the magnetic, magnetostrictive and electrical properties of sol-gel synthesized Zn doped nickel ferrite," *J. Alloy. Comp.,* vol. 509, pp. 5720-5724, 2011.

[52]   S. S. Nair, G. Pookat, V. Saravanan, and M. R. Anantharaman, "Lead free heterogeneous multilayers with giant magneto electric coupling for microelectronics/microelectromechanical systems applications," *J. Appl. Phys.,* vol. 114, p. 064309, 2013.

[53]   R. Goncalves, P. Martins, D. M. Correia, V. Sencadas, J. L. Vilas, L. M. Leon, *et al.*, "Development of magnetoelectric CoFe2O4 /poly(vinylidene fluoride) microspheres," *RSC Advances,* vol. 5, pp. 35852-35857, 2015.
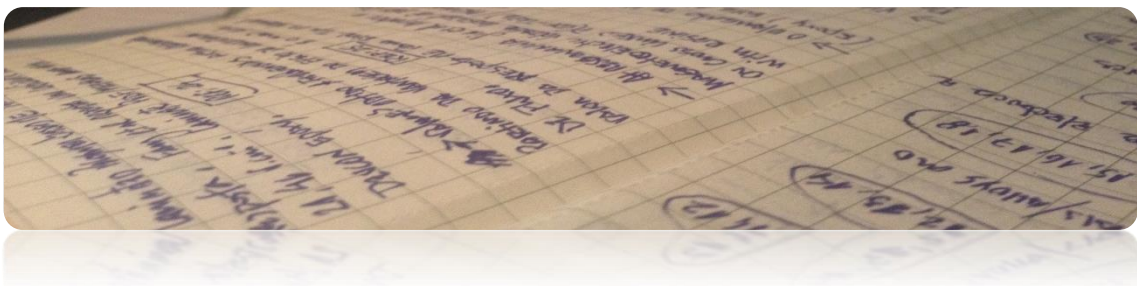
8 Main conclusions and future work

In this chapter the main conclusions of this work and some possibilities for future developments are presented.

8.1 Conclusions

Magnetoelectric (ME) laminate composites have been studied due their technological potential. Among them, polymer based ME laminate composites are a recent approach that allow to solve some of the problems associated with ceramic composites.

This work is focused on the optimization of the different layers involved in the fabrication of laminated composites. The influence of the size of the different layers and the bonding between them were thus addressed, together with the suitability of the materials for energy harvesting and sensor applications.

The main conclusions of this work are the following:

- A Magnetoelectric Characterization System was sucesfully developed.

- The effect of the bonding layer type and piezoelectric layer thickness on the ME response of the composites was reported. It was observed an increase of the magnetoelectric (ME) voltage coefficient from 45 $V.cm^{-1}.Oe^{-1}$ to 53 $V.cm^{-1}.Oe^{-1}$ with increasing PVDF thickness from 28 μm to 110 μm and a reduction of the ME voltage coefficient from 53 $V.cm^{-1}.Oe^{-1}$ to 6 $V.cm^{-1}.Oe^{-1}$ with increasing Young Modulus from 9.0×10^9 Pa to 2.7×10^8 Pa

- Increasing temperature affects the stability and functionality of the composites. The coupling coefficient (k) decreases down to 0.11 with increasing temperatures due to interface detachment and led to reduced transduction and magnetoelectric response, in particular for temperatures above 80ºC.

- The influence of the size of the magnetostrictive and piezoelectric elements as well as different geometries on the ME response was investigated. It is concluded that the ME voltage coefficient increases with decreasing longitudinal aspect ratio (LAR). On the other hand, ME laminates with lowest transversal aspect ratio (TAR) resulted in better ME performance when compared with higher TAR.

- Tri-layered composites configurations (M/P/M type) show a higher ME response (75 V.cm^{-1}.Oe^{-1}) than the M/P bi-layer configuration (66 V.cm^{-1}.Oe^{-1}).

- The ME output voltage and optimum magnetic field can be controlled by changing the number of magnetostrictive layers, which allows these composites to be promising candidate for magnetic sensors and energy harvesting applications.

- For sensor applications, sensibility and resolution values 30 mV.Oe^{-1} and 8 μOe for the DC magnetic field sensor and 992 mV.Oe^{-1} and 0.3 μOe for the AC magnetic field sensors, respectively, were found to be positively comparable with the ones reported in literature for polymer-based ME sensors. Further, the correlation coefficient, linearity and accuracy values DC (0.995, 95.9% and 99.4%) and AC (0.9998, 99.4% and 99.2%) certify the applicability of polymer based ME materials as innovative AC/DC magnetic field sensors

- It has been successfully demonstrated the development of an innovative magnetic harvester based on (magnetostrictive / piezoelectric polymer / magnetostrictive) ME laminate composites with optimized harvesting circuits. Power$_{density}$=0.9 mW.cm^{-3} and Power=12 μW values were obtained for the developed harvester, showing its high application potential.

- It was developed a new method for the measurement of the magnetostriction of nanoparticles based on the ME effect measured on polymer-based ME composite materials. This is a new method with high application potential.

8.2 Future work

This work allowed to determine the fabrication parameters optimizing the response of polymer based ME laminates and proved the suitability of ME composites for sensors and energy harvesting devices. This work also introduced a new application of the ME effect for the determination of the magnetostrictive coefficient of nanoparticles, however some additional studies are needed/desired.

For some applications, biocompatibility of the materials is a key issue in the successful implementation of the devices, in this way a future challenge is to develop fully biocompatible ME sensors and/or harvesters,.

Another important aspect is to eliminate the adhesive layer between magnetostrictive and piezoelectric elements, leading to even more efficient composites, less expensive and with simple structures.

The optimization of the electronic components for energy harvesting devices reported in this work needs to be extended for sensor and actuator applications.

The possibility of developing ME inks for suitable printing technologies (inkjet and screen printing) also needs to be addressed in order to optimize the scalability of the production and implementation of the devices.